

# Investigation of the Homopolar Inductor Alternator for Automotive Applications

By

Leandro M. Lorilla

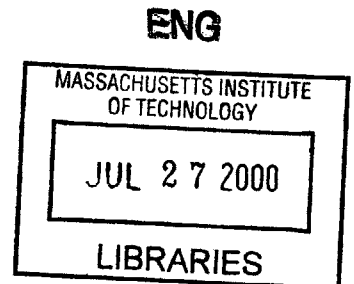
Submitted to the Department of Electrical Engineering and Computer Science  
in Partial Fulfillment of the Requirements for the Degrees of  
Bachelor of Science in Electrical Science and Engineering and  
Master of Engineering in Electrical Engineering and Computer Science  
at the Massachusetts Institute of Technology

May 19, 2000

June 2000

Copyright 2000 MM Leandro M. Lorilla. All rights reserved.

The author hereby grants to M.I.T. permission to reproduce and  
distribute publicly this paper and electronic copies of this thesis  
and to grant others the right to do so.



Author \_\_\_\_\_

Department of Electrical Engineering and Computer Science  
May 19, 2000

Certified by \_\_\_\_\_  
*[Handwritten signature]*

Jeffrey H. Lang  
Thesis Co-Supervisor

Certified by \_\_\_\_\_

Thomas A. Keim  
Thesis Co-supervisor

Accepted by \_\_\_\_\_  
*[Handwritten signature]*

Arthur C. Smith  
Chairman, Department Committee on Graduate Theses

# **Investigation of the Homopolar Inductor Alternator for Automotive Applications**

by

Leandro M. Lorilla

Submitted to the  
Department of Electrical Engineering and Computer Science

May 19, 2000

In Partial Fulfillment of the Requirements for the Degree of  
Bachelor of Science in Electrical Science and Engineering and  
Master of Engineering in Electrical Engineering and Computer Science

## **ABSTRACT**

Increased power consumption and new standards for fuel consumption in automobiles have led to the need for increases in power ratings and efficiency of alternators. To address this need, the MIT/ Industry Consortium on Advanced Automotive Electrical and Electronic Systems has set new output power requirements of 4 kW at 600 rpm increasing linearly to 6 kW at 6000 rpm. The Consortium has also imposed an efficiency of at least 75% at an engine speed of 1500 rpm and power output of 3250 W. In this thesis, the Homopolar Inductor Alternator is designed and optimized for the challenging specifications. The alternator is a brushless, solid rotor, high speed machine that creates AC flux by having a varying reluctance around the air gap. The machine is analyzed as part of a simplified automotive electrical system by developing a lumped parameter model. The alternator is optimized for cost by employing a two stage Monte-Carlo method which performs a random search over the entire design space, and following this, a search around each of the optimistic design points from the first stage. The results obtained are favorable. The optimum machines have fairly competitive costs at high speeds and pole counts. Compared with the wound-field alternator, the machine can be run at higher speeds and pole counts by virtue of its brushless, robust rotor. In addition, it does not have the scaling issues that limits the use of the Lundell alternator for high power applications. These make the Homopolar Inductor Alternator a favorable choice for use in next generation automobiles.

Thesis Co-Supervisor: Jeffrey H. Lang

Title: Professor, Associate Director, Laboratory for Electromagnetic and Electronic Systems

Thesis Co-Supervisor: Dr. Thomas A. Keim

Title: Principal Research Engineer

## Acknowledgements

I would like to thank Prof. Jeffrey Lang and Dr. Thomas Keim, for their supervision throughout this graduate year. It has been a great experience working with them.

I would like to thank the MIT/Industry Consortium on Advanced Automotive Electrical and Electronic Systems for the guidance and funding for this research.

I am thankful for the company of my friends here at the LEES lab. They are a lot of fun to be around with... just great people.

I'd like to thank all my friends. Their presence has made life much more worth it. The experiences I've shared with them are priceless.

And finally, I would like to thank my family. I'd like to thank my grandfather, for his guidance and being a source of inspiration. I am grateful for having my brothers, for so many reasons. And to my parents, who have always been there for me, ever since, thank you. I can hardly find the words and ways to express my sincere gratitude to you.

## Table of Contents

<b>Chapter 1 Introduction</b>	7
1.1 Background	7
1.2 Problem Statement	8
1.3 Thesis Overview	9
<b>Chapter 2 Overall Problem</b>	11
2.1 Electrical and Mechanical Specifications	11
2.2 Electrical Circuit	12
2.3 Principles of Operation of the Homopolar Inductor Alternator	13
<b>Chapter 3 Monte Carlo Optimization</b>	16
<b>Chapter 4 Lumped Parameter Modeling</b>	20
4.1 Stator-Frame Inductances	20
4.1.1 Permeance Function for the Air Gap	23
4.1.2 Magnetomotive Forces	24
4.1.2.1 Field MMF	24
4.1.2.2 Stator Phase MMF	25
4.1.3 Air Gap Flux Densities	26
4.1.3.1 Flux Densities due to Field Winding	26
4.1.3.2 Flux Densities due to Armature Winding	26
4.1.4 Field Self Inductance	27
4.1.5 Armature-Field Mutual Inductance	28
4.1.6 Armature Self and Mutual Inductances	29
4.1.7 Leakage Inductances	30
4.1.8 Winding Factor	31
4.1.9 Inductance Matrix	32
4.2 Direct and Quadrature Reactances	33
4.3 Resistances	35
4.3.1 Field Resistance	35
4.3.2 Armature Resistance	36
4.4 Summary	36

<b>Chapter 5 Equivalent Circuit</b>	38
5.1 Equivalent armature reactance and resistance	38
5.1.1 Phasor Analysis	38
5.1.2 Term-Matching	41
5.2 Equivalent Load	43
<b>Chapter 6 Alternator Design</b>	45
6.1 Meeting the Electrical and Mechanical Requirements	45
6.1.1 Power Requirement	45
6.1.2 Efficiency	46
6.1.2.1 Copper Losses	47
6.1.2.2 Diode Losses	47
6.1.3 Flux Density Requirements (Saturation)	47
6.1.3.1 Centerpiece	48
6.1.3.2 Rotor Poles	48
6.1.3.3 Stator Yoke and Back Iron	49
6.1.3.4 Stator Teeth	51
6.1.4 Thermal Limits	51
6.1.4.1 Field Winding Current Density	51
6.1.4.2 Armature Winding Current Density	51
6.2 Electrical Design	52
<b>Chapter 7 Results</b>	55
<b>Chapter 8 Conclusions and Future Work</b>	61
8.1 Concluding remarks	61
8.2 Possible future work	62
<b>Appendix A Nomenclature</b>	64
<b>Appendix B Armature Winding</b>	68
B.1 Winding Pattern	68
B.2. Mean Path Length	69
<b>Appendix C Pole Face Losses</b>	71
<b>Appendix D Simulation Code</b>	77

## List of Figures

Figure 2.1 Power and Efficiency Requirements	11
Figure 2.2 Simplified Electrical Circuit	12
Figure 2.3 Simplified view of a Homopolar Inductor Alternator	13
Figure 2.4 Simplified machine	14
Figure 3.1 Dimensions of simplified machine	17
Figure 3.2 Monte-Carlo Simulation Flow Chart	19
Figure 4.1 Simple Magnetic Circuit	21
Figure 4.2 Equivalent Magnetic Circuit	23
Figure 4.3 Rotor Teeth	24
Figure 4.4 Ampere loop used to determine Field MMF	25
Figure 4.5 Stator Slot Diagram	31
Figure 5.1 Equivalent Unloaded Armature Circuit	38
Figure 5.2 Phasor Diagram for a Single Phase of a Generator	39
Figure 5.3 Phasor Diagram Used for Determining Equivalent Circuit	30
Figure 5.4 Complete Three-Phase Circuit	43
Figure 5.5 Equivalent Three-Phase Circuit	43
Figure 6.1 Flowchart for electrical design process	53
Figure 7.1 Cost Curves from both broad and refined searches	55
Figure 7.2 Optimal 8 pole machine (\$75.51)	57
Figure 7.3 Optimal 10 pole machine (\$65.31)	57
Figure 7.4 Optimal 12 pole machine (\$62.70)	58
Figure 7.4 Optimal 12 pole machine (\$52.40)	58
Figure 7.4 Optimal 12 pole machine (\$52.78)	58
Figure 7.4 Optimal 12 pole machine (\$50.33)	59
Figure 7.4 Optimal 12 pole machine (\$43.89)	59
Figure 7.9 Optimum machine characteristics	60
Figure B.1 Armature Winding Pattern	68
Figure B.2 Top View of Windings	69
Figure B.3 Top View of One Armature Winding Turn	70
Figure C.1 Developed View of Air Gap	71

# Chapter 1

## Introduction

### 1.1 Background

In recent years, automotive engineers have focused on improving many aspects of automobile performance. One goal is to improve fuel economy, and another is to modify the electrical system to provide sufficient power due to increases in the number of loads and some of their power ratings. The addition of new loads, like electromechanical valve actuators, active suspension, power steering, air conditioning, and an engine cooling fan, will increase the power requirements from the current 800W to around 2.5 kW with a peak of 12 kW by the year 2005 [1]. Part of the fuel economy problem can be approached by improving and modifying the alternator, which supplies electrical energy to the automobile. Improving its efficiency by 5% will save the car 15 L of fuel in one year, which is around 1% of annual consumption [2]. With increased efficiency, the increased power requirement can be more readily met by an increase in the power output of the alternator.

In this light, the MIT/ Industry Consortium on Advanced Electrical Components and Systems has set new requirements for the alternator and is conducting research in the area. Currently, an alternator has a maximum power output of around 2 kW and an efficiency of 50% at 6000 rpm. The new specifications for the alternator are that it must be able to provide 4 kW at 600 rpm increasing linearly to 6 kW at 6000 rpm. This is a substantial increase from the power output of around 1.4 kW at 6000 rpm in today's automobiles [3]. The alternator must be at least 75% efficient at an interior operating point of 1500 rpm and 3.25 kW. Also, the alternator must function with the use of minimal power electronics; the standard electronics include a three-phase bridge rectifier with a constant voltage load at the output. In order to meet these new requirements, the current claw-pole (Lundell) alternator could be redesigned and optimized again. In addition, novel alternators could be designed and evaluated.

The alternator currently being used in cars today is the claw-pole or Lundell alternator. Having been the alternator of choice over decades, this alternator has been optimized to minimize cost somewhat at the expense of efficiency and power density. This alternator performs well over a wide range of speeds and under elevated temperatures [3]. The alternator optimizes to small dimensions and thus easily meets its space requirement, and is relatively cheap. Several disadvan-

tages of the alternator are its high rotor inertia which makes it susceptible to belt slippage, and its adverse overvoltage following load dump [3]. Engineers have contemplated modifying this alternator to meet the new requirements. Having been optimized for cost and not power output, the power limits have yet to be reached. More powerful claw-pole alternators are certainly possible. However, there are some obstacles to increasing its power output. At present, it is around 50% efficient. This low value of efficiency is due to high losses, which results in the need for extensive cooling [3]. Increasing its efficiency to 75% at 3.25 kW and 1500 rpm would be a challenge if costs are to be kept down. Increasing the power rating without a considerable increase in efficiency would further increase the need for cooling. In order to increase the power rating of the alternator, either its size or its speed could be increased. Either way, the centrifugal forces on the machine are likely to rise to intolerable levels because of the claw-like construction of the rotor. Although improving the claw-pole alternator remains a possibility worthy of pursuit, the consortium decided to conduct research on the use of novel alternator designs.

A family of wound field synchronous alternators were previously designed and evaluated for both a direct-drive and a geared-drive configuration operating at twice engine speed. Its known advantages are that of high efficiency, adequate power density, and the ability to function without the need for commutation brushes [3]. In addition to the aforementioned specifications, thermal and saturation limits were set. The machine was thoroughly analyzed and subsequently modeled in Matlab. A two-stage Monte Carlo synthesis process was run over pole counts ranging from 4 to 20. The cheapest machine that met the power density, efficiency, saturation, and current density requirements for each pole count was obtained. The results were favorable. The cheapest among all the acceptable alternators had costs of around \$40. A comparison of the results is provided in Chapter 7.

## **1.2 Problem Statement**

The goal of this thesis project is to investigate the use of the homopolar inductor alternator (HIA) as the next high-power, high-efficiency alternator for automobiles and to compare its performance to that of the Lundell claw-pole alternator and the wound-field synchronous alternator. This alternator has been previously used for power generation in automobiles, and for aeronautical and aerospace applications. Engineers have considered its potential use in hybrid cars. The HIA is a high speed alternator capable of operating at higher ambient temperatures, under hostile environmental conditions and over long periods of time [4]. The rotor is easy to construct,



robust, and can withstand high mechanical stresses. In fact, at high speeds, the rotor of the homopolar inductor alternator is more structurally robust than the claw-pole alternator [4]. In addition, it does not require the use of slip rings or brushes.

The homopolar inductor alternator also tends to have higher power/mass and power/volume ratios compared to conventional machines. Being a high speed machine, it will tend to have smaller dimensions at the same power ratings, thus resulting in materials savings and minimizing cost. This machine has been directly coupled to gas turbines in aircrafts and ships [4,7]. It has also been used as a load-leveler for engines.

The objective of this thesis then is to understand the important aspects of the alternator under steady state operation, create a lumped-parameter model of the machine, determine the equivalent load circuit, and optimize the machine for cost, given the electrical and mechanical requirements as constraints. In the end, the performance and cost of the machine will be compared to that of the wound-field synchronous alternator that has been previously optimized for the same requirements and using the same algorithm.

### **1.3 Thesis Overview**

This thesis is organized into eight chapters. The first part of Chapter 2 will cover in more detail the specifications set for next generation alternators. The second part of the chapter will show the circuit for the loaded alternator. The last part of Chapter 2 will illustrate the principles of operation of the homopolar inductor alternator, explore in more detail which aspects make it different from other synchronous machines, and which characteristics put it at an advantage or disadvantage when compared to other machines. Chapter 3 will provide an overview of the entire design and optimization process used here. The alternator is modeled using a lumped-parameter approach. It is optimized using Monte-Carlo methods where the optimizer synthesizes and evaluates a large number of machines randomly over a restricted design space and selects the cheapest acceptable ones. Chapter 4 covers the derivations used in determining the lumped parameter model for the three-phase alternator. Chapter 5 explores the methods used in determining the equivalent electrical circuit external to the alternator. Chapter 6 presents the details of how the different electrical requirements are implemented in the Monte-Carlo algorithm, and provides a detailed coverage of the electrical design process. Chapter 7 presents the results of the design process. It includes cost curves showing how the costs of the optimum machines vary with pole count. Diagrams of the optimum or cheapest machines are also shown. An analysis of the results

is also included in that chapter. Chapter 8 concludes this thesis paper. It summarizes the key results, and provides a comparison between the homopolar inductor alternator and the wound-field synchronous alternator.

## Chapter 2

### Overall Problem

#### 2.1 Mechanical and Electrical Specifications

Most of the requirements for the alternator can be expressed as constraints on the mechanical and electrical properties of the alternator. The mechanical requirements for the alternator are set mostly by space constraints in the automobile. These are achieved by imposing limits on the dimensions of the machine. The maximum outer diameter of the machine is set at 300 mm. The minimum air gap width is set at 0.33 mm.

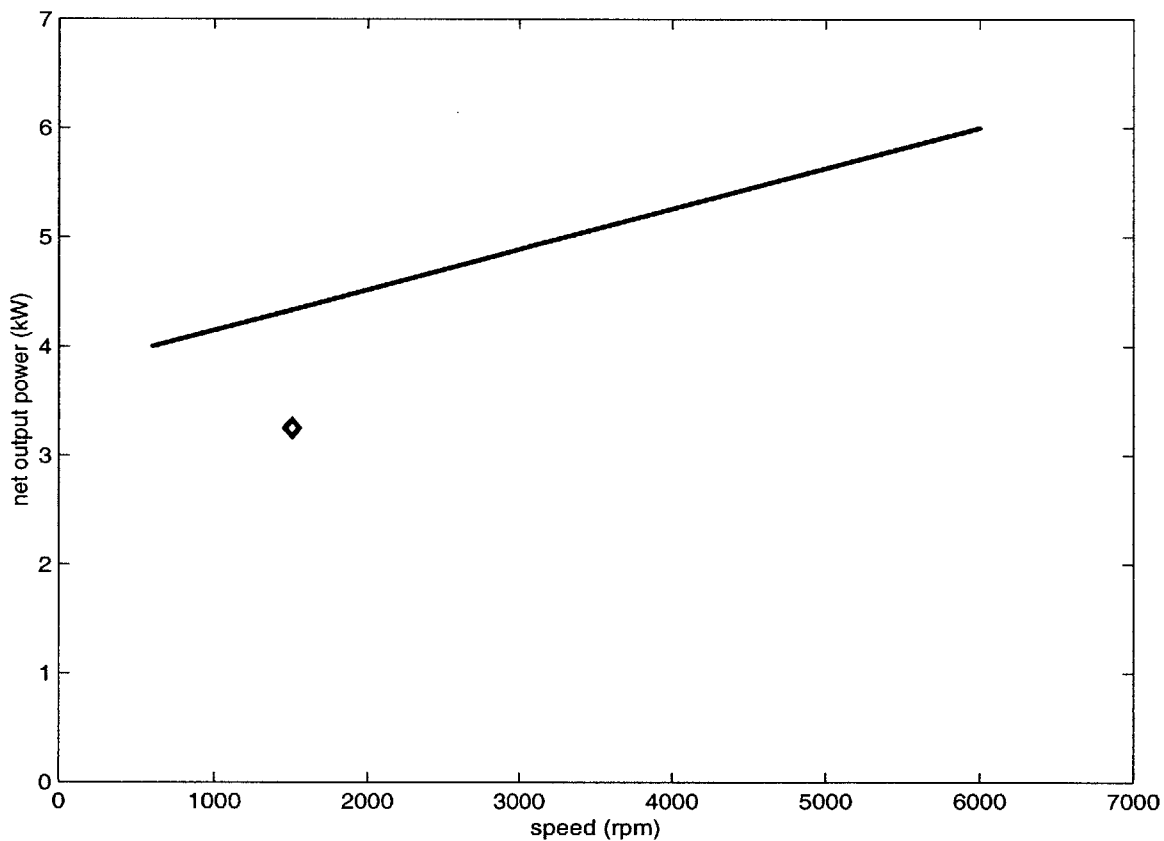


Figure 2.1 Power and Efficiency Requirements

The alternator must meet the requirements shown in Figure 2.1 which were determined based on the new automobile electrical system. These were decided upon by the MIT/Industry Consortium on Advanced Automotive Electrical/Electronic Components and Systems. Shown in Figure 2.1 are the generating requirements for the alternator. The alternator must be able to pro-

vide at least 4 kW at idle speed (600 rpm), increasing linearly to 6 kW at maximum speed (6000 rpm). At a cruising speed of 1500 rpm and a power output of 3250 W, the efficiency of the alternator has to be at least 75%. In this thesis, the alternator speed will be assumed to be three times the engine speed. The alternator is connected to a rectifier where the output voltage is assumed to be 42V. In addition to these requirements, the steel flux densities should be limited to 1.8 Tesla, in order to ensure operation in the linear region. Limits will also be set on the winding current densities, and effectively, the slot current densities, in order to ensure that reasonable thermal performance is maintained. The maximum limit chosen for this purpose is 2000 A/cm<sup>2</sup>.

## 2.2 Electrical Circuit

A simplified model of the electrical circuit into which the three-phase alternator fits involves a rectifier at the output which drives a load voltage,  $V_o$ , of 42 V. This voltage is the voltage of choice for next generation automobiles again decided upon by the MIT/Industry Consortium. The circuit is summarized in Figure 2.2. The power requirements set for the system are those at the output of the rectifier as opposed to the output of the generator itself.

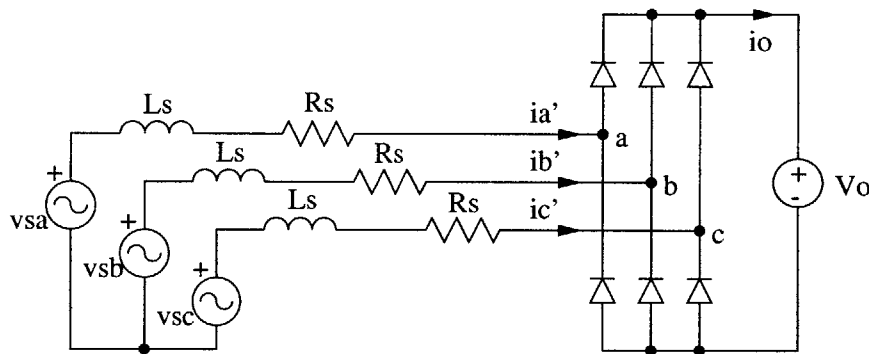


Figure 2.2 Simplified electrical circuit

### 2.3 Principles of Operation of the Homopolar Inductor Alternator

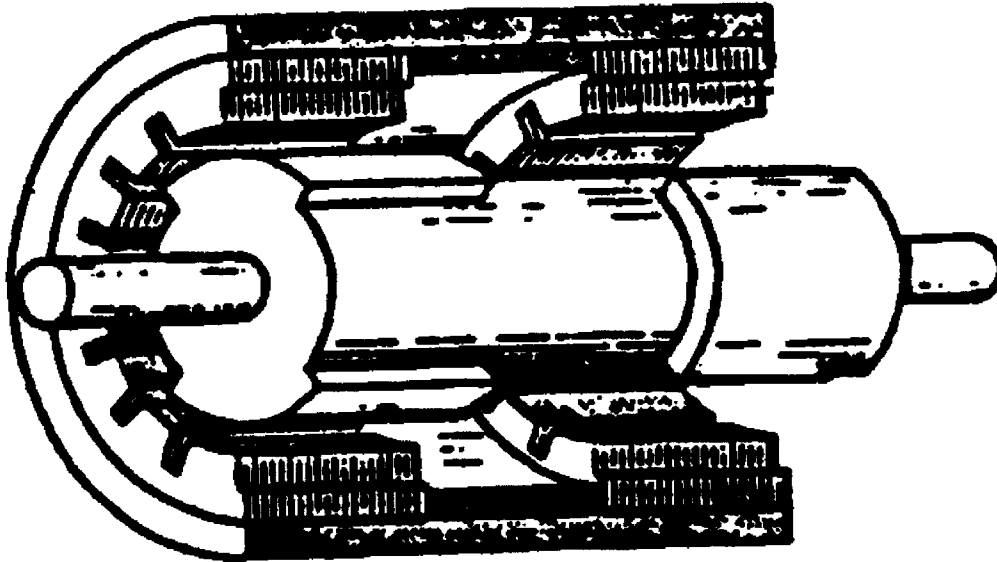


Figure 2.3 Simplified view of a Homopolar Inductor Alternator  
(Taken from [5]).

The homopolar inductor alternator shown in Figure 2.3 is a synchronous machine that creates alternating flux densities in the air gap through a variation in the reluctance of the rotor. The field winding is housed next to the stator which allows for the rotor to be free of brushes and slip rings. This winding drives axial flux through the rotor, creating one North end and one South end. The machine has two distinct stacks of stator laminations, one using the flux from the rotor's north pole and the other using flux from the rotor's south pole. Circumferential variations in the flux in the stacks (necessary to induce voltage in response to rotation) are induced by salient poles on both north and south ends of the rotor. The machine is called homopolar because of the flux being in the same radial direction on each stack. The flux due to the field is directed radially outward on one stack and radially inward in the other. The solid rotor is robust and relatively easy to produce out of ferromagnetic steel. It has salient poles in the region of the stator teeth. The poles adjacent to one stack are offset by 180 electrical degrees relative to poles of the other stack. The

poles are structured in this manner so that the induced voltages in the armature windings due to the field flux on both stacks sum up instead of cancelling each other out. This can be understood by looking at both the armature and the field winding. Notice that the armature winding is wound across both stacks. The field winding, being concentric with the rotor, sends flux axially across the centerpiece, radially outward in all directions on one stack, axially through the back-iron and radially inward in all directions through the opposite stack. This means that the MMF excitation due to the field is constant with a positive value in one stack and an equally opposite negative value in the other stack. Since the alternating flux results from modulation of the field by the rotor poles and interpolar gaps, which essentially means a multiplication of the MMF drop across the air gap by the permeance per unit area of the air gap, the flux densities along the same angle on both stacks will have the same magnitudes but opposite signs if the poles are not offset apart. This would result in cancellation of the flux linked by each of the armature windings and zero induced voltage. However, because the poles are offset, such cancellation does not occur.

To a first order approximation, the flux densities due to the field winding look like a raised sinusoid whose minimum possible value is close to zero and maximum possible value is limited by saturation. Hence, the flux densities have peak-to-peak values of around half that obtained from conventional machines where the flux densities can assume both positive and negative values [15].

The advantages of the homopolar inductor alternator are achieved when operated at high frequencies. It is operated as a high speed machine mainly because of the simplicity and robustness of the rotor. Since output power is the product of torque and speed, high speed machines would require less torque to provide the same amount of power. Since torque scales approximately as the volume of the machine, lower torque implies a smaller machine. A smaller machine results in cheaper costs, thus justifying the consideration of this particular type of alternator for the cost-driven automotive industry.

A rotor mechanical pole pitch spans a pair of magnetic poles and thus, given a rotor pole fraction of a half, a full-pitch armature coil will span the width of a pole or an interpolar gap. Conventional salient pole machines where the field windings are wound around the salient poles

would have the angle between two poles spanning a pole pitch as compared to the homopolar inductor alternator where one mechanical pole spans a pole pair.

The cross-sectional and sectional views of a 12-pole alternator are shown in Figure 2.4. A 12-pole alternator would have 12 poles on both stacks, six on one stack which are offset from six on the other stack. The rotor poles have sidewalls that are directed radially outward. On the other hand, the stator teeth have parallel sidewalls. The number of stator slots per pole used is six. The stator slots have closings or depressions in order to reduce the effects of torque pulsations.

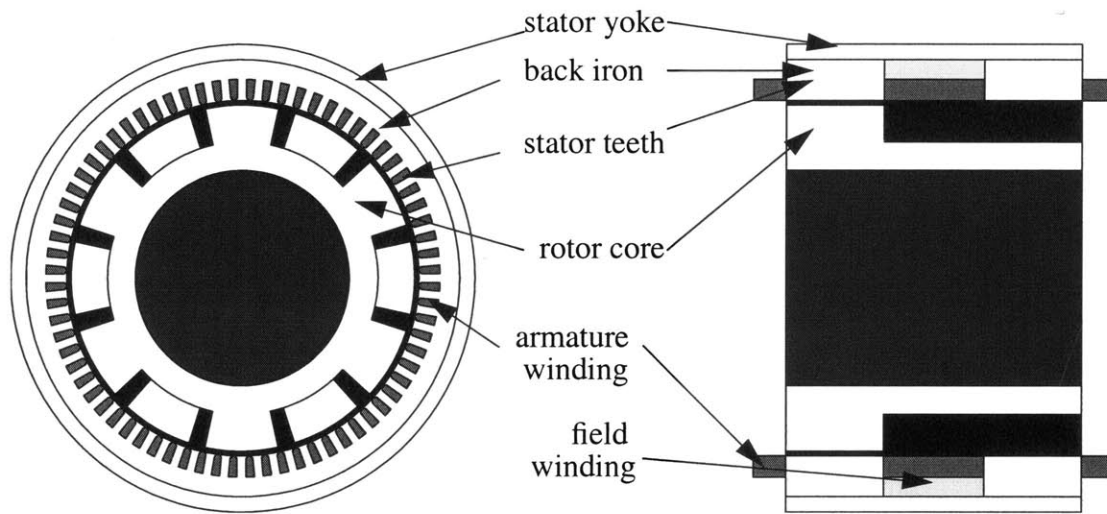


Figure 2.4 Simplified machine

## Chapter 3

### Design by Monte-Carlo Synthesis and Model-Based Evaluation

In this thesis, the HIA is designed through a combination of Monte-Carlo synthesis and model-based analysis. Monte-Carlo synthesis involves randomly selecting the design of the alternator from within a restricted design space. Model-based analysis involves using electromechanical models to evaluate the performance of each synthesized alternator. After a newly synthesized alternator is analyzed, its performance is compared to that of the alternators that came before it, and a list of the best alternators is kept as the basis of this comparison. Poorly performing alternators are discarded. The primary advantage of this approach to design is that it uniformly covers the design space as it searches for an optimal alternator and is not attracted to false optima. The primary disadvantage is that it may take a long time to converge. In fact, millions of machines will be synthesized and analyzed in the process. To speed up the process, convergence is actually obtained with a constrained Monte-Carlo optimization once the Monte-Carlo synthesis has identified the most promising regions of the design space.

A flowchart of the overall design process is shown in Figure 3.2. The beginning of the process involves initialization. This includes setting the requirements, both electrical and mechanical, initializing the constants, and initializing some of the parameters. Next, at the beginning of each iteration, a new geometry is synthesized. That is, the variables noted in Figure 3.1 are chosen randomly from within the permissible design space. The possible values that each of the variables may assume are uniformly distributed within certain limits. The variables that are first chosen get to span the entire range given by the mechanical specifications. The ranges of the variables that follow are determined based on the values that have been determined before them to ensure that the geometry is sensible. For example, the stator bottom radius has to be between the stator slot bottom radius and the outer radius. The variables in the order in which they are generated include the rotor pole and stator tooth angles, rotor pole and slot air gap widths, the rotor slot bottom radius, the stator inside or top radius, the stator slot bottom radius, the stator outside or bottom radius, the stack length, and the inter-stack length, all of which amount to ten dimensions. The rotor top radius is the difference between the stator inside radius and the rotor outside radius. The inner (shaft) and outer radii are to be determined later. Each randomized parameter is generated



from a uniform distribution with the range of possible values falling within the set mechanical limits. Given the geometry, the lumped-parameter model for the alternator is derived assuming one armature turn per coil. The alternator is evaluated for electrical performance. At this point, the design program attempts to obtain the optimum number of armature turns per coil. However, it is possible that the particular geometry of the machine prevents the machine from meeting all the requirements even for any number of armature turns. If the machine satisfies all the requirements with some allowable number of armature turns, then the cost of the machine is determined, otherwise, the machine is discarded. Only the cheapest few machines are kept; the rest are discarded. The cost used for each machine will simply be its materials cost multiplied by an overhead factor of two. The materials cost is equal to the cost of copper used added to the cost of steel. The iterations on different geometries continue until a certain number of alternators have been designed and evaluated. This number depends roughly on the number of parameters randomly chosen for each design as well as the number of constraints imposed on the machine. The number of iterations has to be large enough such that all characteristic geometries for the alternator can be evaluated.

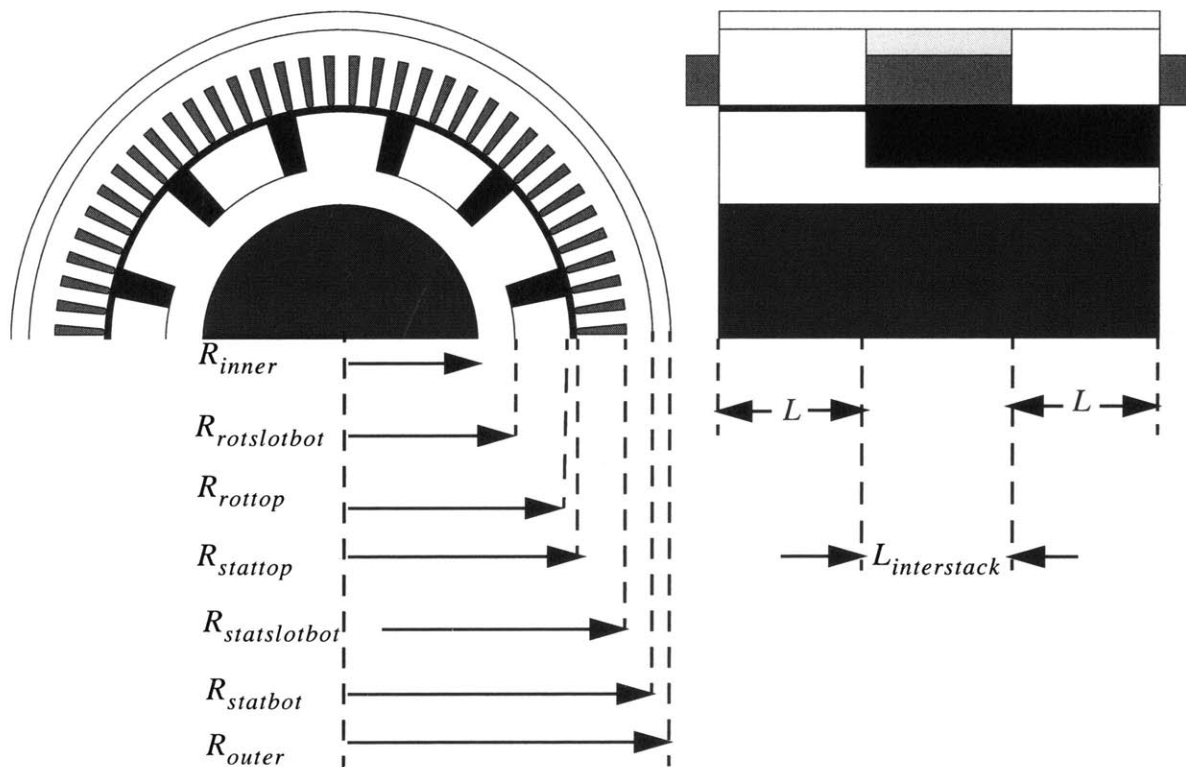
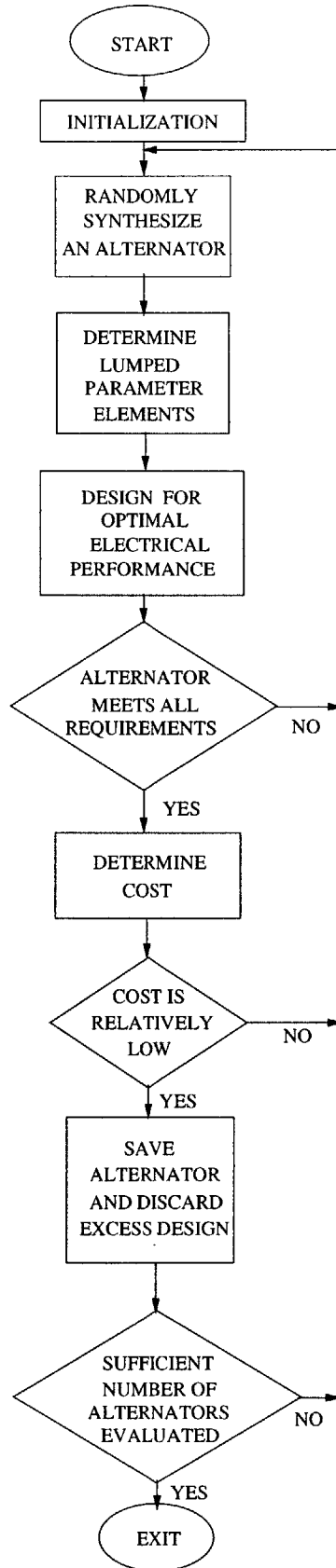


Figure 3.1 Dimensions of simplified machine

The entire design process is divided into two stages: the broad and refined searches. The broad search allows for geometries that fall within the entire range allowed by the mechanical requirements set. A million alternators are synthesized, designed, and evaluated for this stage. From this first stage, the optimum machine almost entirely based on cost and partly on manufacturability, is obtained. The refined search is then performed during which a hundred thousand machines will be synthesized whose geometrical properties are constrained to be within a reduced local design space centered around the optimum machine from the broad search. This is expected to yield cheaper machines and thus further drive down cost.

Figure 3.2  
Monte-Carlo  
simulation  
flowchart



## Chapter 4

### Lumped Parameter Modeling

As part of the design process, it is necessary to evaluate the performance of each synthesized alternator. This is done using the lumped-parameter electromechanical models. In general, each phase of a synchronous machine can be modeled as a back-electromotive force in series with a synchronous inductance and armature resistance. This chapter explains the models used to evaluate these lumped-parameter elements of the homopolar inductor alternator.

#### 4.1 Stator-Frame Inductances

The inductance matrix relates the currents in the windings to the flux linked by the windings. Since the alternator has a field winding (f) and three-phase armature windings (a,b, and c), the flux linkages and currents are related according to

$$\begin{bmatrix} \lambda_a \\ \lambda_b \\ \lambda_c \\ \lambda_f \end{bmatrix} = \begin{bmatrix} L_{aa} & L_{ab} & L_{ac} & L_{af} \\ L_{ba} & L_{bb} & L_{bc} & L_{bf} \\ L_{ca} & L_{cb} & L_{cc} & L_{cf} \\ L_{fa} & L_{fb} & L_{fc} & L_{ff} \end{bmatrix} \begin{bmatrix} i_a \\ i_b \\ i_c \\ i_f \end{bmatrix} \quad 4.1$$

where  $\lambda$  denotes flux linkage,  $i$  denotes current and  $L$  denotes inductance. The convention used is for a motor where the currents are positive into the positive terminal of each phase. Using the equations for a generator would simply mean having the armature currents being positive out of the positive terminal and thus adding a negative sign to them. Using the generator convention, the armature currents would be  $i_a' = -i_a$ ,  $i_b' = -i_b$ , and  $i_c' = -i_c$ . This notation will be used for some of the figures.

The variable  $L_{xy}$  in 4.1 is the inductance associated with the flux linked by winding x due to the current in winding y. The self-inductance of a winding relates the flux linked by the winding due to its own current, and has the same two subscripts. The flux linked in a winding due to current in another winding is referred to as the mutual inductance, and  $L$  has two different subscripts. Because of reciprocity,  $L_{xy} = L_{yx}$ , resulting in a symmetric matrix in 4.1.

Finding each winding inductance involves finding the flux  $\lambda$  linked by the winding, with current  $i$  flowing only in the source winding. The inductance can be obtained from the flux linkage

and source current through  $L = \lambda / i$ . The flux linked by the winding is the integral of the flux density over the area of the winding.

$$\lambda = \int_S \vec{B} \cdot d\vec{S} \quad 4.2$$

The principles used for computing the flux density in the air gap can be understood by looking at the simplified magnetic circuit shown in Figure 4.1.

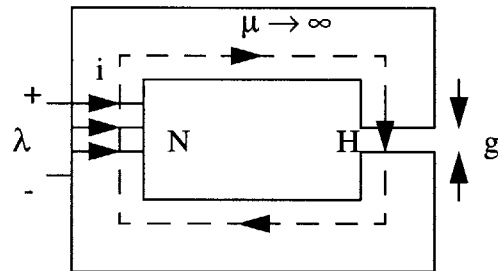


Figure 4.1 Simple magnetic circuit

Ampere's law state that

$$\oint_C \vec{H} \cdot d\vec{l} = \oint_S \vec{J} \cdot d\vec{a} \quad 4.3$$

where  $\vec{H}$  is the magnetic field intensity around the loop, and  $\vec{J}$  is the surface current density through the loop. From this law, the magnetomotive force may be defined as

$$F = \int_C \vec{H} \cdot d\vec{l} \quad 4.4$$

The variable  $F$  will be quite often used to stand for MMF drop. The source of flux around the core is also called the source of MMF, which in this case is the number of ampere turns in the excitation winding,  $Ni$  in the above circuit. Using Ampere's law and assuming that the core is infinitely permeable, the MMF drop across the air gap is:

$$F = H_g g = Ni \quad 4.5$$

where  $H_g$  is the magnetic field intensity in the air gap,  $g$  is the air gap width,  $N$  is the number of series turns, and  $i$  is the current in the winding.

The flux in the air gap is

$$\Phi = B_g A = \mu_o H_g A = \frac{\mu_o A}{g} F = NI \quad 4.6$$

where  $B_g$  is the flux density in the air gap,  $A$  is the cross-sectional area of the air gap and  $\mu_o$  is the permeability of free space. The reluctance of the air gap can be defined as

$$R = \frac{F}{\Phi} = \frac{g}{\mu_o A} \quad 4.7$$

Note that magnetic reluctance is analogous to electrical resistance.

Thus, the flux could be expressed as

$$\Phi = \frac{F}{R} \quad 4.8$$

Following this analogy, an electrical circuit equivalent of the magnetic circuit could be drawing as shown in Figure 4.2. In this circuit, the magnetomotive force is analogous to voltage, flux is analogous to current, and reluctance is analogous to resistance. The reciprocal of reluctance,  $R$ , is termed permeance,  $P$ , which is analogous to conductance. The flux density in the air gap can then be expressed as

$$B_g = \frac{\Phi}{A} = \frac{F}{RA} = F \frac{P}{A} = F\Lambda \quad 4.9$$

The variable  $\Lambda$  is the permeance per unit area of the air gap. The final expression shows that the flux density along a particular path in the air gap could be found as the product of the MMF drop across the air gap and the permeance per unit area along that path. Determining the flux density in the air gap of the homopolar inductor alternator is just a direct extension of this principle to the alternator where there are various excitation windings or MMF sources. The assumption of an infinitely permeable core is made when determining the inductances, and the permeance per unit area varies across the air gap.

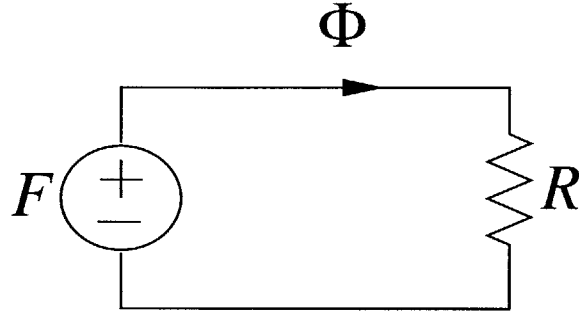


Figure 4.2 Equivalent magnetic circuit

#### 4.1.1 Permeance Function for the Air Gap

In order to find the flux density in the air gap of the HIA, an expression for the permeance function must be derived. A simplified view of the air gap around one end of the rotor laid out flat is shown in Figure 4.3. The permeance per unit area along a magnetic path is defined as

$$\Lambda = \frac{\mu_o}{g(\theta)} \quad 4.10$$

The permeance function for one stack of the rotor, arbitrarily called the left stack ( where the subscript  $L$  is used), taken from [10] is expressed as:

$$\Lambda_L(\theta - \theta_r) = \sum_{m=0}^{\infty} \Lambda_m \cos(mp(\theta - \theta_r)) \quad 4.11$$

where  $m$  indexes the  $m$ th harmonic,  $p$  is the number of pole pairs,  $\theta$  is the mechanical angle around the air gap from the stator reference axis, and  $\theta_r$  is the mechanical angle of the rotor from the stator reference, which is zero when the center of the tooth is aligned with phase A. The harmonic amplitudes are

$$\Lambda_o = \mu_o \left( \frac{1}{g_2} + \beta \left( \frac{1}{g_1} - \frac{1}{g_2} \right) \right) \quad m = 0 \quad 4.12$$

$$\Lambda_m = \frac{2\mu_o}{m\pi} \left( \frac{1}{g_1} - \frac{1}{g_2} \right) \sin(m\beta\pi) \quad m \geq 0 \quad 4.13$$

where  $g_1$  is the air gap width over a rotor pole, and  $g_2$  is the interpolar gap. The rotor pole fraction is

$$\beta = \frac{\theta_t}{\left(\frac{2\pi}{p}\right)} \quad 4.14$$

where  $\theta_t$  is the rotor tooth width in mechanical radians and  $2\pi/p$  shown in Figure 2.3 is the rotor mechanical pole pitch which spans a magnetic pole pair. The other stack of the rotor would have essentially the same permeance function except for a shift in  $\theta_r$  by  $\pi/p$ , thus replacing  $\theta_r$  by  $\theta_r - \pi/p$

$$\Lambda_R(\theta - \theta_r) = \sum_{m=0}^{\infty} \Lambda_m \cos\left(mp\left(\theta - \left(\theta_r - \frac{\pi}{p}\right)\right)\right) \quad 4.15$$

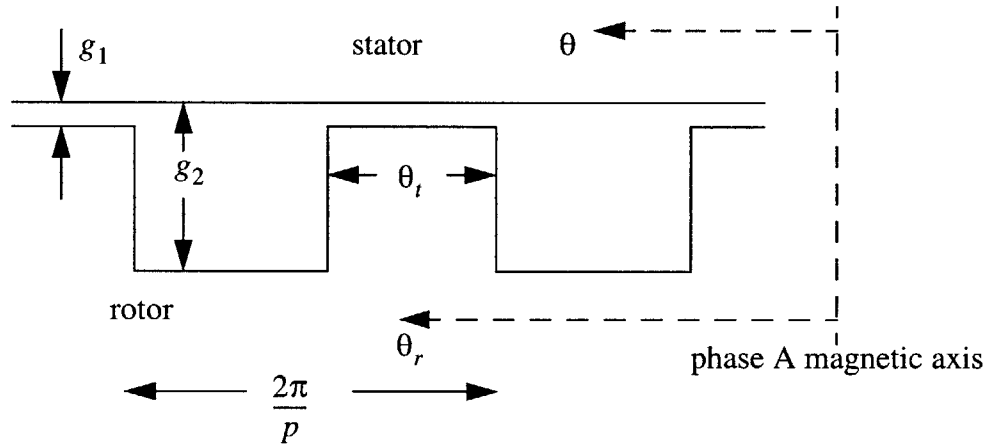


Figure 4.3 Rotor teeth

## 4.1.2 Magnetomotive Forces

### 4.1.2.1 Field MMF

The MMF drop across the air gap due to the field MMF alone could be obtained by analyzing a simplified diagram of the alternator shown in Figure 4.4. Applying Ampere's law on a twisted loop which traverses the same air gap width on both stacks (both teeth or both slots),

$$N_f i_f = 2H_g L_g = 2F_{fL} \quad 4.16$$



where  $F_{fL}$  is the MMF drop across the air gap in the left stack. The MMF is arbitrarily defined as positive going radially outward. Solving for  $F_{fL}$

$$F_{fL} = \frac{N_f i_f}{2} \quad 4.17$$

The MMF drop across the opposite or right stack will have essentially the same form, except for a minus sign

$$F_{fR} = -\frac{N_f i_f}{2} \quad 4.18$$

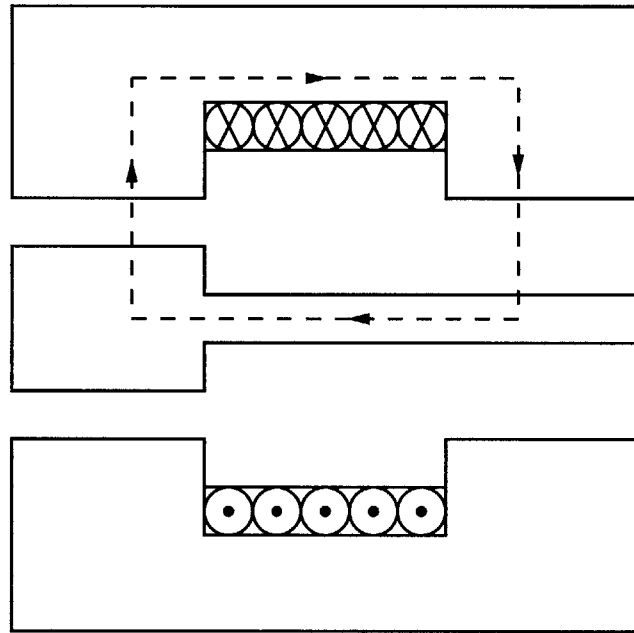


Figure 4.4 Ampere loop used to determine field MMF

#### 4.1.2.2 Stator phase MMF

The MMF distribution due to each phase can be determined by analyzing the winding pattern. The MMF wave per phase is a rectangular wave composed of a fundamental and higher-order odd harmonics. The MMF around the gap due to phase A alone can be expressed as

$$F_a = \sum_{\substack{n=1 \\ n \text{ odd}}}^{\infty} \frac{4}{n\pi} \left( \frac{k_{wn}}{a} \right) \frac{N_s i_a}{2p} \cos(np\theta) \quad 4.19$$

where  $n$  represents the  $n$ th harmonic, and  $N_s$  is the total number of armature turns for each armature phase,  $a$  is the number of parallel windings, and  $k_{wn}$  is the winding factor corresponding to the  $n$ th harmonic. Those for phases B and C lag by  $2\pi/3$  and  $4\pi/3$ , respectively so that

$$F_b = \sum_{\substack{n=1 \\ n \text{ odd}}}^{\infty} \frac{4}{n\pi} \left( \frac{k_{wn}}{a} \right) \frac{N_s i_b}{2p} \cos \left( n \left( p\theta - \frac{2\pi}{3} \right) \right) \quad 4.20$$

$$F_c = \sum_{\substack{n=1 \\ n \text{ odd}}}^{\infty} \frac{4}{n\pi} \left( \frac{k_{wn}}{a} \right) \frac{N_s i_c}{2p} \cos \left( n \left( p\theta + \frac{2\pi}{3} \right) \right) \quad 4.21$$

### 4.1.3 Air Gap Flux Densities

#### 4.1.3.1 Flux Densities due to Field Winding

The air gap flux density in the left-stack air gap due to the field winding alone is

$$B_{fL} = F_{fL} \Lambda_L = \left( \frac{N_f i_f}{2} \right) \left( \sum_{m=0}^{\infty} \Lambda_m \cos(mp(\theta - \theta_r)) \right) \quad 4.22$$

Along the right stack, the uniaxial flux is pointing in the negative direction, and the rotor saliency is skewed by 180 electrical degrees, so the flux density is

$$B_{fR} = F_{fR} \Lambda_R = \left( - \left( \frac{N_f i_f}{2} \right) \right) \left( \sum_{m=0}^{\infty} \Lambda_m \cos mp \left( \theta - \left( \theta_r - \frac{\pi}{p} \right) \right) \right) \quad 4.23$$

#### 4.1.3.2 Flux Densities due to Armature Winding

The flux densities due to each of the stator phases on the left stack are

$$B_{aL} = F_a \Lambda_L = \left( \sum_{\substack{n=1 \\ n \text{ odd}}}^{\infty} \frac{4}{n\pi} \frac{N_s i_a}{2p} \left( \frac{k_{wn}}{a} \right) \cos np\theta \right) \left( \sum_{m=0}^{\infty} \Lambda_m \cos mp(\theta - \theta_r) \right) \quad 4.24$$

$$B_{bL} = F_b \Lambda_L = \left( \sum_{\substack{n=1 \\ n \text{ odd}}}^{\infty} \frac{4}{n\pi} \frac{N_s i_b}{2p} \left( \frac{k_{wn}}{a} \right) \cos n \left( p\theta - \frac{2\pi}{3} \right) \right) \left( \sum_{m=0}^{\infty} \Lambda_m \cos mp(\theta - \theta_r) \right) \quad 4.25$$

$$B_{cL} = F_c \Lambda_L = \left( \sum_{\substack{n=1 \\ n \text{ odd}}}^{\infty} \frac{4 N_s i_c \left( \frac{k_{wn}}{a} \right)}{n\pi 2p} \cos n \left( p\theta + \frac{2\pi}{3} \right) \right) \left( \sum_{m=0}^{\infty} \Lambda_m \cos mp(\theta - \theta_r) \right) \quad 4.26$$

On the right stack, the permeance functions are shifted by 180 electrical degrees thus replacing  $\theta_r$  by  $\theta_r - \pi/p$  in determining  $B_{aR}$ ,  $B_{bR}$ , and  $B_{cR}$ .

$$B_{aL} = F_a \Lambda_R = \left( \sum_{\substack{n=1 \\ n \text{ odd}}}^{\infty} \frac{4 N_s i_a \left( \frac{k_{wn}}{a} \right)}{n\pi 2p} \cos np\theta \right) \left( \sum_{m=0}^{\infty} \Lambda_m \cos mp \left( \theta - \left( \theta_r - \frac{\pi}{p} \right) \right) \right) \quad 4.27$$

$$B_{bL} = F_b \Lambda_R = \left( \sum_{\substack{n=1 \\ n \text{ odd}}}^{\infty} \frac{4 N_s i_b \left( \frac{k_{wn}}{a} \right)}{n\pi 2p} \cos n \left( p\theta - \frac{2\pi}{3} \right) \right) \left( \sum_{m=0}^{\infty} \Lambda_m \cos mp \left( \theta - \left( \theta_r - \frac{\pi}{p} \right) \right) \right) \quad 4.28$$

$$B_{cL} = F_c \Lambda_R = \left( \sum_{\substack{n=1 \\ n \text{ odd}}}^{\infty} \frac{4 N_s i_c \left( \frac{k_{wn}}{a} \right)}{n\pi 2p} \cos n \left( p\theta + \frac{2\pi}{3} \right) \right) \left( \sum_{m=0}^{\infty} \Lambda_m \cos mp \left( \theta - \left( \theta_r - \frac{\pi}{p} \right) \right) \right) \quad 4.29$$

#### 4.1.4 Field Self Inductance

To derive the field winding self-inductance, the flux leaving one stack or entering the other is calculated. Since this same flux links each turn of the field winding, the inductance can be obtained by multiplying this flux by the number of field turns and dividing by the field current

$$\lambda_{ff} = N_f \int_0^{2\pi} B_{fL} L R d\theta = N_f^2 R L \pi \Lambda_o i_f \quad 4.27$$

$$L_{ff} = \frac{\lambda_{ff}}{i_f} = N_f^2 R L \pi \Lambda_o \quad 4.28$$

where  $R$  is the average air gap radius, and  $L$  is the length of one stack.

#### 4.1.5 Armature-Field Mutual Inductance

The armature-field mutual inductance can be calculated by first finding  $\lambda_{af}$ , the flux linked by the armature phase A winding due to the field. Only the fundamental flux linkages are considered. Thus, flux is given by

$$\lambda_{af} = N_s \left( \frac{k_w}{a} \right) \int_{-\frac{\pi}{2p}}^{\frac{\pi}{2p}} B_{fL} LR d\theta + N_s \left( \frac{k_w}{a} \right) \int_{\frac{\pi}{2p}}^{\frac{\pi}{2p}} B_{fR} LR d\theta \quad 4.29$$

where  $k_w$  is the winding factor associated with the first harmonic ( $k_w = k_{w1}$ ). The total flux linked is the flux linked in one side or stack added to that linked in the other. The mutual inductance is obtained by dividing the flux linked  $\lambda_{af}$  by the field current so that

$$L_{af} = \frac{\lambda_{af}}{i_f} = \frac{2N_s N_f RL}{p} \left( \frac{k_w}{a} \right) \left( \sum_{m=1, 5, 9, 13, \dots}^{\infty} \frac{\Lambda_m}{m} \cos mp\theta_r \right) \quad 4.30$$

The 3rd, 7th, 11th, 15th, ... , harmonics are cancelled out due to the presence of two stacks with the permeance functions offset by 180 electrical degrees. For the rest of this chapter, the flux densities will be lumped in one single integral, as opposed to 4.29 with two separate integrals, but will actually mean two different stacks as shown above. The other mutual inductances can be determined in a similar fashion as

$$\lambda_{bf} = N_s \left( \frac{k_w}{a} \right) \int_{\left(\frac{2\pi}{3p} - \frac{\pi}{2p}\right)}^{\left(\frac{2\pi}{3p} + \frac{\pi}{2p}\right)} (B_{fL} + B_{fR}) LR d\theta \quad 4.30$$

$$\lambda_{cf} = N_s \left( \frac{k_w}{a} \right) \int_{\left(\frac{-2\pi}{3p} - \frac{\pi}{2p}\right)}^{\left(\frac{-2\pi}{3p} + \frac{\pi}{2p}\right)} (B_{fL} + B_{fR}) LR d\theta \quad 4.31$$

$$L_{bf} = \frac{\lambda_{bf}}{i_f} = \frac{2N_s N_f RL}{p} \left( \frac{k_w}{a} \right) \left( \sum_{m=1, 5, 9, 13, \dots}^{\infty} \frac{\Lambda_m}{m} \cos m \left( p\theta_r - \frac{2\pi}{3} \right) \right) \quad 4.32$$

$$L_{cf} = \frac{\lambda_{cf}}{i_f} = \frac{2N_s N_f R L}{p} \left( \frac{k_w}{a} \right) \left( \sum_{m=1, 5, 9, 13, \dots}^{\infty} \frac{\Lambda_m}{m} \cos m \left( p\theta_r + \frac{2\pi}{3} \right) \right) \quad 4.33$$

#### 4.1.6 Armature Self and Mutual-Inductances

To calculate the armature self and mutual inductances between phases, the armature flux linkages due to the different armature currents have to be determined. Note that only the fundamental flux linkages are considered. Because of reciprocity, only half the number of armature mutual inductances must be obtained. The armature inductances can be derived as

$$\lambda_{aa} = N_s \left( \frac{k_w}{a} \right) \int_{-\frac{\pi}{2p}}^{\frac{\pi}{2p}} (B_{aL} + B_{aR}) LR d\theta \quad 4.34$$

$$\lambda_{bb} = N_s \left( \frac{k_w}{a} \right) \int_{\left(\frac{2\pi}{3p} - \frac{\pi}{2p}\right)}^{\left(\frac{2\pi}{3p} + \frac{\pi}{2p}\right)} (B_{bL} + B_{bR}) LR d\theta \quad 4.35$$

$$\lambda_{cc} = N_s \left( \frac{k_w}{a} \right) \int_{\left(\frac{-2\pi}{3p} - \frac{\pi}{2p}\right)}^{\left(\frac{-2\pi}{3p} + \frac{\pi}{2p}\right)} (B_{cL} + B_{cR}) LR d\theta \quad 4.36$$

$$L_{aa} = \frac{\lambda_{aa}}{i_a} = \frac{8N_s^2 R L}{\pi p^2} \left( \frac{k_w}{a} \right)^2 \left( \Lambda_o + \frac{\Lambda_2}{2} \cos(2p\theta_r) \right) \quad 4.37$$

$$L_{bb} = \frac{\lambda_{bb}}{i_b} = \frac{8N_s^2 R L}{\pi p^2} \left( \frac{k_w}{a} \right)^2 \left( \Lambda_o + \frac{\Lambda_2}{2} \cos\left(2\left(p\theta_r - \frac{2\pi}{3}\right)\right) \right) \quad 4.38$$

$$L_{cc} = \frac{\lambda_{cc}}{i_c} = \frac{8N_s^2 R L}{\pi p^2} \left( \frac{k_w}{a} \right)^2 \left( \Lambda_o + \frac{\Lambda_2}{2} \cos\left(2\left(p\theta_r + \frac{2\pi}{3}\right)\right) \right) \quad 4.39$$

$$\lambda_{ab} = N_s \left( \frac{k_w}{a} \right) \int_{-\frac{\pi}{2p}}^{\frac{\pi}{2p}} (B_{bL} + B_{bR}) LR d\theta \quad 4.40$$

$$\lambda_{ac} = N_s \left( \frac{k_w}{a} \right) \int_{-\frac{\pi}{2p}}^{\frac{\pi}{2p}} (B_{cL} + B_{cR}) LR d\theta \quad 4.41$$

$$\lambda_{bc} = N_s \left( \frac{k_w}{a} \right) \int_{\left(\frac{2\pi}{3p} - \frac{\pi}{2p}\right)}^{\left(\frac{2\pi}{3p} + \frac{\pi}{2p}\right)} (B_{cL} + B_{cR}) LR d\theta \quad 4.42$$

$$L_{ab} = \frac{\lambda_{ab}}{i_b} = \frac{8N_s^2 RL}{\pi p^2} \left( \frac{k_w}{a} \right)^2 \left( \Lambda_o \left( \frac{-1}{2} \right) + \frac{\Lambda_2}{2} \cos \left( 2p\theta_r - \frac{2\pi}{3} \right) \right) \quad 4.43$$

$$L_{ac} = \frac{\lambda_{ac}}{i_c} = \frac{8N_s^2 RL}{\pi p^2} \left( \frac{k_w}{a} \right)^2 \left( \Lambda_o \left( \frac{-1}{2} \right) + \frac{\Lambda_2}{2} \cos \left( 2p\theta_r + \frac{2\pi}{3} \right) \right) \quad 4.44$$

$$L_{bc} = \frac{\lambda_{bc}}{i_c} = \frac{8N_s^2 RL}{\pi p^2} \left( \frac{k_w}{a} \right)^2 \left( \Lambda_o \left( \frac{-1}{2} \right) + \frac{\Lambda_2}{2} \cos(2p\theta_r) \right) \quad 4.45$$

In equation 4.29 to 4.45, only fundamental flux linkages are calculated. The associated voltages correspond to the fundamental.

#### 4.1.7 Leakage Inductance

Not all the flux produced by the armature windings ends up as useful flux in the air gap. Some of it crosses the slots of the stator and ends up as leakage flux. This leakage flux contributes to what is called leakage inductance. Other forms of leakage inductance will be ignored.

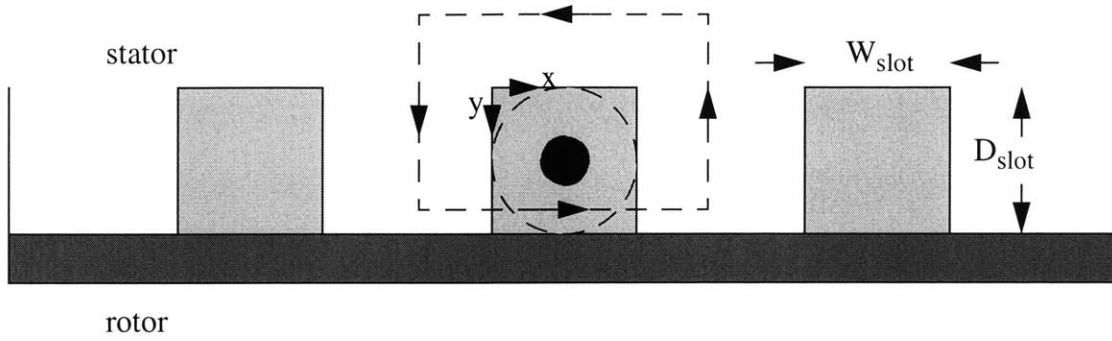


Figure 4.5 Stator slot diagram

By analyzing one slot and applying Ampere's Law as illustrated in Figure 4.3,

$$H_x W_{slot} = \left(\frac{N_s}{2p}\right) \left(\frac{I_s}{a}\right) \left(\frac{y}{D_{slot}}\right) \quad 4.46$$

where  $W_{slot}$  and  $D_{slot}$  are the width and depth of a slot respectively,  $N_s/2p$  is the number of series armature turns per pole, and  $H_x$  is the magnetic field crossing the slot. It is assumed for purposes of calculation that the permeability of iron is infinite. Having calculated the magnetic field intensity, the total energy stored in the slots can be computed. This is done by determining the energy in one slot and multiplying it by the number of slots containing the same phase.

$$E = \left[ (2L) W_{slot} \int_0^{D_{slot}} \frac{1}{2} \mu_o H_x^2 dy \right] \left(\frac{n_{sp}}{3}\right) (2p) = \frac{1}{2} L_l I_s^2 \quad 4.47$$

where  $n_{sp}$  is the number of stator slots per pole. From this equation, the leakage inductance

$$L_l = \frac{\mu_o (2L) D_{slot}}{3 W_{slot}} \left(\frac{N_s}{2p}\right)^2 \left(\frac{1}{a}\right) \left(\frac{n_{sp}}{3}\right) (2p) \quad 4.48$$

is obtained.

#### 4.1.8 Winding Factor

Since the armature windings are not concentrated, the MMFs produced by the armature currents of the same phase which are in separate slots are displaced from each other by the electrical angle between slots. Also, the fluxes linked by the coils of the same phase in different slots will be phase displaced from each other by the electrical angle between slots. Thus the total flux linkage for each phase when the windings are distributed will be less than that obtained when they are

concentrated. This is accounted for by the breadth factor. Since the pitch factor is unity for the particular winding pattern being used, the winding factor equals the breadth factor alone. The winding factor associated with the  $n$ th harmonic can be expressed as

$$k_{wn} = \frac{\sin\left(\frac{nm_{spp}\gamma}{2}\right)}{m_{spp}\sin\left(\frac{n\gamma}{2}\right)} \quad 4.49$$

where  $m_{spp} = \frac{n_{sp}}{3}$  is the number of slots per pole per phase, and  $\gamma = \frac{180^\circ}{n_{sp}}$  is the number of electrical degrees between slots. Since only the first harmonic flux linkages and voltages are considered, only  $k_{w1}$  will survive in the equations, which is also represented by  $k_w$ .

#### 4.1.9 Inductance Matrix

Having derived all the inductances, the flux linkage equations are complete. They can be assembled in vector matrix form according to

$$\begin{bmatrix} \lambda_a \\ \lambda_b \\ \lambda_c \\ \lambda_f \end{bmatrix} = \begin{bmatrix} L_o + L_2 \cos 2p\theta_r + L_l & -0.5L_o + L_2 \cos\left(2p\theta_r - \frac{2\pi}{3}\right) & -0.5L_o + L_2 \cos\left(2p\theta_r + \frac{2\pi}{3}\right) & L_{afm} \cos p\theta_r \\ -0.5L_o + L_2 \cos\left(2p\theta_r - \frac{2\pi}{3}\right) & L_o + L_2 \cos\left(2\left(p\theta_r - \frac{2\pi}{3}\right)\right) + L_l & -0.5L_o + L_2 \cos 2p\theta_r & L_{afm} \cos\left(p\theta_r - \frac{2\pi}{3}\right) \\ -0.5L_o + L_2 \cos\left(2p\theta_r + \frac{2\pi}{3}\right) & -0.5L_2 + L_2 \cos 2p\theta_r & L_o + L_2 \cos\left(2\left(p\theta_r + \frac{2\pi}{3}\right)\right) + L_l & L_{afm} \cos\left(p\theta_r + \frac{2\pi}{3}\right) \\ L_{afm} \cos(p\theta_r) & L_{afm} \cos\left(p\theta_r - \frac{2\pi}{3}\right) & L_{afm} \cos\left(p\theta_r + \frac{2\pi}{3}\right) & L_{ff} \end{bmatrix} \begin{bmatrix} i_a \\ i_b \\ i_c \\ i_f \end{bmatrix} \quad 4.50$$

where

$$L_o = \frac{8N_s^2 RL}{\pi p^2} \left(\frac{k_w}{a}\right)^2 \Lambda_o \quad 4.51$$

$$L_2 = \frac{4N_s^2 RL}{\pi p^2} \left(\frac{k_w}{a}\right)^2 \Lambda_2, \quad 4.52$$

$$L_{afm} = \frac{2N_s N_f RL}{p} \left(\frac{k_w}{a}\right) \quad 4.53$$



A similar derivation was made in [11]. Note that for the armature-field mutual inductance, the higher harmonics are ignored.

#### 4.2 Direct and Quadrature Reactances

For the purpose of finding the equivalent reactance of the alternator, a  $DQ\phi$ -transformation is applied. The transformation translates the reference frame from one on the stator to one that is synchronous with the rotor. As the transformation is applied here, the quadrature axis leads the direct axis with the direct-axis aligned with the rotor position  $p\theta_r$ . The rotor angle  $\theta_r$  is zero when the tooth is aligned with the stator phase A axis. The Park power-invariant transformation taken from [8] is used

$$\begin{bmatrix} S_d \\ S_q \\ S_o \end{bmatrix} = \sqrt{\frac{2}{3}} \begin{bmatrix} \cos(p\theta_r) & \cos\left(p\theta_r - \frac{2\pi}{3}\right) & \cos\left(p\theta_r + \frac{2\pi}{3}\right) \\ -\sin(p\theta_r) & -\sin\left(p\theta_r - \frac{2\pi}{3}\right) & -\sin\left(p\theta_r + \frac{2\pi}{3}\right) \\ \frac{1}{\sqrt{2}} & \frac{1}{\sqrt{2}} & \frac{1}{\sqrt{2}} \end{bmatrix} \begin{bmatrix} S_a \\ S_b \\ S_c \end{bmatrix} \quad 4.54$$

The symbol  $S$  in the matrix represents any electrical variable. Examples of these are flux linkages, currents, and voltages. The electrical variable in phases a,b, and c is converted to its equivalent with d,q, and zero sequence (o) components in the rotating frame. As stated earlier, balanced operation is used. From Faraday's law, the back-emf of each phase is the time derivative of the field flux linked by that phase. Thus,

$$E_{af} = \frac{d\lambda_{af}}{dt} \quad , \quad E_{bf} = \frac{d\lambda_{bf}}{dt} \quad , \quad E_{cf} = \frac{d\lambda_{cf}}{dt} \quad 4.55$$

The currents in the armature winding are expressed as

$$i_a = I_s \sin(p\theta_r - \theta_i) \quad 4.56$$

$$i_b = I_s \sin\left(p\theta_r - \theta_i - \frac{2\pi}{3}\right) \quad 4.57$$

$$i_c = I_s \sin\left(p\theta_r - \theta_i + \frac{2\pi}{3}\right) \quad 4.58$$

The angle  $\theta_i$  is the internal power angle and is the angle by which the armature currents (using the generator convention) lag the back-emf. Using the flux linkage equations in 4.50 , the flux linkages  $\lambda_a$ ,  $\lambda_b$ , and  $\lambda_c$  are derived when there is no field excitation. In this case

$$\lambda_a = \frac{3}{2}(L_o \sin(p\theta_r - \theta_i) - L_2 \sin(p\theta_r + \theta_i))I_s \quad 4.59$$

$$\lambda_b = \frac{3}{2}\left(L_o \sin\left(p\theta_r - \theta_i - \frac{2\pi}{3}\right) - L_2 \sin\left(p\theta_r + \theta_i - \frac{2\pi}{3}\right)\right)I_s \quad 4.60$$

$$\lambda_c = \frac{3}{2}\left(L_o \sin\left(p\theta_r - \theta_i + \frac{2\pi}{3}\right) - L_2 \sin\left(p\theta_r + \theta_i + \frac{2\pi}{3}\right)\right)I_s \quad 4.61$$

Using the DQ-transformation,  $\lambda_d$ ,  $\lambda_q$ ,  $i_d$ , and  $i_q$  can be determined

$$\lambda_d = \frac{-3I_s}{2\sqrt{2}}(L_o + L_2)\sin\theta_i \quad 4.62$$

$$\lambda_q = \frac{-3I_s}{2\sqrt{2}}(L_o - L_2)\cos\theta_i \quad 4.63$$

$$i_d = \frac{-I_s}{\sqrt{2}}\sin\theta_i \quad 4.64$$

$$i_q = \frac{-I_s}{\sqrt{2}}\cos\theta_i \quad 4.65$$

from which  $L_d$  and  $L_q$  can be determined

$$L_d = \frac{\lambda_d}{i_d} = \frac{3}{2}(L_o + L_2) + L_l \quad 4.66$$

$$L_q = \frac{\lambda_q}{i_q} = \frac{3}{2}(L_o - L_2) + L_l \quad 4.67$$

$$L_o = L_l \quad 4.68$$

With a rotor pole fraction of a half ( $\beta = 0.5$ ), the inductance due to the second harmonic permeance term is zero, the direct- and quadrature synchronous inductances are equal ( $L_d = L_q$ ), and the alternator becomes a cylindrical air gap alternator. An HIA with rotor slots as wide as its rotor poles can be analyzed using a cylindrical air gap machine model. This is a result of having

the slots and poles on opposite stacks skewed by 180 electrical degrees. Any angular location which faces rotor slot on one stack aligns with a rotor pole on the other stack.

Again, using the flux linkage equations in 4.50,  $\lambda_a$ ,  $\lambda_b$ , and  $\lambda_c$  can be derived when the armature windings are open circuited, thus showing only the effects of the field winding.

$$\lambda_a = L_{afm} \cos(p\theta_r) i_f \quad 4.69$$

$$\lambda_b = L_{afm} \cos\left(p\theta_r - \frac{2\pi}{3}\right) i_f \quad 4.70$$

$$\lambda_c = L_{afm} \cos\left(p\theta_r + \frac{2\pi}{3}\right) i_f \quad 4.71$$

$$\lambda_d = \sqrt{\frac{3}{2}} L_{afm} i_f \quad 4.72$$

$$L_{df} = \sqrt{\frac{3}{2}} L_{afm} \quad 4.73$$

The flux linkage equations in the rotating frame can be summarized as

$$\begin{bmatrix} \lambda_d \\ \lambda_q \\ \lambda_f \end{bmatrix} = \begin{bmatrix} L_d & 0 & L_{df} \\ 0 & L_q & 0 \\ L_{df} & 0 & L_{ff} \end{bmatrix} \begin{bmatrix} i_d \\ i_q \\ i_f \end{bmatrix} \quad 4.74$$

The zero sequence component can be ignored assuming balanced loads and using a Wye configuration. The convention used for the flux linkage equations is still for motoring. The third equation of 4.74 is derived from the fourth equation of 4.50 in the fixed reference frame flux linkage equations

$$\lambda_{ff} = L_{afm} \cos(p\theta_r) i_a + L_{afm} \cos\left(p\theta_r - \frac{2\pi}{3}\right) i_b + L_{afm} \cos\left(p\theta_r + \frac{2\pi}{3}\right) i_c + L_{ff} i_f \quad 4.75$$

where it can be recognized that

$$\sqrt{\frac{3}{2}} i_d = i_a \cos(p\theta_r) + i_b \cos\left(p\theta_r - \frac{2\pi}{3}\right) + i_c \cos\left(p\theta_r + \frac{2\pi}{3}\right) \quad 4.76$$

so that  $L_{afm}$  can be factored out of 4.75 and the 3rd equation in 4.74 can be obtained.

## 4.3 Resistances

### 4.3.1 Field Resistance

The resistance of a conductor is modeled by

$$R = \frac{l}{\sigma A} \quad 4.77$$

where  $l$  is the length of the conductor,  $\sigma$  is its conductivity, and  $A$  is the cross-sectional area of the conductor. This may be directly applied to the field winding, resulting in the resistance

$$R_{field} = \frac{N_f \left( \frac{2\pi(R_{statbotrad} + R_{statslotbot})}{2} \right)}{\sigma_{Cu} A_{armwire}} \quad 4.78$$

where  $R_{statbot}$  is the radius to the stator bottom, and  $R_{statslotbot}$  is the radius to the bottom of the stator slot. The relation

$$A_{fieldslot} k_{pf} = A_{fieldwire} N_f \quad 4.79$$

holds between the field wire cross-sectional area ( $A_{fieldwire}$ ), and the housing or slot area for the field ( $A_{fieldslot}$ ), where the area for the field slot is

$$A_{fieldslot} = (R_{statbot} - R_{statslotbot}) L_{interstack}$$

The final expression for the field resistance is

$$R_{field} = \frac{N_f^2 \left( 2\pi \left( \frac{R_{statbot} + R_{statslotbot}}{2} \right) \right)}{\sigma_{Cu} (k_{pf}) (R_{statbot} - R_{statslotbot}) L_{interstack}} \quad 4.80$$

where  $k_{pf}$  is the packing factor and  $L_{interstack}$  is the length in between stacks.

### 4.3.2 Armature Resistance

To determine the armature resistance, the resistance of each turn in parallel is divided by the number of wires in parallel. Thus,

$$R_{arm} = \frac{\left( \frac{N_s L_{oneturn}}{a} \right)}{\sigma A_{armwire}} \left( \frac{1}{a} \right) \quad 4.81$$

where  $A_{armwire}$  is the cross-sectional area of each wire, and  $L_{oneturn}$  is the length of one turn. The numerator in 4.80 is the equivalent length of each one of the wires in parallel. Next, apply the relation

$$A_{armslot} k_{pf} = A_{armwire} n_{turnperslot} \quad 4.82$$

where  $A_{slot}$  is the cross-sectional area of each slot,  $n_{turnsper slot}$  is the number of turns per slot and is equal to  $N_s/(2p)$ . The resistance per phase of the armature winding is then

$$R_{arm} = \frac{(N_s L_{oneturn}) \left( \frac{N_s}{2p} \right) \left( \frac{1}{a} \right)}{\sigma_{Cu} (k_{pf}) (A_{arm slot})} \quad 4.83$$

#### 4.4 Summary

The important lumped parameter elements are the armature-field mutual inductance, found in 4.52, the direct-and quadrature-axis inductances found in 4.65 and 4.66, and the field and armature resistances found in 4.78 and 4.81. The armature-field mutual inductance is used to relate the field current to the back-emf. The direct- and quadrature-axis inductances, and armature resistance are used to determine the equivalent armature circuit. The resistances are also used for calculating conduction losses.

## Chapter 5

### Equivalent Circuit

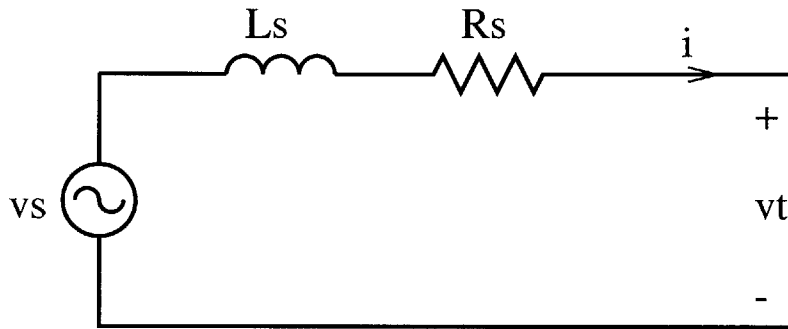


Figure 5.1 Equivalent unloaded armature circuit (single-phase)

The transformation of electrical variables to the DQ frame resulted in expressions for the direct and quadrature reactances. From these reactances, an equivalent circuit for the machine shown in Figure 5.1 can be obtained. This will be shown using two methods. The first is based on a phasor analysis. The second is based on what can be called term-matching, which is elaborated on later.

#### 5.1 Equivalent armature reactance and resistance

##### 5.1.1 Phasor Analysis

Since the inductor alternator can be analyzed as a salient-pole machine, a phasor diagram typical for a salient-pole machine will be used. The phasor diagram for a single phase of the generator is shown in Figure 5.2 where  $\hat{E}_{af}$  is the back-emf,  $\hat{V}$  is the terminal voltage,  $\hat{I}$  is the armature current (generator convention),  $\hat{I}_d = \hat{I} \sin \theta_i$  is the direct-axis current,  $\hat{I}_q = \hat{I} \cos \theta_i$  is the quadrature-axis current,  $r_a$  is the armature resistance,  $X_d$  is the direct-axis reactance, and  $X_q$  is the quadrature-axis reactance. The diagram taken from [8] shows that the excitation voltage or back-emf is equal to the sum of the terminal voltage, the resistive drop, and the direct- and quadrature-reactance voltage drops. The angle  $\psi$  is the external power angle, and  $\theta_i$  is the internal power angle or the angle by which the armature current lags the back voltage. Following an analysis of the circuit when connected through a rectifier to a constant voltage load [9], the internal power angle can be found analytically.



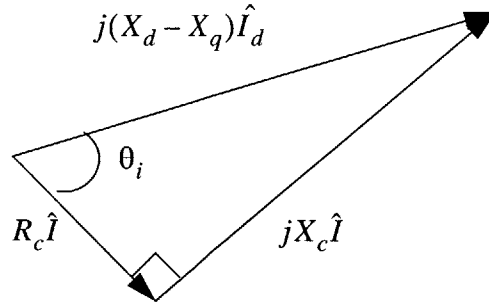


Figure 5.3 Phasor diagram used for determining equivalent circuit

From Figure 5.3, the phasor  $j(X_d - X_q)\hat{I}_d$  can be decomposed into a sum of two orthogonal phasors as

$$j(X_d - X_q)\hat{I}_d = R_c\hat{I} + jX_c\hat{I} \quad 5.4$$

The equivalent resistance  $R_c$  and reactance  $X_q + X_c$  due to armature reaction can be found using the steps that follow. The Pythagorean theorem can be used to show that

$$\sqrt{(R_c^2 + X_c^2)}\hat{I} = (X_d - X_q)\hat{I}_d \quad 5.5$$

where as shown earlier

$$\hat{I}_d = \hat{I} \sin \theta_i \quad 5.6$$

Also, a relation between the internal power angle and the two sides of the right triangle can be found

$$\tan \theta_i = \frac{X_c \hat{I}}{R_c \hat{I}} \quad 5.7$$

These equations yield the values of the equivalent resistance and reactance due to armature reaction

$$R_c = \left( \frac{X_d - X_q}{2} \right) \sin 2\theta_i \quad 5.8$$



$$X_s = X_q + X_c = X_q + \left( \left( \frac{X_d - X_q}{2} \right) - \left( \frac{X_d - X_q}{2} \right) \cos 2\theta_i \right) = \left( \frac{X_d + X_q}{2} \right) - \left( \frac{X_d - X_q}{2} \right) \cos 2\theta_i \quad 5.9$$

The equivalent unloaded circuit for a single phase of the alternator can be shown in Figure 5.1

where  $R_s = r_a + R_c$ , and the synchronous inductance is,  $L_s = \frac{X_s}{\omega}$ , where  $\omega$  is the stator electrical frequency, and  $v_s$  is the back-emf in the time domain. The elements shown in the circuit are equivalent elements. The resistor  $R_c$  is actually a generating term corresponding to the reluctance torque. It can either produce or consume electrical energy. It can assume both negative and positive values.

### 5.1.2 Term-matching

The second approach to determining  $R_s$  and  $L_s$  is to determine the flux linked in a single phase due to the combined effect of the three-phase armature currents, then determine the back-emf as the time derivative of the flux linkage. The back-emf can then be broken down into an in phase and out of phase part. The combined MMF due to all three phases is

$$F = F_a + F_b + F_c \quad 5.10$$

$$F = \sum_{n=1, 7, 13, \dots, 6k+1}^{\infty} \left( \frac{3}{2} \right) \frac{4 N_s I_s k_{wn}}{n\pi 2p} \frac{1}{a} \sin(p\theta_r - \theta_i - np\theta) + \sum_{n=5, 12, \dots, 6k-1}^{\infty} \left( \frac{3}{2} \right) \frac{4 N_s I_s k_{wn}}{n\pi 2p} \frac{1}{a} \sin(p\theta_r - \theta_i + np\theta) \quad 5.11$$

The flux density in the left stack due to the three-phase armature currents is

$$B_L = F \Lambda_L \quad 5.12$$

The fundamental flux density is a function of the fundamental MMF wave ( $n$  equals one), and the zeroth and second harmonic components of the permeance function ( $m$  equals zero or two).

This can be expressed as

$$B_{1L} = \left( \frac{3}{2} \right) \frac{4 N_s I_s k_w}{\pi 2p} \frac{1}{a} \left( \Lambda_o \sin(p(\theta_r - \theta) - \theta_i) - \frac{\Lambda_2}{2} \sin(p(\theta_r - \theta) + \theta_i) \right) \quad 5.13$$

The fundamental flux density in the right stack is the same despite the offset because the effective permeance function for the right side equals that for the left when  $m$  is equal to zero or two. Therefore,

$$B_{1R} = B_{1L} \quad 5.14$$

The flux linked in phase A due to the balanced armature currents is

$$\lambda_a = N_s \frac{k_w}{a} \int_{-\frac{\pi}{2p}}^{\frac{\pi}{2p}} (B_{1L} + B_{1R}) LR d\theta \quad 5.15$$

Using the relation  $p\theta_r = \omega t + \delta$ , where  $\delta$  is the initial rotor angle in electrical degrees, the back-emf of phase a is

$$\frac{d\lambda_a}{dt} = \frac{3}{2}\omega(L_o - L_2 \cos 2\theta_i)(I_s \cos(\omega t + \delta - \theta_i)) + \frac{3}{2}\omega(L_2 \sin 2\theta_i)(I_s \sin(\omega t + \delta - \theta_i)) \quad 5.16$$

This time derivative of flux linkage can also be represented as a voltage drop across an inductor and a resistor in series such that

$$\frac{d\lambda_a}{dt} = \frac{X_s di_a}{\omega dt} + R_c i_a \quad 5.17$$

Then, using term-by-term matching, the effective reactance and resistance due to armature reaction can be found.

$$X_s = \frac{3}{2}\omega(L_o - L_2 \cos 2\theta_i) \quad 5.18$$

$$R_c = \frac{3}{2}\omega L_2 \sin 2\theta_i \quad 5.19$$

This result agrees with the values obtained in part 5.1.

## 5.2 Equivalent Load

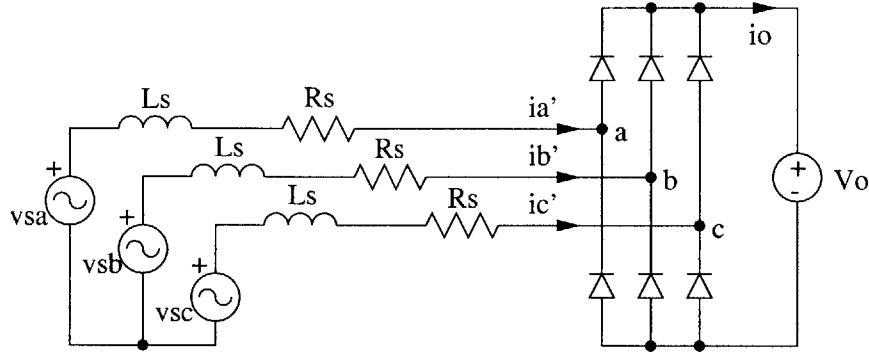


Figure 5.4 Complete three-phase circuit

The three-phase alternator circuit is connected to a three-phase bridge rectifier with a constant-voltage load at the output as shown in Figure 5.4. As stated earlier, the currents are assumed to be balanced and sinusoidal. This particular circuit has been analyzed in [9]. The following useful results are taken from [9]. The three-phase bridge rectifier with a constant voltage load can be converted into a set of balanced resistive loads as shown in Figure 5.5.

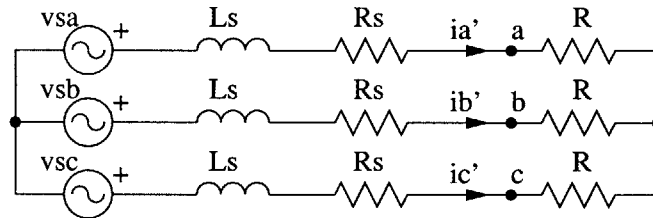


Figure 5.5 Equivalent three-phase circuit

Each resistance has the value

$$R = \frac{\left(\frac{4V_{hll}}{\pi}\right)R_s + \sqrt{X_s^2\left(V_s^2 - \left(\frac{4V_{hll}}{\pi}\right)^2\right) + R_s^2V_s^2}}{V_s^2 - \left(\frac{4V_{hll}}{\pi}\right)^2} \quad 5.20$$

where  $V_{hll}$  is half the line-to-line voltage  $= (V_o + 2V_d)/2$ ,  $V_s$  is the amplitude of the field excitation voltage (back-emf),  $V_o$  is the constant load voltage of 42 V, and  $V_d$  is the voltage drop across a

diode. If the armature resistance  $R_s$  is ignored ( $R_s=0$ ), the power angle can be explicitly obtained as

$$\theta_i = \arctan\left(\frac{X_s}{R}\right) = \arccos\left(\frac{4V_{hll}}{\pi V_s}\right) \quad 5.21$$

This power angle is independent of the equivalent reactance and load resistance. The equivalent reactance can be found using this power angle.

If the armature resistance is not ignored, the power angle can be expressed as

$$\tan(\theta_i) = \left(\frac{X_s}{R + R_s}\right) \quad 5.22$$

The load resistance  $R$  is a function of  $V_s$  and  $\theta_i$  while  $X_s$  and  $R_s$  are both functions of  $\theta_i$ . Numerical methods must be used to determine the internal power angle  $\theta_i$ .

The amplitude of armature current can be found as

$$I_s = \frac{V_s}{\sqrt{X_s^2 + (R + R_s)^2}} \quad 5.23$$

from which the average current at the output of the rectifier can be found to be

$$\langle i_o \rangle = \frac{3}{\pi} I_s \quad 5.24$$

Given this average output current, the average power at the output of the rectifier is found

$$P_{gross} = V_o \langle i_o \rangle \quad 5.25$$

## Chapter 6

### Alternator Design

#### 6.1 Meeting the Electrical and Mechanical Requirements

Given the complete lumped-parameter model, the next stage of the design process involves designing the alternator such that all the electrical and mechanical requirements are met. In order to meet some of the mechanical requirements, the dimensions which are randomly generated will be constrained to be within the allowable limits. The alternator will then be designed such that the electrical requirements are met. However, there are some dimensions that will be determined after some of the electrical properties are obtained. If these dimensions do not meet the mechanical specifications, then the particular machine being evaluated will be discarded. Other specifications that must be met include the power, efficiency, saturation (flux density), and thermal (winding current density) requirements.

##### 6.1.1 Power Requirement

Although the net output power must be at least 4 kW at 600 rpm, increasing linearly to 6 kW at 6000 rpm, only the power outputs at the engine speeds of 600 rpm and 6000 rpm are evaluated when designing the alternator. The gross power at the output of the rectifier must be at least the sum of the net required output power and the field losses. The power required for the field winding is considered as separate from the power required for the loads. The required gross output power for the alternator is therefore

$$P_{gross} = P_{net} + P_{fieldloss} \quad 6.1$$

Since the power dissipated in the field winding is resistive in nature, using Equation 5.26, the gross output power requirement can be expressed as

$$V_o \langle i_o \rangle = P_{net} + i_f^2 R_{field} \quad 6.2$$

The field current determines how much back voltage is induced:

$$V_s = \omega L_{afm} i_f \quad 6.3$$

Based on the analysis made in [9], if the equivalent series armature resistance is ignored, the amplitude of the armature phase current is

$$I_s = \frac{3}{\pi} \frac{\sqrt{V_s^2 - \left(\frac{2V_o + 4V_d}{\pi}\right)^2}}{X_s} \quad 6.4$$

To obtain  $X_s$ , an expression for  $\cos 2\theta_i$  must be found. Equation 5.22 yields

$$\cos 2\theta_i = 2(\cos \theta_i)^2 - 1 = 2\left(\frac{4V_{hll}}{\pi V_s}\right)^2 - 1 \quad 6.5$$

From Equations 6.5 and 5.8, the back-emf can be determined

$$\frac{3}{\pi} \frac{\sqrt{V_s^2 - \left(\frac{2V_o + 4V_d}{\pi}\right)^2}}{\left(\left(\frac{X_d + X_q}{2}\right) - \frac{(X_d - X_q)}{2} \left(2\left(\frac{4V_{hll}}{\pi V_s}\right)^2 - 1\right)\right)} = \frac{P_{out}}{V_o} + \left(\frac{V_s}{\omega L_{afm}}\right)^2 R_{field} \quad 6.6$$

The above calculations result in approximations to the back-emf and power angle because the series resistance is ignored. These are used for the broad search. For the refined search, however, the exact back-emf and power angles are obtained using Newton's Method. In this case, Equations 5.23 and 5.24 are used instead of 6.4 and 6.5 as expressions for the armature phase current and power angle, respectively. The approximate analysis is used during the broad search because the exact calculations slow down the analysis considerably. Also, the back-emf and power angle approximations are fairly reliable such that the machines from the broad search can be slightly modified to obtain satisfactory machines when the exact calculations are made.

### 6.1.2 Efficiency

At the internal operating point of 1500 rpm engine speed, which is around cruising speed, and a net output power of 3250 watts, the alternator must be at least 75% efficient. The efficiency of an alternator can be defined as the output electrical power divided by the input mechanical power. Since the input power is equal to the sum of the output power and the losses, percentage efficiency can be expressed as

$$\eta = \frac{P_{net}}{P_{net} + P_{loss}} \times 100 \quad 6.7$$

where  $P_{net}$  is the net output electrical power, and  $P_{loss}$  is the total amount of losses. Initially, the losses that were thought to be significant were the copper (winding), iron (eddy current), and diode losses. However, it was found that the iron losses could be ignored. Recall that the alternator is composed of a solid rotor, laminated stator teeth and a solid back iron. The stator teeth are laminated in order to minimize losses due to eddy currents which result from alternating flux in the teeth. Since the rotor is solid and is subject to high frequency flux, which is a result of modulation due to the stator teeth, the rotor iron losses were first assumed to be significant. However, following a thorough analysis, the rotor iron losses were found to be negligible. The supporting calculations can be found in Appendix D. Thus, only the copper and diode losses are included in the final design process. The total losses can be expressed as

$$P_{loss} = P_{copperloss} + P_{diodeloss} \quad 6.8$$

### 6.1.2.1 Copper Losses

The copper losses due to both the field and armature winding are resistive in nature. This makes determining them relatively straightforward. The field losses are

$$P_{fieldloss} = i_f^2 R_{field} \quad 6.9$$

The armature losses are due to the sinusoidal three-phase armature currents:

$$P_{armatureloss} = \frac{3}{2} I_s^2 R_{arm} \quad 6.10$$

The total copper losses are therefore

$$P_{copperloss} = P_{fieldloss} + P_{armatureloss} \quad 6.11$$

### 6.1.2.2 Diode Losses

The diode losses are the power dissipated in the diodes of the rectifier. Since two diodes are on at any particular instant, and the average current that flows through them is  $\langle i_o \rangle$ , the power dissipated in the diodes can be expressed as

$$P_{diodeloss} = 2V_d \langle i_o \rangle \quad 6.12$$

### 6.1.3 Flux Density Requirement (Saturation)

Since steel saturates as its flux density is increased beyond some point, with a resultant increase in losses, a limit is imposed on the steel flux density. Based on the magnetization curve

for M-19 steel, a maximum flux density of 1.8 T is set in order to avoid saturation. The machine is dimensioned in order to avoid saturating steel. The parts of the alternator can be analyzed separately.

### 6.1.3.1 Centerpiece

The centerpiece must have a cross-sectional area wide enough in order to carry the axially directed flux due to the field winding. The flux through the centerpiece is

$$\lambda_{cp} = B_{cpa}A_{cp} = N_f i_f RL\Lambda_o\pi \quad 6.13$$

where  $B_{cpa}$  is the flux density directed axially through the centerpiece and  $A_{cp}$  is the cross-sectional area of the center-piece. The cross-sectional area of the centerpiece is

$$A_{cp} = \pi(R_{rotslotbot}^2 - R_{inner}^2) \quad 6.14$$

Solving for the inner radius yields

$$R_{inner} = \sqrt{R_{rotslotbot}^2 - \frac{N_f i_f RL\Lambda_o}{B_{cpa}}} \quad 6.15$$

Substituting for  $B_{cpa}$  the maximum value of 1.8 T would yield the maximum inner radius that can be used.

Another constraint that must be satisfied when determining the inner radius is that the centerpiece must be wide enough to carry the flux in the azimuthal direction from a half-pole in the air gap. In order to solve this problem, the maximum flux density possible in the air gap must be calculated. This occurs when the combined MMFs due to the armature currents is a maximum. The maximum armature MMF is

$$F_{smax} = \frac{3N_s I_s}{2} \left(\frac{1}{a}\right) \quad 6.16$$

The maximum MMF due to the field is constant as shown previously in Equation 4.17 or 4.18.

The maximum flux density occurs when the air gap width is a minimum, that is when

$$\Lambda = \frac{\mu_o}{g_1} \quad 6.17$$

The maximum flux density in the air gap is then

$$B_{airgap} = \left(\frac{N_f i_f}{2} + \frac{3N_s I_s}{2} \left(\frac{1}{a}\right)\right) \left(\frac{\mu_o}{g_1}\right) \quad 6.18$$



Assuming that all the flux spanning a half pole from the air gap traverses the centerpiece in the azimuthal direction,

$$B_{airgap}LR\left(\frac{2\pi}{4p}\right) = B_{cpl}T_{cp}L \quad 6.19$$

where  $B_{cpl}$  is the flux density directed laterally, and  $T_{cp}$  is the thickness of the centerpiece.

The minimum width  $T_{cp}$  can be obtained when  $B_{apl}$  assumes the maximum allowable value of 1.8 T. Thus

$$T_{cp} = \frac{B_{airgap}R}{B_{cpl}}\left(\frac{\pi}{2p}\right) \quad 6.20$$

The inner radius must be at most

$$R_{inner} = R_{rotslotbot} - T_{cp} \quad 6.21$$

In order to satisfy both constraints, the smaller of the two inner radii obtained from Equation 6.15 and 6.21 is used.

### 6.1.3.2 Rotor Poles

A limit must be set on the rotor tooth fraction such that the neck or base of each rotor pole is not saturated. This problem can be solved by assuming the worst case situation were the air gap flux over each pole traverses the base of each pole.

$$B_{airgap}LR\left(\frac{2\pi}{2p}\right) = B_{rottoothbase}LR_{rotslotbot}\left(\frac{2\pi}{p}\beta\right) \quad 6.22$$

where  $\beta$  is the rotor tooth fraction. The flux density at the base of each rotor pole is therefore

$$B_{rottoothbase} = \frac{B_{airgap}R}{2R_{rotslotbot}\beta} \quad 6.23$$

This value must be less than 1.8 T.

### 6.1.3.3 Stator Yoke and Back-iron

The stator yoke is the solid steel from the stator bottom radius to the machine's outer radius. The stator back-iron is the laminated steel between the rotor slot bottom and the stator bottom. The flux due to the field passes radially through the back-iron and then is directed axially through the stator yoke.

The stator back-iron must be wide enough to carry the air gap flux which traverses it in the circumferential direction. This is done by equating the flux through a half-pole in the air gap and the back iron. This yields

$$B_{airgap}LR\left(\frac{2\pi}{4p}\right) = B_{bil}T_{bi}L \quad 6.24$$

where  $B_{airgap}$  is the amplitude of the flux density in the air gap,  $B_{bil}$  is the flux density in the back-iron flowing laterally, and  $T_{bi}$  is the back-iron thickness. This yields a thickness which must also be met by the centerpiece as shown earlier. This results in a back-iron thickness of

$$T_{bi} = \frac{B_{airgap}R}{B_{bil}}\left(\frac{\pi}{2p}\right) \quad 6.25$$

Substituting in 1.8 tesla for  $B_{bil}$  will give the minimum back-iron thickness allowable. The minimum outer radius is:

$$R_{statbot} = T_{bi} + R_{statslotbot} \quad 6.26$$

The stator yoke must have a cross-sectional area wide enough to carry the uniaxial flux due to the field. The constraint is similar to that used for the centerpiece. The uniaxial flux through the stator yoke is

$$\lambda_{bi} = B_{bia}A_{bi} = N_f i_f R L \Lambda_o \pi \quad 6.27$$

where  $B_{bia}$  is the flux density directed axially in the stator yoke and

$$A_{bi} = \pi(R_{outer}^2 - R_{statbot}^2) \quad 6.28$$

The outer radius is then obtained as

$$R_{outer} = \sqrt{\frac{N_f i_f R L \Lambda_o}{B_{bi}} + R_{statbot}^2} \quad 6.29$$

#### 6.1.3.4 Stator Teeth

The stator teeth are more easily saturated since they are relatively narrow and each tooth has to carry the flux spanning a tooth pitch. This is expressed as

$$B_{airgap}R\theta_{toothslot}L = B_{tooth}R\theta_{tooth}L \quad 6.30$$

where  $\theta_{stattooth}$  is the angle spanning a stator tooth, and  $\theta_{stattoothslot}$  is the tooth pitch.

The tooth flux density can be obtained from the air gap flux density as

$$B_{tooth} = B_{airgap} \frac{\theta_{stattoothslot}}{\theta_{stattooth}} \quad 6.31$$

The obtained tooth flux density must be below the upper limit of 1.8 T. This means that the stator teeth must be wide enough to allow flux to pass through.

#### 6.1.4 Thermal Limits

Instead of conducting an in-depth thermal analysis of the machine, a limit is set on the winding current densities such that the thermal characteristics of the machine are reasonable and the machine does not overheat. The winding current density is defined as the total amount of current flowing through the slot divided by the total area of copper in the slot. Both field and armature winding current densities must be less than 2000 A/cm<sup>2</sup>.

##### 6.1.4.1 Field Winding Current Density

The field slot current is equal to the number of field ampere turns. The field winding current density is then determined to be

$$J_{field} = \frac{N_f i_f}{L_{interstack}(R_{statbot} - R_{statslotbot})k_{pf}} \quad 6.32$$

This winding current density must be less than the allowable limit of 2000 A/cm<sup>2</sup>.

##### 6.1.4.2 Armature Winding Current Density

A procedure similar to that used to derive Equation 6.32 is used to determine the armature winding current density. The total rms current in the slot is equal to the number of rms ampere turns. Thus,

$$J_{armature} = \frac{1}{\sqrt{2}} \frac{\left(\frac{N_s}{2p}\right)\left(\frac{I_s}{a}\right)}{A_{statslot}k_{pf}} \quad 6.33$$

The area of each stator slot is:

$$A_{statslot} = \frac{\pi(R_{statslotbot}^2 - R_{stattop}^2) - N_{statteeth}(W_{tooth}(R_{statslotbot} - R_{stattop}))}{N_{statslot}} \quad 6.34$$

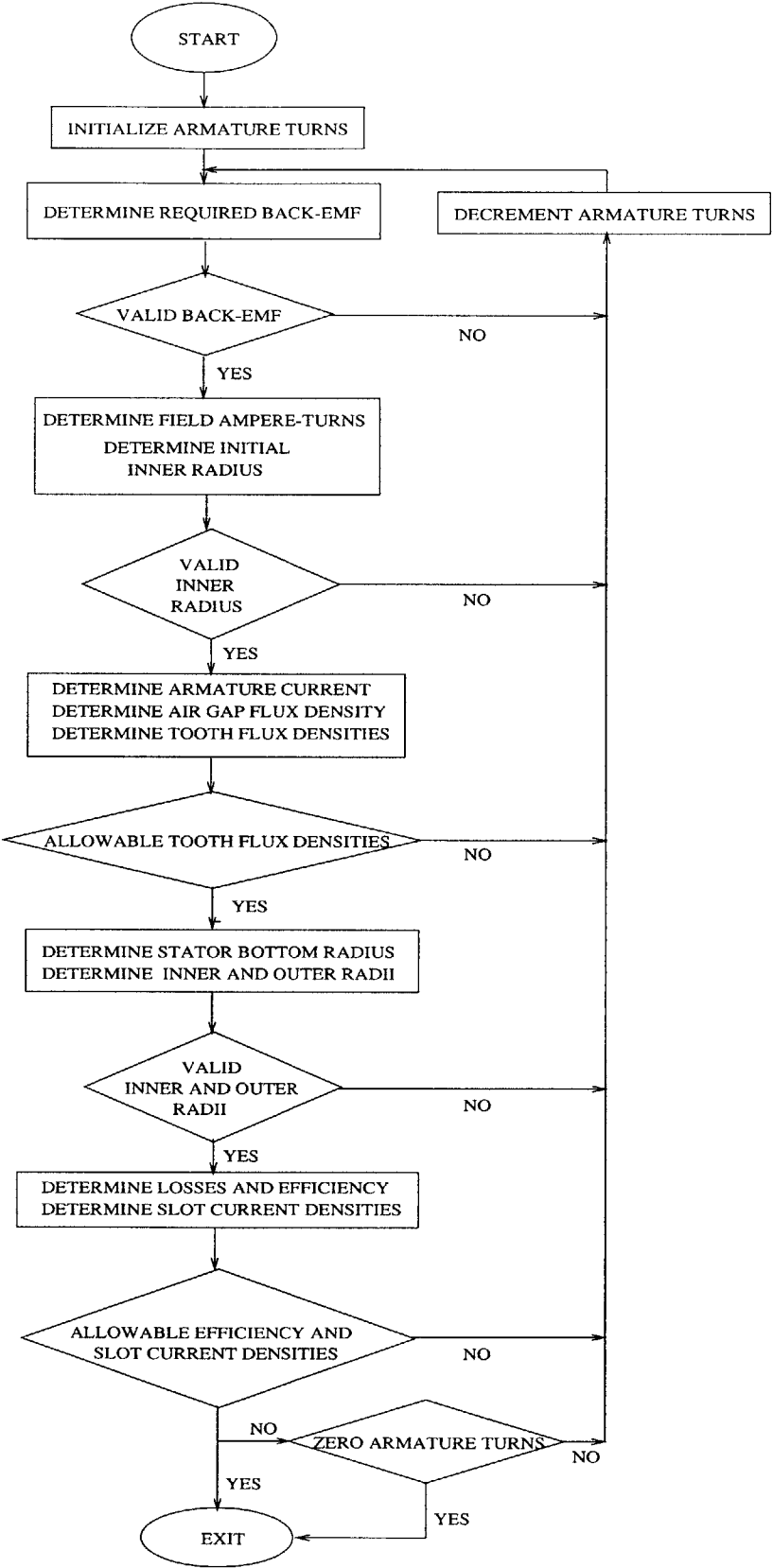
where  $N_{statteeth}$  and  $N_{statslot}$  are the number of stator teeth and slots which are equal, and  $W_{tooth}$  is the width of a stator tooth. The armature current in Equation 6.33 must be less than the allowable limit of 2000 A/cm<sup>2</sup>.

## 6.2 Electrical Design

Based on all the requirements and the procedures used for meeting them, the electrical design of the alternator can be summarized in the flow chart shown below in Figure 6.1. This constitutes the stages “DESIGN FOR OPTIMAL ELECTRICAL PERFORMANCE” and “ALTERNATOR MEETS ALL REQUIREMENTS” of Figure 3.2. The first step involves initializing the number of armature turns per coil. This number is picked to be the largest number such that the machine meets the winding current density requirements specified by Equation 6.33. Next, the required back-emf is determined using the power requirements of the alternator, and the equivalent circuit for the system comprising the alternator and external rectifier circuit with constant voltage load. It is possible that the machine will not be able to meet the power requirements. If it does not, then the armature turns is decremented and a new back-emf is calculated. Given the back-emf, the number of field-ampere turns can be determined using equation 6.3. The field ampere-turns sets a maximum inner radius for the centerpiece through Equation 6.15. If the inner radius exceeds the mechanical limits, then a fewer number of armature turns is used, and the machine is reevaluated from the beginning of the loop. If the inner radius is acceptable, the armature current is then calculated using 6.6. Knowledge of the field and armature excitations next specifies the flux densities in the air gap, and the tooth flux densities can be obtained to check for saturation in Equations 6.23 and 6.31. If either of the teeth saturate, then the analysis returns to the beginning of the loop. If the teeth are not saturated, then another minimum inner radius is obtained using Equation 6.21, such that saturation of the centerpiece is avoided. The minimum inner radius is picked to be the smaller of the two inner radial limits obtained. The stator slot bottom radius is determined based on 6.26. The outer radius is obtained using equation 6.29. If the radii exceed the prescribed limits, then the analysis returns to the beginning of the loop. If valid radii are obtained, then the losses and efficiency are calculated. In addition to this, the field and armature winding current densities are determined. The efficiency and winding current densities have to satisfy the requirements set earlier in order for the machine to be acceptable. To summarize, the analysis starts at a certain number of armature turns and evaluates the machine. If the machine is unacceptable, then the number of armature turns is decremented and the machine is reevaluated. This process is repeated until a satisfactory machine is obtained. The simulation exits the electrical design stage and evaluates the cost of the machine corresponding to the “DETERMINE COST” stage in Figure 3.2. If no satisfactory machine is obtained for any positive number of turns, then the

machine is discarded and a new geometry is synthesized corresponding to the remaining stages in Figure 3.2.

Figure 6.1.  
Flowchart  
for the  
electrical  
design  
process



## Chapter 7

### Results

The design procedure was run for a wide range of pole counts. The costs of the optimum machines from both the broad search and the refined search are plotted in Figure 7.1. Note that the broad search employs the approximate electrical analysis while the refined search uses the more accurate electrical analysis.

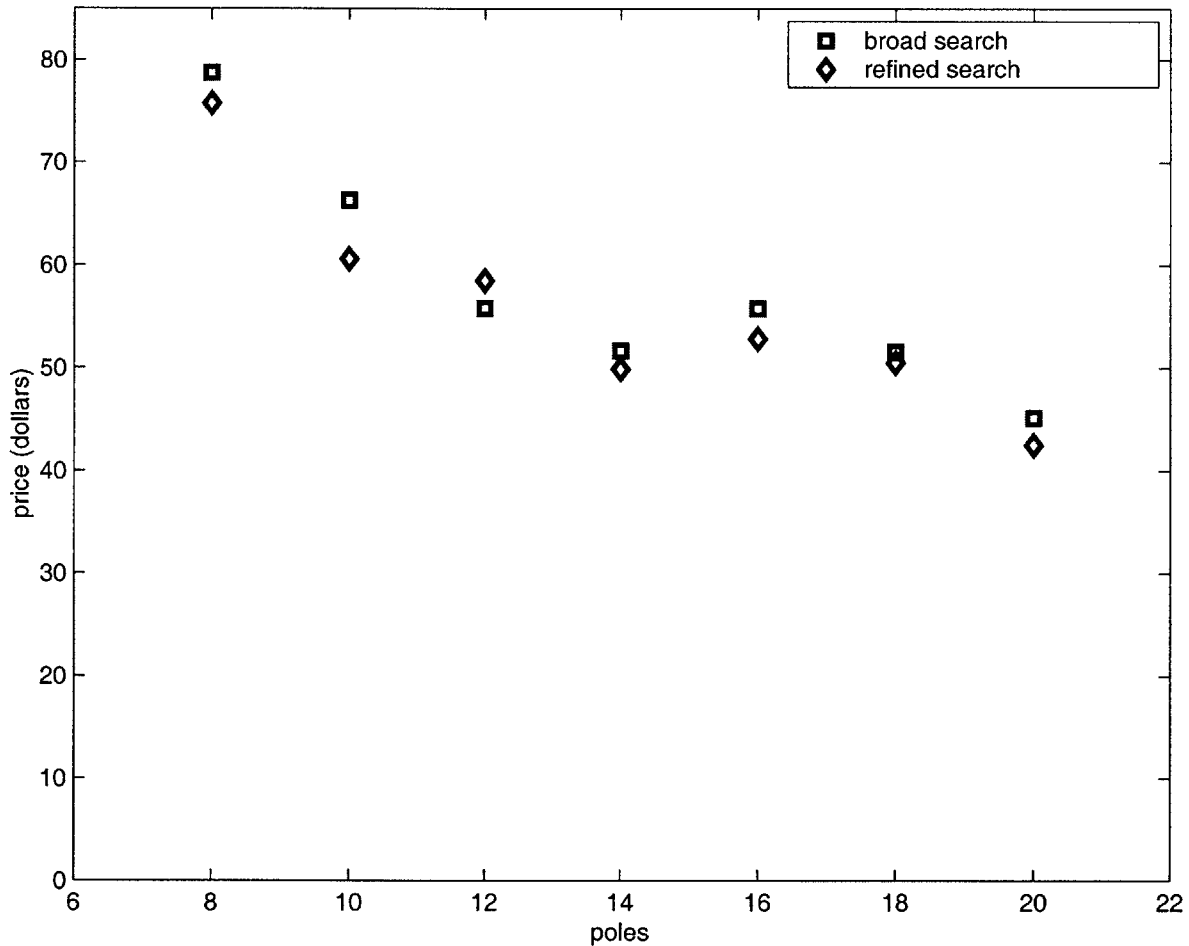


Figure 7.1 Cost curves from both broad and refined searches

Figure 7.1 shows a decrease in cost as the number of poles are increased. This makes higher-pole-count machines more favorable. Compared with conventional machines, it is easier to construct the homopolar inductor alternator with high pole counts because the number of poles is equal to the number of rotor teeth, and the rotor is devoid of windings. Aside from this, the total number of field ampere turns, in general, does not have to increase with pole count, unlike in con-

ventional wound-rotor machines. The power per unit weight of a machine is roughly proportional to the electrical frequency of operation. This implies that it is easier to meet a given power requirement with a higher-pole-count than a lower-pole-count machine. However, the pole count can also be too high to be reasonable. This is because the stator slots become too narrow and the machine becomes harder to wind. Also a higher-pole-count machine takes longer to wind due to the increased number of slots. Thus, overhead costs tend to increase with increasing pole count. Yet another disadvantage of higher pole counts are higher frequencies and larger iron losses. Thus, at higher frequencies, thermal issues are more important. To treat this, a more detailed thermal analysis is required, instead of having an upper limit on the winding current densities.

Higher pole count machines are cheaper for several reasons. One factor that contributes to this is that the back-iron and centerpiece are allowed to become thinner as the pole count increases since their thicknesses are determined by the amount of flux spanning a half-pole in the air gap; this flux decreases as the pole count is increased. Assuming constant dimensions and peak flux densities, a decrease in flux per pole allows for a thinner back iron. Beyond this, the length of the end turns decrease with increases in pole count. In choosing the optimum machine, a compromise has to be made between choosing between a cheap machine and one with a reasonable pole count. This would mean selecting a machine whose cost occurs after a significant decrease in the cost curve and precedes a gradual decrease as the pole count is increased. If the cost curve looks linear, then the choice of pole count is highly subjective. The main basis for selecting the best machine must be the estimate of the cost of the machine while taking into consideration a more accurate overhead cost function which increases with pole count.

From Figure 7.1, it can be seen that the costs of the optimum machines from the refined search are for the most part, slightly less than those from the broad search. It should be noted though that the refined search is not necessarily based on the cheapest machine from the broad search. In order for an alternator to be used as a basis for the refined search, it must be selected from among the cheapest machines from the broad search which meet the requirements when exact back-emf calculations are used. It also must look manufacturable, which means having reasonable dimensions, like for example, slot widths. Since the set of machines used as the basis for the refined search have costs near the minima from the broad search, the costs of the optimum machines from the refined search are slightly cheaper than the minimum cost machines from the broad search.



Shown in Figures 7.2 to 7.8 are the optimum machines from the refined searches. These machines were selected from among the cheapest ones obtained from the search. However, manufacturability was taken into consideration when selecting them. That is, the machines selected were those with wider slots for easier assembly.

Noticeable from Figures 7.2 to 7.8 are some favorable properties. The armature windings can be wound relatively easily since the slots are wide enough. The rotor tooth fraction is close to a half, implying that it is possible to design a machine which can be treated as having a round rotor. The ratios of slot depths to widths seem reasonable. The maximum outer diameters of the alternators are close to 220 mm, which is much less than the upper limit. The aspect ratios are also reasonable.

0 50 (mm)  
 H H H H H

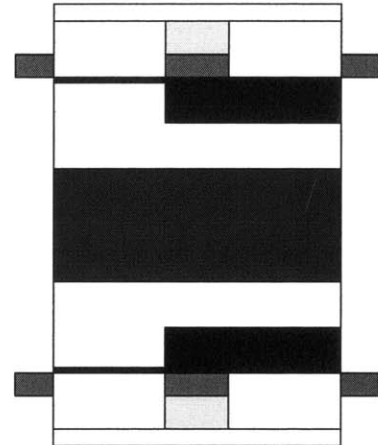
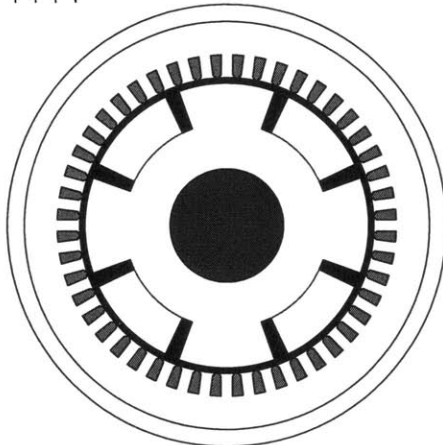


Figure 7.2 Optimal 8 pole machine (\$75.51)

0 50 (mm)  
 H H H H H

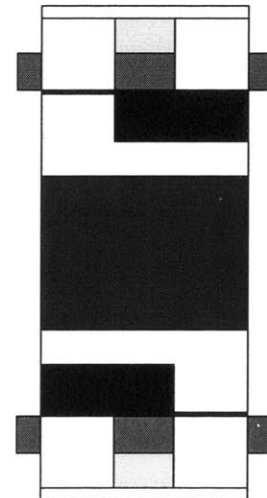
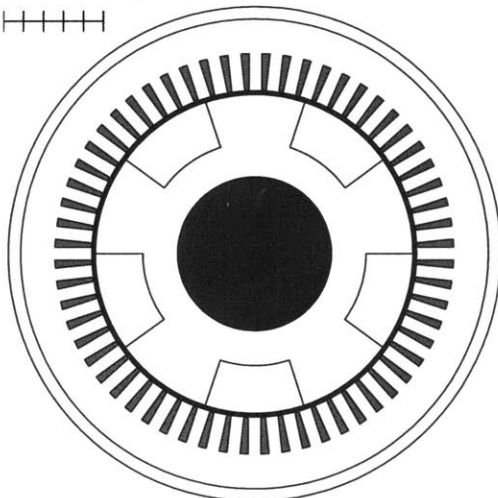


Figure 7.3 Optimal 10 pole machine (\$65.31)

0 50 (mm)  
+++++

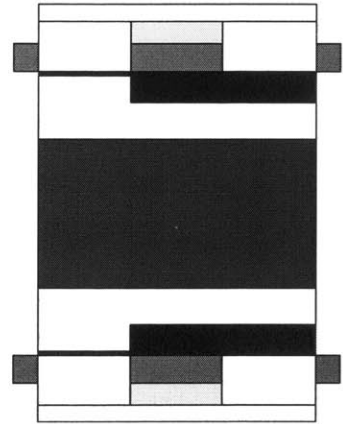
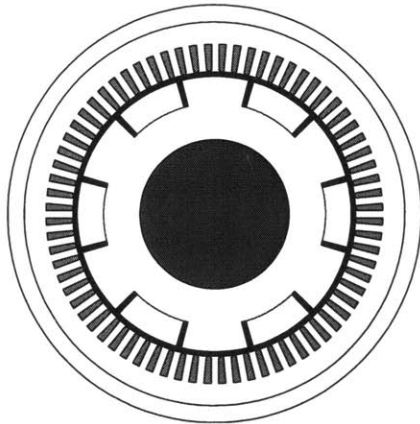


Figure 7.4 Optimal 12 pole machine (\$62.70)

0 50 (mm)  
+++++

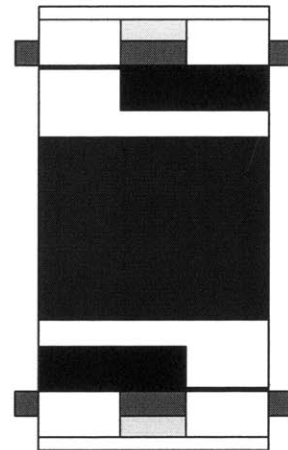
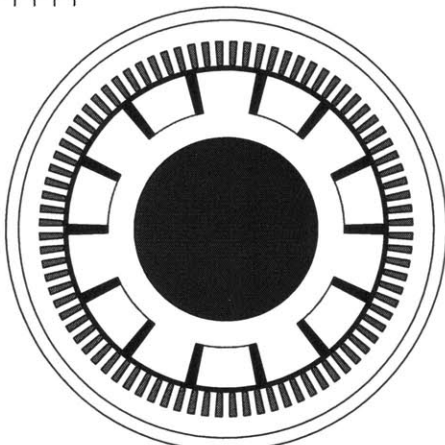


Figure 7.5 Optimal 14 pole machine (\$52.40)

0 50 (mm)  
+++++

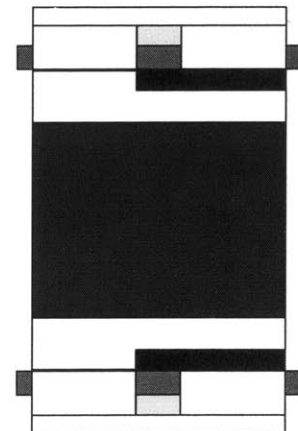
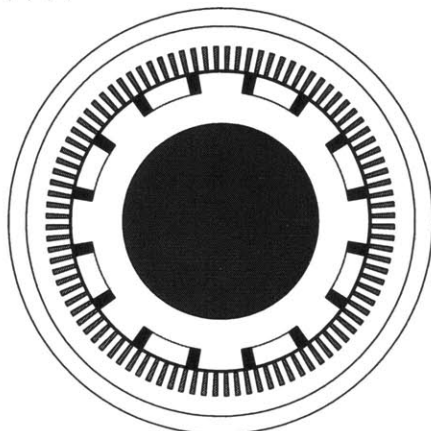


Figure 7.6 Optimal 16 pole machine (\$52.78)

0 50 (mm)  
+++++

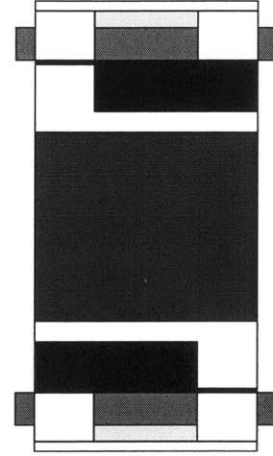
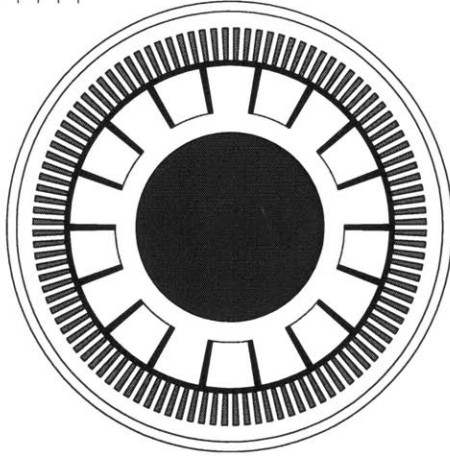


Figure 7.7 Optimal 18 pole machine (\$50.33)

0 50 (mm)  
+++++

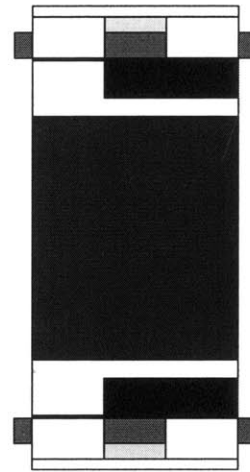
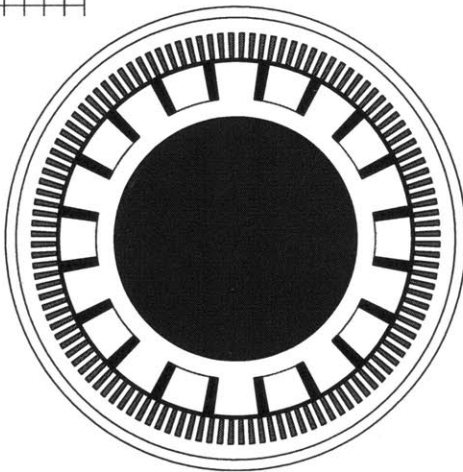


Figure 7.8 Optimal 20 pole machine (\$43.89)

Table 7.1 summarizes the characteristics of the machine selected to be the optimum from the refined search. The alternator selected was the 14-pole machine. The efficiency of the machine is around 85%, which is favorable. The winding current densities lie towards the upper limit which makes it safe to say that the search has fully optimized and that it will be difficult to further reduce cost. Saturation of the stator teeth is not one of the limiting factors. Since further optimi-

zation is achieved by narrowing the stator slots and thus widening the stator teeth, the flux densities in the stator teeth can only decrease with further optimization.

Figure 7.9 Optimal Machine Characteristics

	Optimum 14 pole machine
Cost (\$)	52.40
Pole Count	14
Gear Ratio	3
Outer Diameter (mm)	218.9
Stack Length (mm)	40.6
Inter-stack Length (mm)	32.7
Armature turns per coil	15
Mass (kg)	17.87
Efficiency (%)	84.83
Maximum Tooth Flux Density (T)	1.7203
Field Current Density (A/cm <sup>2</sup> )	1880
Stator Current Density (A/cm <sup>2</sup> )	1888
Maximum tip speed (m/s)	148
Peak shear stress (psi)	1.02
Moment of inertia (kgm <sup>2</sup> )	0.0208

## Chapter 8

### Conclusions and Future Work

#### 6.1 Concluding remarks

The design and search process yielded satisfactory machines that were fairly inexpensive. The overall dimensions and topologies of these machines are reasonable. The outer diameters (OD) of these machines are much less than the upper limit and the dimensions of the machines leave enough clearance for a shaft. The alternator with the pole count of 14 was selected as the optimum. One of the reasons for selecting the machine is the fact that it occurs at a local minimum of the cost curve. And although the materials costs of the machines are still decreasing into the 20s pole count range, the overhead cost is expected to increase. The materials cost of the selected machine was \$26.20, with the actual cost predicted to be twice that, or \$52.40. This is reasonable considering the challenging power requirements that the machine had to meet.

The optimum machines are comparable, in terms of materials costs, with the optimum machines obtained when designing the wound-field synchronous alternator. However, the inductor alternator was optimized at speeds three times the engine speed, compared with the optimum wound field alternators which were optimized at speeds twice the engine speed. The inductor alternator was allowed to run at higher speeds because the typical shear stress present in this machine is less than that of the wound-field synchronous machine. But since the inductor alternator has a simple and robust rotor made up of solid steel, running it at higher tip speeds is allowable.

For both the wound-field and homopolar inductor alternators, the cheap machines have high pole counts with the cost curve still decreasing into the 20 pole range. The homopolar inductor alternators are easier to build at high pole counts because the rotor is free of windings, which make it easier to wind. Also, the number of field ampere turns of the homopolar alternator does not have to increase with pole count, unlike the wound field synchronous machine. At some point, the field excitation for the wound field machine becomes too costly.

A comparison between the homopolar inductor alternator and wound field synchronous alternator indicates that the homopolar inductor alternator is the preferred machine. Compared with the Lundell alternator, there are also several advantages to using the homopolar inductor

alternator. Due to the structure of its rotor, the homopolar machine does not have scaling issues, unlike the Lundell alternator. In order to increase the output power of the Lundell alternator, one way would be to increase its radial or longitudinal dimensions. However, there are limitations to this due to its having cantilevered poles. If these dimensions are to be increased, the speed of the machine has to be decreased. This, however, results in a smaller increase in output power. The other way of increasing power is by increasing speed. However, again, because of the cantilevered rotor structure, there are considerable limitations to such an increase. Thus, increasing output power is a daunting task for the Lundell alternator designer.

To summarize, there are distinct advantages to using the homopolar inductor alternator over either the wound-field synchronous alternator and the Lundell alternator for automobiles when designed for high output power and minimum cost. The costs are reasonable while the inherent properties of the machine make it a machine worthy of consideration for use in future automobiles.

## **6.2 Future Work**

The work done in this thesis comprises a first pass study of the feasibility of the homopolar inductor alternator for automotive applications. There is still room for further study. For example, there is the need for a more comprehensive set of specifications. The thermal requirement, for example, was just a limit on the winding current densities. An in depth thermal analysis is required since cooling the machine should be considered. A transient analysis of the machine should be performed. A finite element analysis of the machine should be conducted in order to make sure that the lumped parameter modeling used is accurate enough. Finally, the control aspects of this machine should be taken into consideration.

A further reduction in the cost of the Homopolar Inductor Alternator can be achieved by placing the field winding right next to the rotor. This topology is magnetically equivalent to the original. The advantage of this, though, is that it will allow for a possible decrease in the stator back-iron thickness since the back-iron thickness is now independent of the field winding current density that has to be below a certain limit. A thinner back-iron implies a lower cost machine. The optimization process should be run on such a topology to assess the expected decrease in cost.

Finally, the Lundell alternator has not yet been optimized for the new electrical system that is being designed for automobiles. Therefore, a study similar to this thesis should address the Lundell machine.

## Appendix A

### Nomenclature

$A_{armslot}$	armature slot area
$A_{fieldslot}$	field slot area
$A_{armwire}$	cross-sectional area of armature winding
$A_{fieldwire}$	cross-sectional area of field winding
$A_{bi}$	cross-sectional area of back-iron
$A_{cp}$	cross-sectional area of centerpiece
$a$	number of parallel armature windings
$B_{airgap}$	maximum flux densities in air gap
$B_{aL}, B_{bL}, B_{cL}$	air gap flux densities in left stack
$B_{aR}, B_{bR}, B_{cR}$	air gap flux densities in right stack
$B_{cpa}$	flux density directed axially in centerpiece
$B_{bia}$	flux density directed axially in back iron
$B_{cpl}$	flux density in centerpiece directed in lateral or azimuthal direction
$B_{rottoothbase}$	flux density in rotor tooth base
$D_{slot}$	depth of a stator slot
$E_{af}, E_{bf}, E_{cf}$	back voltages
$F_{jL}$	MMF drop across left stack
$F_{rL}$	MMF drop across right stack
$F_{smax}$	maximum combined armature MMFs in air gap
$F_a, F_b, F_c$	armature MMF
$g$	air gap width
$g_1$	air gap width above rotor slot (interpole)
$g_2$	air gap width above rotor tooth (pole)
$H_{gL}$	air gap magnetic field intensity in left stack
$H_x$	magnetic field intensity across stator slot
$i_a, i_b, i_c$	armature currents (motor convention)
$i_a', i_b', i_c'$	armature currents (generator convention)
$i_f$	field current
$i_d, i_q$	direct and quadrature axis currents
$I_s$	amplitude of armature phase currents



$J_{fieldslot}$	field winding density
$k_w$	winding factor of first harmonic
$k_{wn}$	nth harmonic winding factor
$k_{pf}$	packing or space factor
$L_{aa}, L_{bb}, L_{cc}$	armature self inductances
$L_{af}, L_{bf}, L_{cf}$	armature field mutual inductances
$L_{df}$	mutual inductance between field and armature direct axis
$L_{ff}$	field self inductance
$L_s$	synchronous inductance
$L_d, L_q, L_o$	armature inductances in dq frame
$L_o, L_2$	amplitudes of inductances associated with armature
$L_{afm}$	amplitude of armature-field mutual inductance
$L_l$	slot leakage inductance
$L_{oneturn}$	length of one turn of armature winding
$m$	mth harmonic of permeance function
$m_{spp}$	number of slots per pole per phase
$n$	nth harmonic of armature MMF
$n_{turnperslot}$	number of armature turns in a slot
$N_f$	number of series field turns
$N_s$	number of armature conductors or turns
$n_{sp}$	number of stator slots per pole
$N_{statteeth}$	number of stator teeth
$N_{statslot}$	number of stator slots
$P_{diodeloss}$	diode losses
$P_{armloss}$	armature winding losses
$P_{fieldloss}$	power required for field winding or field winding losses
$P_{copper}$	total copper or winding losses
$P_{net}$	required net output power
$P_{gross}$	gross power at output of rectifier
$P_{loss}$	total power losses
$p$	number of pole pairs
$R_{field}$	field resistance
$R_{inner}$	rotor inner radius

$R_{outer}$	stator outer radius
$R_{rotslotbot}$	rotor slot bottom radius
$R_{rotop}$	rotor top radius
$R_{statbot}$	stator bottom radius
$R_{statslotbot}$	stator slot bottom radius
$R_{stattop}$	stator top radius
$r_a$	armature resistance
$R_s$	equivalent armature resistance
$T_{cp}$	width or thickness of centerpiece
$T_{bi}$	back iron thickness
$V_{hll}$	half the line-to-line voltage
$V_o$	constant load voltage
$V_s$	amplitude of back-emf
$W_{slot}$	width of a stator slot
$X_d, X_q$	direct and quadrature axis reactances
$X_s$	equivalent synchronous reactance
$\beta$	rotor tooth fraction
$\gamma$	electrical angle between stator slots
$\delta$	initial rotor angle in electrical degrees
$\eta$	efficiency
$\theta$	mechanical angle around stator from phase a magnetic axis
$\theta_i$	internal power angle (between excitation and phase current)
$\theta_r$	mechanical angle between rotor and stator phase A magnetic axis
$\theta_t$	rotor tooth width in radians
$\theta_{stattoothslot}$	stator tooth pitch
$\theta_{stattooth}$	stator tooth width
$\Lambda$	permeance per unit area
$\Lambda_L$	permeance per unit area for left stack
$\Lambda_R$	permeance per unit area for right stack
$\Lambda_m$	amplitude of mth harmonic of permeance function
$\lambda_{aa}, \lambda_{bb}, \lambda_{cc}$	flux linked by armature winding due to itself
$\lambda_{ab}, \lambda_{bc}, \lambda_{ac}$	armature flux linked by one phase due to a different phase
$\lambda_{af}, \lambda_{bf}, \lambda_{cf}$	flux linked by armature winding due to field winding

$\lambda_d, \lambda_q$	direct and quadrature axis flux linkages
$\lambda_{ff}$	flux linked by field due to itself
$\mu_o$	permeability of free space
$\sigma_{Cu}$	copper conductivity

## Appendix B

### Armature Winding

#### B.1. Winding Pattern

The winding pattern shown in Figures B.1 and B.2 is the same as that used for the wound field synchronous machine which was optimized for the same specifications [3]. The winding patterns seen below were taken from [3]. The winding pattern is a double layer, full-pitch winding with two slots per pole per phase. The windings are wound in parallel which results in lower armature inductances. The number of parallel windings is equal to the number of poles ( $a = 2p$ ), and each of the armature coils has  $N_a$  series armature turns. In optimizing the machine, the number of armature turns per coil,  $N_a$ , is varied. In the derivations shown in Chapter 4, the total number of armature turns per phase,  $N_s$ , is used. This is equal to the number of turns per coil, multiplied by the number of slots per phase belt, multiplied by the number of poles. There are two slots per phase per pole. Thus,

$$N_s = N_a m_{spp} (2p) \quad \text{B.1}$$

Since there are  $2p$  wires in parallel, each wire carries a current of  $I_s/(2p)$ . If each coil has only one turn,  $N_a = 1$ , then the total amount of current in the slot is  $I_s/p$ . That is, the minimum slot current is the armature phase current divided by the number of pole pairs.

	$a_1$	$a_2$	$-c_{23}$	$-c_{24}$	$b_1$	$b_2$	$-a_3$	$-a_4$	$c_1$	$c_2$	$-b_3$	$-b_4$
	$a_{23}$	$a_{24}$	$-c_{21}$	$-c_{22}$	$b_{23}$	$b_{24}$	$-a_1$	$-a_2$	$c_{23}$	$c_{24}$	$-b_1$	$-b_2$

Figure B.1 Armature winding pattern

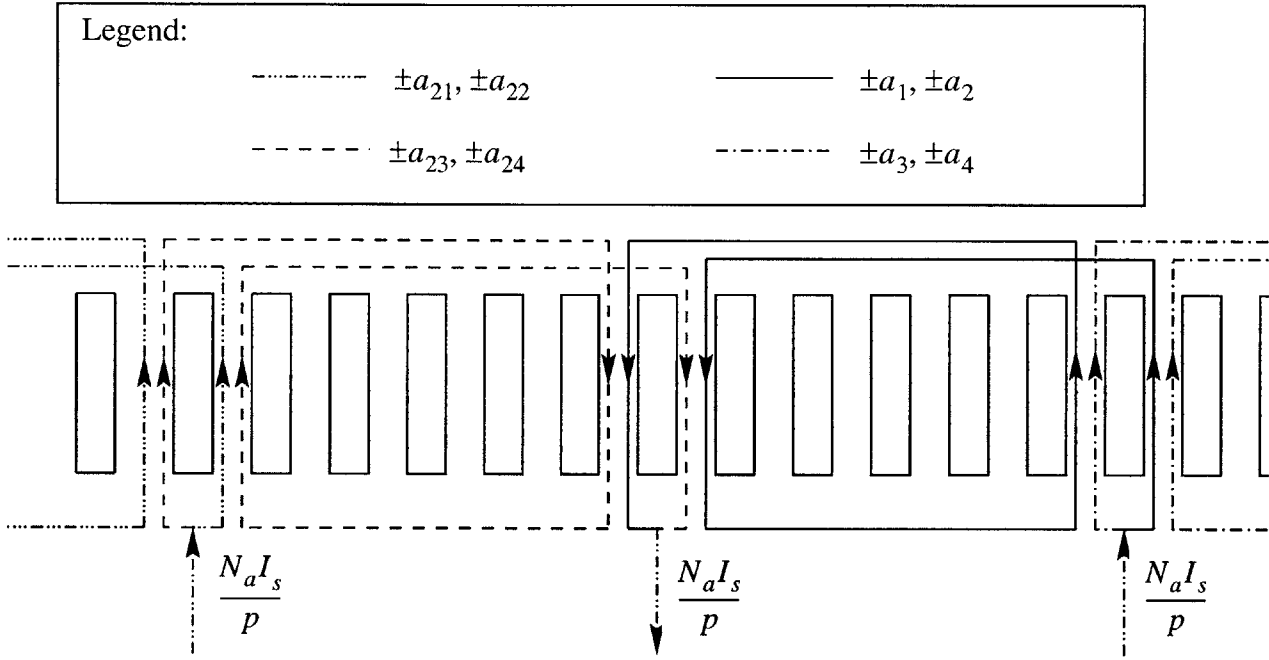


Figure B.2 Top view of windings (end turns not drawn accurately)

## B.2. Mean Path Length

The mean path length can be calculated from Figure B.3. The length used is that drawn in solid which passes through the center of the slot and follows each of the imaginary circles from one point of tangency to the other. The machine length is

$$L_{machine} = 2L_{stack} + L_{interstack} \quad \text{B.2}$$

The angle  $\angle bac$  is equal to  $\phi$ . In order to solve for  $\phi$ , note that

$$\sin \phi = \frac{\text{length}(\overline{bc})}{\text{length}(\overline{ac})} = \frac{W_{tooth}}{W_{tooth} + W_{slot}} \quad \text{B.3}$$

The length of segment  $\overline{de}$  is equal to the length of segment  $\overline{fc}$ . Therefore

$$\text{length}(\overline{fc}) = \frac{3W_{tooth} + 2.5W_{slot}}{\cos \phi} \quad \text{B.4}$$

The mean path length or the length of one turn of a coil is thus

$$L_{oneturn} = 2L_{machine} + 4\text{length}(\overline{de}) + 2\pi \left( \frac{W_{slot}}{2} \right) \quad \text{B.5}$$

where the last term in the expression comes from knowing that the sum of the arc lengths is the circumference of one of the imaginary circles.

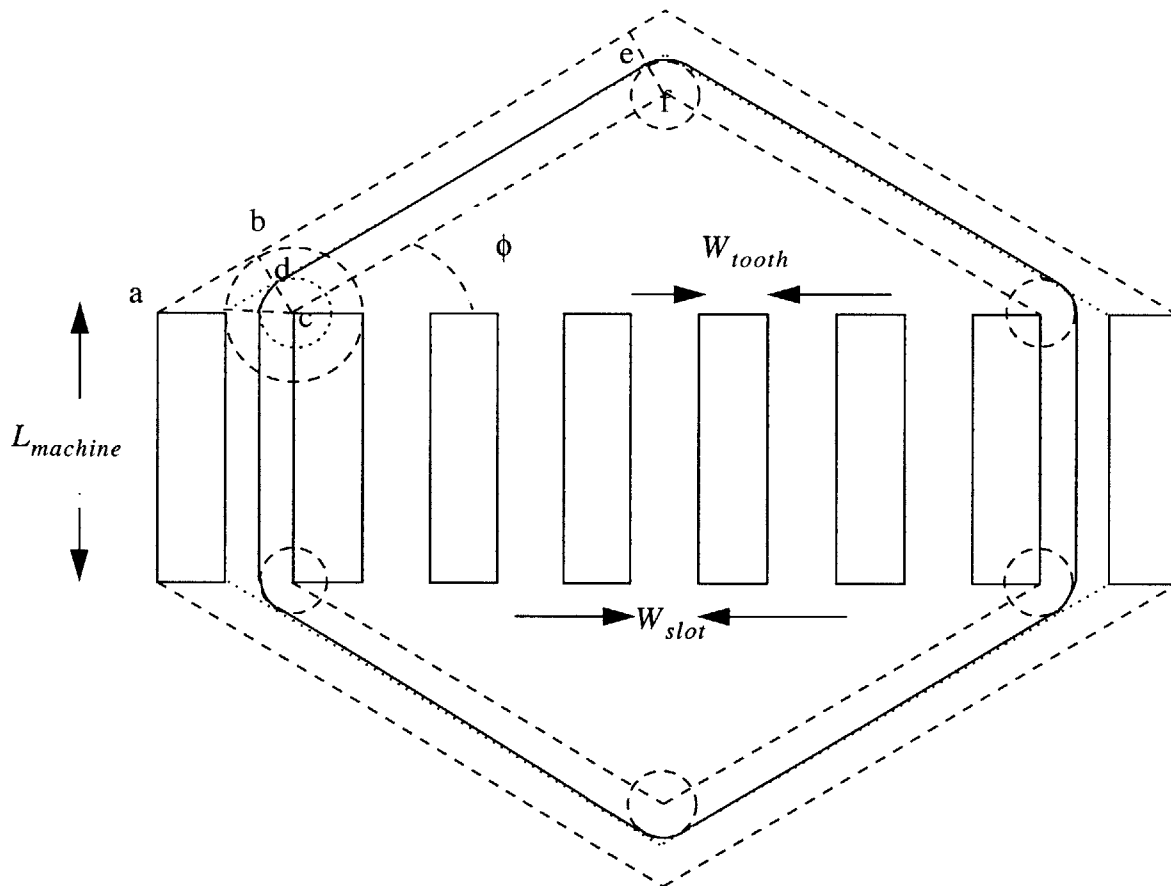


Figure B.3 Top view of one armature winding turn

## Appendix C

### Rotor Pole Face Losses

Since the rotor is made up of solid steel, its eddy current losses must be evaluated. These are the losses in the rotor that come as a result of the modulation of the air gap flux by the stator teeth thus resulting in high frequency flux densities in the air gap diffusing into the solid rotor. A diagram used for the evaluation is shown in Figure C.1.

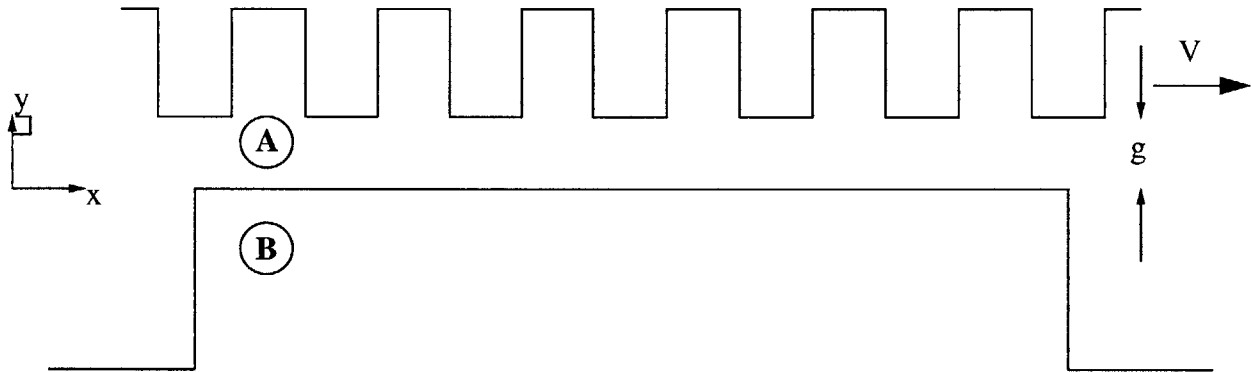


Figure C.1 Developed view of air gap

The air gap region is laid out flat. Evaluating the losses in rectilinear coordinates is easier than in cylindrical coordinates. Furthermore, instead of analyzing the losses in the reference frame where the stator is stationary and the rotor is moving to the left at velocity  $V$ , the rotor assumed to be stationary and the stator is moving to the right with velocity  $V$ . This will simplify the diffusion equation. Finally, the analysis is two-dimensional with everything assumed to be uniform in the  $z$ -direction.

In this analysis, the source of high-frequency flux is the stator teeth. Thus, the source excitation  $B_s$  at  $y = g$  takes the form

$$B_s = B_m \cos(k_m(x - Vt)) \quad \text{C.1}$$

where  $k_m$  is the wavenumber corresponding to the  $m$ th harmonic. The exact amplitude  $B_m$  used is the  $m$ th harmonic of the air gap flux density divided by the stator tooth fraction. Thus,

$$B_m = \frac{(F\Lambda_{L,R} + B_{fL,fR})_m}{\left(\frac{\theta_{stattooth}}{\theta_{stattoothslot}}\right)} \quad C.2$$

where  $F$  is taken from Equation 5.10, the subscript  $m$  in the numerator represents the  $m$ th harmonic which has to be obtained from the product of two summations,  $\Lambda_{L,R}$  is taken from Equation 4.11 or 4.15, and  $B_{fL,fR}$  is taken from Equation 4.22 or 4.23 depending on what stack is being analyzed. The losses in both stacks are the same and so the analysis of one stack is sufficient. The calculations above can be fairly involved. For the purposes of approximating the losses, only the losses due to the fundamental will be calculated. The amplitude of the fundamental ( $m=1$ ) used is the upper bound of

$$B_1 = \frac{\left(\left(\frac{3}{2}\right)\frac{4N_s I_s k_w}{\pi 2p a}\right)\left(\Lambda_o + \frac{\Lambda_2}{2}\right) + \frac{N_{ff} \Lambda_1}{2}}{\left(\frac{\theta_{stattooth}}{\theta_{stattoothslot}}\right)} \quad C.3$$

For the sake of generality, the derivations that follow can be used on any harmonic.

To begin,

$$N_{statteeth} \lambda_{stattooth} = 2\pi R_{airgap} \quad C.4$$

where  $\lambda_{stattooth}$  is the wavelength of one stator tooth, and  $N_{stattooth}$  is the number of stator teeth, and  $R_{airgap}$  which is the midpoint between  $R_{stator}$  and  $R_{rotor}$ , will be used. Equation C.4 shows that  $N_{statteeth}$  wavelengths (fundamental) span the entire circumference of the stator.

The wave number of the fundamental is thus

$$k_1 = \frac{2\pi}{\lambda_{stattooth}} = \frac{N_{statteeth}}{R_{airgap}} \quad C.5$$

The wave number of the  $m$ th harmonic is

$$k_m = mk_1 \quad C.6$$

The velocity of the stator is

$$V = R_{airgap} \frac{\omega}{p} \quad C.7$$

where  $\omega$  is the electrical frequency of excitation.



The complete source excitation is then:

$$B_s = B_m \cos\left(k_m \left(x - \left(\frac{R_{airgap}\omega}{p}\right)t\right)\right) \quad C.8$$

which can then be written as

$$B_s = B_m \cos(\omega_m t - k_m x) \quad C.9$$

where

$$\omega_m = m \left(\frac{N_{stator\text{teeth}}}{p}\right)\omega \quad C.10$$

As shown in Figure C.1, two regions must be analyzed. Region A is the air gap and region B is the solid rotor. Laplace's equation is applied to region A, which is free space, and the diffusion equation is applied to region B, which is the highly-permeable and conducting rotor. The magnetic scalar potential for region A can be expressed as:

$$\Psi_A = \left\{ \psi_s \frac{\sinh(k_m y)}{\sinh(k_m g)} + \psi_r \frac{\sinh k_m (g - y)}{\sinh(k_m g)} \right\} \cos((\omega_m t - k_m x)) \quad C.11$$

where  $\psi_s$  is the potential at the surface of the stator ( $y = g$ ) and  $\psi_r$  is the potential at the surface of the rotor ( $y = 0$ ). The magnetic flux density in region A is the gradient of the potential so that

$$B_A = -\nabla \Psi_A \quad C.12$$

The flux density normal to the boundary at  $y=g$  is continuous. Evaluating the  $y$ -directed flux density  $B_{Ay}$  at the source ( $y=g$ ) yields

$$B_m = -\mu_o k_m \left( \frac{\psi_s}{\tanh(k_m g)} - \frac{\psi_r}{\sinh(k_m g)} \right) \quad C.13$$

The flux in the air gap enters the rotor. The following analysis of magnetic diffusion is typical, and taken from [15]. The magnetic flux density in the rotor satisfies the diffusion equation

$$\frac{1}{\mu\sigma} \nabla^2 \vec{B}_B = \frac{\partial \vec{B}_B}{\partial t} \quad C.14$$

The  $y$ -component of the diffusion equation is

$$\frac{1}{\mu\sigma}\left(\frac{\partial^2 B_{By}}{\partial x^2} + \frac{\partial^2 B_{By}}{\partial y^2}\right) = \frac{\partial B_{By}}{\partial t} \quad \text{C.15}$$

The flux density in the y direction can be represented as

$$B_{By} = \text{Re}(\hat{B}_{By}(y)e^{j(\omega_m t - k_m x)}) \quad \text{C.16}$$

Substituting Equation C.16 into Equation C.15 yields

$$\frac{\partial^2 \hat{B}_{By}}{\partial y^2} - \alpha^2 \hat{B}_{By} = 0 \quad \text{C.17}$$

where

$$\alpha = k_m \sqrt{1 + jS} \quad \text{C.18}$$

and

$$S = \frac{\mu\sigma\omega_m}{k_m^2} \quad \text{C.19}$$

Let

$$\hat{B}_{By} = \hat{C}e^{\alpha y} \quad \text{C.20}$$

The y-directed flux density in region B is then

$$B_{By} = \text{Re}(\hat{C}e^{\alpha y} e^{j(\omega_m t - k_m x)}) \quad \text{C.21}$$

Since  $\nabla \cdot \vec{B}_B = 0$ , the x-directed flux density can be obtained as

$$\hat{B}_{Bx} = \frac{\alpha \hat{C}e^{\alpha y}}{jk_m} \quad \text{C.22}$$

Thus, the flux density in region B is

$$\vec{B}_B = \text{Re}\left(\left(\hat{x}\frac{\alpha}{jk_m} + \hat{y}\right)\hat{C}e^{\alpha y} e^{j(\omega_m t - k_m x)}\right) \quad \text{C.23}$$

The normal flux densities at the surface of the rotor ( $y = 0$ ) are continuous. From this, it follows that

$$\hat{C} = -\mu_o\left(\Psi_s \frac{k_m}{\sinh(k_m g)} + \Psi_r \frac{k_m}{\tanh(k_m g)}\right). \quad \text{C.24}$$

The tangential flux densities at the surface of the rotor are also continuous since there is no surface current at  $y = 0$ . Therefore

$$\hat{C} = -\frac{\mu_o \Psi_r k_m^2}{\alpha} \quad \text{C.25}$$

The value of  $\hat{C}$  can be then explicitly determined to be

$$\hat{C} = \frac{\frac{k_m}{\alpha} B_m}{\left( \left( \frac{k_m}{\alpha} + \frac{1}{\tanh(k_m g)} \right) \cosh(k_m g) - \frac{1}{\sinh(k_m g)} \right)} \quad \text{C.26}$$

The expression for the current density in region B is finally

$$\bar{J}_B = \frac{\nabla \times \hat{B}_B}{\mu} = \frac{1}{\mu} \text{Re} \left( -\frac{\mu \sigma \omega_m}{k_m} \hat{C} e^{\alpha y} e^{j(\omega_m t - k_m x)} \right) \hat{z} \quad \text{C.27}$$

The time-averaged force-density (per volume) in the x-direction is

$$\langle F_x \rangle = \frac{1}{2} \text{Re}(-\hat{J}_{Bz} \hat{B}_{By}) = \frac{\sigma \omega_m}{k_m} (e^{2\text{Re}(\alpha)y}) \frac{\hat{C} \hat{C}^*}{2} \quad \text{C.28}$$

The time-averaged traction in the x-direction (per unit x-z area) is:

$$\langle T_x \rangle = \int_{-\infty}^0 \langle F_x \rangle dy = \frac{\sigma \omega_m}{k_m} \left( \frac{\hat{C} \hat{C}^*}{2} \right) \left( \frac{1}{2\text{Re}(\alpha)} \right) \quad \text{C.29}$$

The power per unit x-z area is the average traction multiplied by the velocity  $V$ . The total power dissipated in the rotor is this power per unit area multiplied by the total surface area of the rotor teeth where the air gap flux enters. Therefore,

$$\langle P_{rotorloss} \rangle = \left( \frac{\sigma \omega_m}{k_m} \left( \frac{\hat{C} \hat{C}^*}{2} \right) \left( \frac{1}{2\text{Re}(\alpha)} \right) \right) \left( R_{airgap} \frac{\omega}{p} \right) (2\pi R_{airgap} (2L_{stack}) \beta)$$

The same results can be obtained when a similar approach is carried out using the time-averaged power dissipation per unit volume. This yields

$$\langle P_{rotorloss} \rangle = (2\pi R_{airgap} (2L_{stack}) \beta) \int_{-\infty}^0 \frac{1}{2} \text{Re} \left( \frac{\hat{J}_B \hat{J}_B^*}{\sigma} \right) dy$$

To verify that the pole face losses are negligible, calculations are made for a 12-pole machine. To do so, let  $R_{airgap} = 69.1$  mm,  $L_{stack} = 35.7$  mm,  $n = 1500$  rpm,  $B_1 = 0.61$  T, and  $p = 6$ . The pole face losses calculated for this machine amount to 28.6 mW. The diode loss is

157.3 W and the winding losses are 470.7 W. The core losses are indeed negligible compared to the other losses.

## Appendix D

### Simulation Code

#### gendesign.m

```
%%%gendesign.m%%  
%%%simulation runs for broad search%%  
%%%OPTIONS%%  
start=0; % 0 continues  
willsavecheap=1; % 0 saves all satisfactory machines; be aware of file size  
totcheapmachines=100; % number of cheapest machines to be saved  
totmachines=5e5; % total number of geometries evaluated  
gearratio=3;  
pp=4; % pole pairs  
origfield=1; % 0 for modified structure (field winding adjacent to rotor)  
filename='temp.mat'; %file to which results are saved  
backemfaccuracy=3; % 1 to be exact (refined search)  
    % 2 to ignore resistance (broad search)  
    % 3 to ignore resistance and saliency  
    % 4 to use exact but calculate all three options above  
%%  
  
counter=0; % number of satisfactory machines found; do not set  
desno=1; % current number of machines evaluated; do not set  
if willsavecheap  
    dimensions=ones(totcheapmachines,13)*9e9; %% using savecheap.m  
else  
    dimensions=ones(1,13)*9e9; %%using saveall.m  
end  
if (start==0)  
    load(eval('filename'))  
end  
init; %initialization script  
while desno<=totmachines,  
    fprintf('\nHomopolar Inductor Alternator: Broad Search %dx-Geared Design Number  
%d\n',gearratio,desno);  
    fprintf('Saving to: %s\n',filename);  
    sdim; %randomly synthesizes dimensions  
    cdim; %generates remaining dimensions  
    lumpparam; %determines lumped parameters  
    perf; %optimizes for electrical performance  
    cost; %determines cost of satisfactory machines  
    if willsavecheap  
        savecheap; %saves a set number of cheapest machines  
    else  
        saveall; %saves all satisfactory machines
```

```

end
desno=desno+1;
fprintf('poles=%g\ncounter=%d\nBest Cost=%g\n',2*pp,counter,min(dimensions(:,13)));
end

save(eval('filename'), 'dimensions', 'desno', 'counter', 'pp', 'garratio','origfield','backemfaccuracy');

```

### **gendesignr.m**

```

%%%gendesignr.m%%%
%%%simulation run for refined search%%%
%%%OPTIONS%%%
load temp.mat %file used as basis for refined search
[val,index]=min(dimensions(:,13)); %use minimum cost machine from file above
%index=3; % select machine to be used as basis for refined search
start=0; %0 continues
willsavecheap=1; % 0 saves all machines, 1 saves set no. of cheapest machines
totcheapmachines=100;%number of machines to be saved if willsavecheap is 1
totmachines=5e5; %total number of geometries evaluated
garratio=3;
pp=5; %pole pairs
origfield=1; % 0 for modified structure (field winding adjacent to rotor)
filename='tempref.mat'; %file to which results are saved
backemfaccuracy=1; % 1 to be exact (refined search)
    % 2 to ignore resistance (broad search)
    % 3 to ignore resistance and saliency
    % 4 to use exact but calculate all three options above
%%%%%%%%%%
counter=0; %%%no. of satisfactory machines found; do not set
desno=1; %%%current number of machines evaluated; do not set
initr; %initialization script
if willsavecheap
    dimensions=ones(totcheapmachines,13)*9e9; %% using savecheap.m
else
    dimensions=ones(1,13)*9e9; %%using saveall.m
end
if (start==0)
    load(eval('filename'))
end

while desno<=totmachines,
    fprintf('\nHomopolar Inductor Alternator:Refined Search %dx-Geared Design Number
%d\n',garratio,desno);
    fprintf('Saving to: %s\n',filename);
    sdimr; %randomly synthesizes dimensions
    cdim; %synthesizes remaining dimensions

```

```

lumpparam; %determines lumped parameters
perf; %optimizes for electrical performancs
cost;
if willsavecheap
    savecheap; %saves a set number of cheapest machines
else
    saveall; %saves all satisfactory machine
end
desno=desno+1;
fprintf('poles=%g\ncounter=%d\nBest Cost=%g\n',2*pp,counter,min(dimensions(:,13)));
end
save(eval('filename'),'dimensions','desno','counter','pp','gearratio','origfield','backemfaccuracy');
init.m
%%%init.m%%%
%%%initialization script for broad search%%%
outerradmax= 0.15; %maximum outer radius

airgapwid1min= 0.33e-3; %minimum air gap width over pole

maxtominairgapwid1=10; %ratio of maximum to minimum airgapwid1

minairgapwid2toairgapwid1=2; %minimum ratio of airgapwid2 to airgapwid1

maxairgapwid2toairgapwid1=12; %maximum ratio of airgapwid2 to airgapwid1

outerradmin= maxairgapwid2toairgapwid1*maxtominairgapwid1*airgapwid1min; %minimum
outer radius

innerradmin= 1e-6; %minimum inner radius

aspectratiomin=0.1; %aspectratio=stacklen/(2*outerrad); %minimum aspect ratio

aspectratimax=2; % maximum aspect ratio

minrotslotbotradtoouterrad=0.2;

mininterstacktostacklen= .25; %k=stacklen/interstacklen; %minimum interstack to stack length

maxinterstacktostacklen= 4; %maximum interstack to stack length

minrottoothfrac=0.1; %minimum rotor tooth fraction

maxrottoothfrac=0.9; %maximum rotor tooth fraction

minbackirontoouterrad=0.1; %minimum back iron thickness to outer radius ratio

```

```

dollarsperpoundsteel=0.45;
dollarsperpoundcopper=2.27;
dollarsperkgsteel=dollarsperpoundsteel*2.205; %2.205 lbs per kg
dollarsperkgcopper=dollarsperpoundcopper*2.205; %2.205 lbs per kg
steeldensity=7462; %kg per m^3
copperdensity=8960; %kg per m^3
dollarspervolsteel=dollarsperkgsteel*steeldensity;
dollarspervolcopper=dollarsperkgcopper*copperdensity;
packingfactor=0.35; %fraction of copper per unit area
statsp = 6; % stator slots per pole
Nap=2; %minimum series turns per pole per phase
speed=gearratio.*[600,1500,6000]; %alternator speed
netoutputpower=[4000,3250,6000];
loadvoltage=42;
diodedrop=1;
freq=pp*speed/60; %Hz
omegaelec=2*pi*freq; %rad/s %electrical frequency
omegamech=2*pi*speed/60; %rad/s %mechanical frequency
Jfieldmax=2e7; %A/m^2 %maximum field winding current density
Jarmmax =2e7; %A/m^2 %maximum armature winding current density
Bsat=1.8; %T %maximum steel flux density
copperconductivity = 4.45e7; %mhos/m
steelconductivity = 1/25 *1e8; %mhos/m

```



```

mu0=4*pi*(1e-7); %H/m %permeability of free space

musteel=4.5e3*mu0; %H/m %permeability of steel

armwindingfac=cos(pi/12); %fundamental armature winding factor

statslots = 2 * statsp * pp; %number of stator slots

statstang= 2*pi/statslots; % stator slot and tooth angle

rotslots = 2 * pp; %number of rotor slots on both stacks

rotstang=2*pi/rotslots; %pole span

initr.m
%%%initr.m%%%
%%%initialization file for refined search%%%
outerrad = dimensions(index,1);
statbotrad = dimensions(index,2);
statslotbotrad = dimensions(index,3);
airgapwid1 = dimensions(index,4);
airgapwid2 = dimensions(index,5);
rotslotbotrad = dimensions(index,6);
innerrad = dimensions(index,7);
stattoothang = dimensions(index,8);
rottoothang = dimensions(index,9);
stacklen = dimensions(index,10);
interstacklen = dimensions(index,11);
stattoprad = rotslotbotrad + airgapwid2;
rotoprad = rotslotbotrad+ airgapwid2 - airgapwid1;

outerradmax=min(outerrad*1.2,0.15); %maximum outer radius

airgapwid1max=airgapwid1*1.2; %maximum airgapwid1

airgapwid1min=max(airgapwid1*0.8,0.33e-3); %minimum airgapwid1

airgapwid2max=airgapwid2*1.2; %maximum airgapwid2

airgapwid2min=airgapwid2*0.8; %minimum airgapwid2

maxtominairgapwid1=10; %ratio of maximum to minimum airgapwid1

maxairgapwid2toairgapwid1=12; %maximum ratio of airgapwid2 to airgapwid1

```

```

outerradmin1= maxairgapwid2toairgapwid1*maxtominairgapwid1*airgapwid1min;
outerradmin=max(outerrad*0.8, outerradmin1); %minimum outer radius
innerradmin=1e-6; %minimum inner radius
rotslotbotradmax=rotslotbotrad*1.2; %maximum rotor slot bottom radius
rotslotbotradmin=rotslotbotrad*0.8; %minimum rotor slot bottom radius
minrotslotbotradtoouterrad=0.2;
minbackirontoouterrad=0.1; %minimum back iron thickness to outer radius ratio
stattopradmax=rotslotbotradmax+airgapwid2max-airgapwid1min; %maximum stator top radius
stattopradmin=rotslotbotradmin+airgapwid2min-airgapwid1max; %minimum stator top radius
statslotbotradmax=statslotbotrad*1.2; %maximum stator slot bottom radius
statslotbotradmin=statslotbotrad*0.8; %minimum stator slot bottom radius
statbotradmax=statbotrad*1.2; %maximum stator bottom radius
statbotradmin=statbotrad*0.8; %minimum stator bottom radius
stacklenmax=stacklen*1.2; %maximum stack length
stacklenmin=stacklen*0.8; %minimum stack length
interstacklenmax=interstacklen*1.2; %maximum inter-stack length
interstacklenmin=interstacklen*0.8; %minimum inter-stack length
stattoothangmax = stattoothang*3/2; %maximum stator tooth angle
stattoothangmin = stattoothang*2/3; %minimum stator tooth angle
rottoothangmax = rottoothang*3/2; %maximum rotor tooth angle
rottoothangmin = rottoothang*2/3; %minimum rotor tooth angle
dollarsperpoundsteel=0.45;
dollarsperpoundcopper=2.27;

```

dollarsperkgsteel=dollarsperpoundsteel\*2.205; %2.205 lbs per kg  
dollarsperkgcopper=dollarsperpoundcopper\*2.205; %2.205 lbs per kg  
steeldensity=7462; %kg per m^3  
copperdensity=8960; %kg per m^3  
dollarspervolsteel=dollarsperkgsteel\*steeldensity;  
dollarspervolcopper=dollarsperkgcopper\*copperdensity;  
packingfactor=0.35; %fraction of copper per unit area  
statsp = 6; % stator slots per pole  
Nap=2; %minimum series turns per pole per phase  
speed=gearratio.\*[600,1500,6000]; %rpm %alternator speed  
netoutputpower=[4000,3250,6000];  
loadvoltage=42;  
diodedrop=1;  
freq=pp\*speed/60; %Hz  
omegaelec=2\*pi\*freq; %rad/s %electrical frequency  
omegamech=2\*pi\*speed/60; %rad/s %mechanical frequency  
Jfieldmax=2e7; %A/m^2 %maximum field winding current density  
Jarmmax =2e7; %A/m^2 %maximum armature winding current density  
Bsat=1.8; %T %maximum steel flux density  
copperconductivity = 4.45e7; %mhos/m  
steelconductivity = 1/25 \*1e8; %mhos/m  
mu0=4\*pi\*(1e-7); %H/m %permeability of free space  
musteel=4.5e3\*mu0; %premeability of steel

```

armwindingfac=cos(pi/12); %fundamental armature winding factor

statslots = 2 * statsp * pp; %number of stator slots

statstang= 2*pi/statslots; % stator slot and tooth angle

rotslots = 2 * pp; %number of rotor slots on both stacks

rotstang=2*pi/rotslots; %pole span
sdim.m
%%%sdim.m%%
%%%synthesizes dimensions for broad search
randmat=rand(10,1);
order=randperm(10);
%stator tooth angle
stattoothang= 0 + randmat(order(1))*(statstang-0);

%rotor tooth angle
rottoothang=minrottoothfrac*(2*rotstang) + randmat(order(2))*(maxrottoothfrac*(2*rotstang)-
minrottoothfrac*(2*rotstang));

%outer radius
outerrad = outerradmin + randmat(order(3)) * (outerradmax-outerradmin);

%air gap width over pole
airgapwid1 = airgapwid1min + randmat(order(4)) * (maxtominairgapwid1*airgapwid1min -
airgapwid1min);

%air gap width over interpole
airgapwid2 = minairgapwid2toairgapwid1*airgapwid1 + randmat(order(5)) *
(maxairgapwid2toairgapwid1*airgapwid1 - minairgapwid2toairgapwid1*airgapwid1);

%rotor slot bottom radius
rotslotbotrad = minrotslotbotradtoouterrad*outerrad + randmat(order(6)) * ((1-minbackirontoou-
terrad)*outerrad-airgapwid2 - minrotslotbotradtoouterrad*outerrad);

%rotor slot top radius
stattoprad = rotslotbotrad + airgapwid2;

%stator slot bottom radius
statslotbotrad = stattoprad + randmat(order(7)) * (outerrad - stattoprad);

%stator bottom radius
statbotrad = statslotbotrad + randmat(order(8)) * (outerrad - statslotbotrad);

%rotor top radius

```

```

rotoprad = rotslotbotrad + airgapwid2 - airgapwid1;

%stack length
stacklen = aspectratiomin * 2 * outerrad + randmat(order(9)) * (aspectratiomax-aspectratiomin) *
2 * outerrad ;

%inter stack length
interstacklen = mininterstacktostacklen * stacklen + randmat(order(10)) * (maxinterstack-
tostacklen-mininterstacktostacklen) * stacklen;
sdimr.m
%%%sdimr.m%%%
%%%synthesizes dimensions for refined search%%%
randmat=rand(10,1);
order=randperm(10);
%stator tooth angle
stattoothang= stattoothangmin + randmat(order(1))*(stattoothangmax-stattoothangmin);

%rotor tooth angle
rottoothang=rottoothangmin + randmat(order(2))*(rottoothangmax-rottoothangmin);

%outer radius
outerrads = outerradadmin + randmat(order(3)) * (outerradsmax-outerradadmin);

%air gap width over rotor pole
airgapwid1 = airgapwid1min + randmat(order(4)) * (airgapwid1max -airgapwid1min);

%air gap width over rotor interpole
airgapwid2 = airgapwid2min + randmat(order(5)) * (airgapwid2max - airgapwid2min);

%rotor slot bottom radius
rotslotbotrad = max(rotslotbotradadmin,minrotslotbotradtoouterrads*outerrads) + randmat(order(6)) *
(min(rotslotbotradmax,(1-minbackirontouterrads)*outerrads-airgapwid2) - max(rotslotbotrad-
min,minrotslotbotradtoouterrads*outerrads));

%stator top radius
stattoprad = rotslotbotrad + airgapwid2;

%stator slot bottom radius
statslotbotrad = max(statslotbotradadmin,stattoprad) + randmat(order(7)) * (min(statslotbotrad-
max,outerrads) - max(statslotbotradadmin,stattoprad));

%stator bottom radius
statbotrad = max(statbotradadmin,statslotbotrad) + randmat(order(8)) * (min(statbotradmax,outer-
rad) - max(statbotradadmin,statslotbotrad));

%rotor top radius

```

```

rotoprad = rotslotbotrad + airgapwid2 - airgapwid1;

%stack length
stacklen = stacklenmin + randmat(order(9)) * (stacklenmax-stacklenmin) ;

%inter stack length
interstacklen = interstacklenmin + randmat(order(10)) * (interstacklenmax-interstacklenmin);
cdim.m
%%%%cdim.m%%
%%%%Determines remaining dimensions%%
%%

%stator slot angle
statslotang= statstang - stattoothang;

%rotor tooth fraction
rottoothfrac=rottoothang/(2*rotstang);

%for drawing purposes only
if rottoothfrac<0.5
rotslotang = rotstang-rottoothang;
else
rotslotang = 2*rotstang-rottoothang;
end

%average armature winding radius
avearmrad=(stattoprad+statslotbotrad)/2;

%average air gap radius
aveairgaprad=(rotoprad+stattoprad)/2;

%stator tooth top angle
stattoothtopang=stattoothang;

%stator tooth bottom angle
stattoothbotang=2*asin(stattoprad*sin(stattoothtopang/2)/statslotbotrad);

%half stator slot top angle
halfstatslottopang=(statstang-stattoothtopang)/2;

%half stator slot bottom angle
halfstatslotbotang=(statstang-stattoothbotang)/2;

%stator tooth width
stattoothwid=2*stattoprad*sin(stattoothtopang/2);

%average stator tooth width

```

```

avestattoothwid=stattoothwid;

%average stator slot width
avestatslotwid=((2*stattoprad*halfstatslottopang)+(2*statslotbotrad*halfstatslotbotang))/2;

%angle between end turn and horizontal axis, phi in write up
theta=asin(avestatslotwid/(avestatslotwid+avestattoothwid));

%end turn width
endturnwid = (3*avestattoothwid + 2.5*avestatslotwid)*tan(theta) + avestatslotwid;

%area occupied by field winding
if origfield
fieldcopperarea=(statbotrad-statslotbotrad)*interstacklen*packingfactor;
else
fieldcopperarea=(stattoprad-rotslotbotrad)*interstacklen*packingfactor;
end

% total length
totlen=(2*stacklen+interstacklen);

% length of a diagonal segment of one turn
seglen=(3*avestattoothwid+2.5*avestatslotwid)/cos(theta);

% mean path length o one turn
armmeanpathlen= 2*totlen + 4*seglen + 2*pi*(avestatslotwid/2);

% number of stator teeth
statteeth=statslots;

% area of one stator slot
slotarea=(pi*(statslotbotrad^2-stattoprad^2)-statteeth*stattoothwid*(statslotbotrad-stattoprad))/
statslots;

% area of a stator slot occupied by armature winding
usedslotarea=slotarea*packingfactor;
lumpparam.m
%%%lumpparam.m%%%
%%%Lumped parameters%%%

%field resistance
if origfield
Rfield=1/copperconductivity/packingfactor/interstacklen*((statbotrad+statslotbotrad)/(statbotrad-
statslotbotrad));
else

```

```
Rfield=1/copperconductivity/packingfactor/interstacklen*((stattoprad+rotslotbotrad)/(stattoprad-
rotslotbotrad));
end
```

```
%armature resistance
```

```
Rarm= 1/copperconductivity/usedslotarea*(armmeanpathlen/2)*(statsp/3)*(2*pp)...
/(pp^2); % divide by pp^2 because of pp in parallel
```

```
%permeance harmonic amplitudes
```

```
lambda0=mu0*( (1/airgapwid2) + rottoothfrac * ((1/airgapwid1)-(1/airgapwid2)));
lambda1=2*mu0/pi* ((1/airgapwid1)-(1/airgapwid2))*sin(rottoothfrac*pi);
lambda2=mu0/pi* ((1/airgapwid1)-(1/airgapwid2))*sin(2*rottoothfrac*pi);
```

```
%leakage inductance
```

```
Ll=2*8/3*mu0/(2*pp)*stacklen*(statslotbotrad-stattoprad)/avestatslotwid;
```

```
%direct-axis reactance
```

```
Xd=omegaelec*3/2*(8/pi)*(armwindingfac/2/pp)^2*(2*Nap)^2*avearm-
rad*stacklen*(lambda0+lambda2/2)+omegaelec*Ll;
```

```
%quadrature axis reactance
```

```
Xq=omegaelec*3/2*(8/pi)*(armwindingfac/2/pp)^2*(2*Nap)^2*avearmrad*stacklen*(lambda0-
lambda2/2)+omegaelec*Ll;
```

```
%armature field mutual inductance
```

```
Laf=(armwindingfac/2/pp) * 2 * (2*Nap)*avearmrad*stacklen*lambda1;
```

```
perf.
```

```
%%%perf.m%%%
```

```
%%%Optimizes Electrical Performance%%%
```

```
initphasecur=(pi/3)*netoutputpower/loadvoltage;
```

```
%initial number of armature turns
```

```
initarmturns=floor((Jarmmax*usedslotarea*sqrt(2)*pp)/initphasecur);
```

```
Na=min(initarmturns);
```

```
Ns=0;
```

```
validmachine=0;
```

```
while (Na>=1) & (validmachine==0),
```

```
    if backemfaccuracy==2
```

```
        %%%back emf when ignoring saliency and armature resistance
```

```
        [Eafapprox,validEaf]=backemfapprox(Na,Xd,Xq,loadvoltage,diodedrop,netoutput-
power,Rfield,omegaelec,Laf);
```

```
        Eaf=Eafapprox;
```



```

elseif backemfaccuracy==1
%%%back emf when ignoring equivalent armature resistance
[Eafapprox,validEaf]=backemfapprox(Na,Xd,Xq,loadvoltage,diodedrop,netoutput-
power,Rfield,omegaelec,Laf);
%%%exact back-emf calculations
if validEaf
[Eaf,validEaf,powang]=backemfexact(Na,Xd,Xq,loadvoltage,diodedrop,netoutput-
power,Rfield,Rarm,omegaelec,Laf,Eafapprox);
end

elseif backemfaccuracy==3
[Eafround,validEaf]=backemfcomp(Rfield,omegaelec,Na,Laf,Xd,loadvoltage,diode-
drop,netoutputpower);
Eaf=Eafround;
else
[EafXdonly,validEaf]=backemfcomp(Rfield,omegaelec,Na,Laf,Xd,loadvoltage,diode-
drop,netoutputpower);
[Eafapprox,validEaf]=backemfapprox(Na,Xd,Xq,loadvoltage,diodedrop,netoutput-
power,Rfield,omegaelec,Laf);
%%%exact back-emf calculations
if validEaf
[Eaf,validEaf,powang]=backemfexact(Na,Xd,Xq,loadvoltage,diodedrop,netoutput-
power,Rfield,Rarm,omegaelec,Laf,Eafapprox);
end
end
if validEaf
% fprintf('REACHED1\n');
%field ampere turns
NIfield=Eaf./(omegaelec*Na*Laf);

%inner radius limit based on centerpiece axial flux
innerrad3=sqrt(rotslotbotrad^2-NIfield*aveairgaprad*stacklen*lambda0/1.8); %inner
radii for all three operating points
innerradmin1=min(innerrad3);

if all(imag(innerrad3)==0) & innerradmin1>innerradmin ,
% fprintf('REACHED2\n');

%armature phase current
Iarm=(pi/3)*(netoutputpower+NIfield.^2*Rfield)/loadvoltage;

%field MMF
Fr=(1/2)*NIfield;

```

```

    %armature combined MMF
    Fs=(1/2)*(3/2)*(2*Nap*Na)*(Iarm/2/pp);

    %maximum possible airgap flux density
    Bairgap=mu0*(Fr+Fs)/airgapwid1;

    %stator tooth flux density
    Bstattooth=Bairgap*(statstang/stattoothang);

    %rotor tooth flux density
    Brottooth=Bairgap*aveairgaprad/2/rotslotbotrad/rottoothfrac;

    if max(Bstattooth) <= Bsat & max(Brottooth) <= Bsat,
%   fprintf('REACHED3\n');
    Bs=max(Bairgap);

    %back-iron thickness calculation
    backironthickness = Bs*aveairgaprad/(Bsat*pp)*(pi/2);

    %second minimum value for outer radius
    statbotrad1=statslotbotrad+backironthickness;

    if origfield
        statbotrad=max(statbotrad,statbotrad1);
    else
        statbotrad=statbotrad1;
    end

    if origfield
        fieldcopperarea=(statbotrad-statslotbotrad)*interstacklen*packingfactor;
    else
        fieldcopperarea=(stattoprad-rotslotbotrad)*interstacklen*packingfactor;
    end

    %outer radius based on backiron uniaxial flux
    outerrad=max(sqrt(NIfield*aveairgaprad*stacklen*lambda0/1.8 + statbotrad^2));

    %second maximum value for inner radius
    innerradmin2=rotslotbotrad-backironthickness;
    innerrad = min(innerradmin1,innerradmin2);

    if outerrad < outerradmax & innerrad > innerradmin,
%   fprintf('REACHED4\n');

```

```

        %%% copper losses at second operating point
copperloss2=(3/2)*(Iarm(2))^2*Rarm * Na^2 + (NIfield(2))^2*Rfield;
        %%% armature copper losses at second operating point
armcopperloss2=(3/2)*(Iarm(2))^2*Rarm*Na^2;

        %%% field copper losses at second operating point
fieldcopperloss2=(NIfield(2))^2*Rfield;

        %%% diode losses at second operating point
diodeloss2= 3/pi*Iarm(2)* 2*diodedrop;

        %%% efficiency at second operating point
efficiency2=netoutputpower(2)/(diodeloss2 + copperloss2 + netoutputpower(2));
% field winding current densities
        Jfield=NIfield/fieldcopperarea;

% armature winding current densities
        Jarm=Na*(Iarm/pp)/sqrt(2)/usedslotarea;

if efficiency2 >= 0.75 & max(Jfield) <= Jfieldmax & max(Jarm) <= Jarmmax,
%       fprintf('REACHED5\n');
        validmachine=1;

        Ns=Na;

        %%% copper losses for all operating points
copperloss=(3/2).*Iarm.^2.*Rarm .* Na^2 + (NIfield).^2.*Rfield;
        %%% armature copper losses for all operating points
armcopperloss=(3/2).*(Iarm).^2.*Rarm*Na^2;

        %%% field copperlosses for all operating points
fieldcopperloss=(NIfield).^2.*Rfield;

        %%% diode losses for all operating points
diodeloss=3/pi*Iarm * 2*diodedrop;

        %%% efficiency for all operating points
efficiency=netoutputpower/(diodeloss + copperloss + netoutputpower);

        %%% shear stress
shearstress=(netoutputpower+fieldcopperloss)/(2*pi*rot-
toprad^2*(2*stacklen)*6.895e3*omegamech);

        %%% tip speed
tipspeed=omegamech*rotoprad;

```

```

        %%%mass of centerpiece
        masscenterpiece=pi*(rotslotbotrad^2-innerrad^2)*totlen*steeldensity;
        %%%mass of rotor teeth
        massrotorteeth=rottoothfrac*pi*(rotoprad^2-rotslotbotrad^2)*(2*stacklen)*steel-
density;

        %%%rotor moment of inertia
        inertia=0.5*masscenterpiece*(innerrad^2+rotslotbotrad^2)+0.5*massrotor-
teeth*(rotslotbotrad^2+rotoprad^2);
    end
end
end
    end
end
    Na=Na-1;
end

```

### **backemfcomp.m**

```

function [Eaf,validEaf]=backemfcomp(Rfield,omegaelec,Na,Laf,Xd,loadvoltage,diode-
drop,netoutputpower)
%backemfcomp.m
%rough calculation of back-emf; ignores saliency and armature resistance
A= Rfield./((omegaelec*Na*Laf).^2);
C= (pi*Na^2*Xd)/3;
D= (2*loadvoltage + 4*diodedrop)/pi;
F1=[(A(1)*C(1)/loadvoltage)^2 2*netoutputpower(1)*A(1)*(C(1)/loadvoltage)^2-1
(C(1)*netoutputpower(1)/loadvoltage)^2+D^2];
F2=[(A(2)*C(2)/loadvoltage)^2 2*netoutputpower(2)*A(2)*(C(2)/loadvoltage)^2-1
(C(2)*netoutputpower(2)/loadvoltage)^2+D^2];
F3=[(A(3)*C(3)/loadvoltage)^2 2*netoutputpower(3)*A(3)*(C(3)/loadvoltage)^2-1
(C(3)*netoutputpower(3)/loadvoltage)^2+D^2];

Q1=roots(F1);
Q2=roots(F2);
Q3=roots(F3);
[Eafmat(:,1)]=sqrt(Q1);
[Eafmat(:,2)]=sqrt(Q2);
[Eafmat(:,3)]=sqrt(Q3);
Eaf=[];
if (all(imag(Eafmat(2,:))==0))
    validEaf=1; %Eaf obtained is valid
    Eaf=Eafmat(2,:); %Eaf obtained
else

```

```

    validEaf=0;
end
backemfapprox.m
function [Eaf,validEaf]=backemfapprox(Na,Xd,Xq,loadvoltage,diodedrop,netoutput-
power,Rfield,omegaelec,Laf)
%backemfapprox.m
%calculates backemf while ignoring armature resistance
if Xd==Xq
    Xq=Xq-1e-6;
end
y=((2*loadvoltage+4*diodedrop)/pi)^2;
m=(Na^2)*(Xd+Xq)/2;
n=(Na^2)*(Xq-Xd)/2;
r=netoutputpower./loadvoltage;
s=Rfield/loadvoltage./(omegaelec*Laf*Na).^2;
f=3/pi;
a=s.^2.*(m-n).^2;
b=2*r.*s.*(m-n).^2-f.^2+4*n.*y.*s.^2.*(m-n);
c=f.^2*y+r.^2.*(m-n).^2+8.*n.*y.*r.*s.*(m-n)+4.*n.^2*y.^2.*s.^2;
d=4.*n.*y.*r.^2.*(m-n)+8*n.^2*y.^2.*r.*s;
e=4.*n.^2.*y.^2.*r.^2;

[Eafsqaredmat(:,1)]=roots([a(1),b(1),c(1),d(1),e(1)]);
[Eafsqaredmat(:,2)]=roots([a(2),b(2),c(2),d(2),e(2)]);
[Eafsqaredmat(:,3)]=roots([a(3),b(3),c(3),d(3),e(3)]);

[Eafmat(:,1)]=sqrt(Eafsqaredmat(:,1));
[Eafmat(:,2)]=sqrt(Eafsqaredmat(:,2));
[Eafmat(:,3)]=sqrt(Eafsqaredmat(:,3));
Eaf=[];
validEaf=0;

if(all(imag(Eafmat(2,:))==0))
    validEaf=1;
    Eaf=Eafmat(2,:);
end

if validEaf
Xeq=m+n.*(2*y./(Eaf.^2)-1); %equivalent reactance
powerfactor=sqrt(y./Eaf.^2);
end

```

```

backemfexact.m
function [Eaf,validEaf,powang]=backEafexact(Na,Xd,Xq,loadvoltage,diodedrop,netoutput-
power,Rfield,Rarm,omegaelec,Laf,Eafapprox)

```

```

%backemfexact.m
%exact calculation of back-emf
r=netoutputpower./loadvoltage;
s=Rfield/loadvoltage./(omegaelec*Laf*Na).^2;
Vodp=loadvoltage/2+diodedrop;
k3=(4*Vodp/pi);
powerangle1=acos(4*Vodp/pi./Eafapprox);
if Xd==Xq
    Xq=Xq-1e-6;
end
[Eaftemp powangtemp validEaf]=findet(Na,Xd(1),Xq(1),Eafapprox(1),powerangle1(1),Rarm,r(1),s(1),k3);
Eaf(1)=Eaftemp;
powang(1)=powangtemp;

if validEaf==0
    return
end

[Eaftemp powangtemp validEaf]=findet(Na,Xd(2),Xq(2),Eafapprox(2),powerangle1(2),Rarm,r(2),s(2),k3);
Eaf(2)=Eaftemp;
powang(2)=powangtemp;

if validEaf==0
    return
end

[Eaftemp powangtemp validEaf]=findet(Na,Xd(3),Xq(3),Eafapprox(3),powerangle1(3),Rarm,r(3),s(3),k3);
Eaf(3)=Eaftemp;
powang(3)=powangtemp;

if validEaf==0
    return
end
findet.m
function [Emf,thetai,validEaf]=findet(Na,Xd,Xq,Emf,thetai,Rarm,r,s,k3)
%findet.m
%uses Newton's method to determine back-emf and internal power angle
deltaEmf=1;
deltathetai=1;
f1=1;
f2=1;
h=0.0001;

```

```

iter=0;
validEaf=1;
%implements Newton's method to solve nonlinear equation
while norm([deltaEmf deltathetai])>.01 | norm([f1 f2])>.01
iter=iter+1;

if iter>500
    validEaf=0;
    return;
end

f1=getf1(Na,Xd,Xq,Emf,thetai,Rarm,r,s,k3);
f2=getf2(Na,Xd,Xq,Emf,thetai,Rarm,r,s,k3);

df1bydEmf=cendiff(1,1,Na,Xd,Xq,Emf,thetai,Rarm,r,s,k3,h);
df1bydthetai=cendiff(1,2,Na,Xd,Xq,Emf,thetai,Rarm,r,s,k3,h);
df2bydEmf=cendiff(2,1,Na,Xd,Xq,Emf,thetai,Rarm,r,s,k3,h);
df2bydthetai=cendiff(2,2,Na,Xd,Xq,Emf,thetai,Rarm,r,s,k3,h);
jac=[df1bydEmf df1bydthetai; df2bydEmf df2bydthetai];

xx=inv(jac)*[-f1;-f2];
deltaEmf=xx(1);
deltathetai=xx(2);
Emf=Emf+deltaEmf;
thetai=thetai+deltathetai;
if imag(Emf)~=0 | imag(thetai)~=0
    validEaf=0;
    return
end
end
end
getf1.m
function f1=getf1(Na,Xd,Xq,Emf,thetai,Rarm,r,s,k3)
%getf1.m
%determines first of two nonlinear equations used to determine
%backemf and internal power angle

%equivalent synchronous reactance
Xs=((Na^2)*((Xd+Xq)/2-(Xd-Xq)/2.*cos(2.*thetai)));

%equivalent armature resistance
Rs=((Na^2)*((Xd-Xq)/2.*sin(2.*thetai) + Rarm));

%equivalent load resistance
R=(((k3^2)*Rs+k3*sqrt((Xs.^2).*(Emf.^2-k3^2)+Rs.^2.*Emf.^2))./(Emf.^2-k3^2));

%power requirement equation; searching for zero

```

```

f1=3/pi*Emf/sqrt( Xs^2 + (R+Rs)^2) - r - Emf^2* s;
getf2.m
function f2=getf2(Na,Xd,Xq,Emf,thetai,Rarm,r,s,k3)
%getf2.m
%determines second of two nonlinear equations used to determine
%backemf and internal power angle

%equivalent synchronous reactance
Xs=((Na^2)*((Xd+Xq)/2-(Xd-Xq)/2.*cos(2.*thetai)));

%equivalent armature resistance
Rs=((Na^2)*((Xd-Xq)/2.*sin(2.*thetai) + Rarm));

%power angle equation; searching for zero
R=((k3^2)*Rs+k3*sqrt((Xs.^2).*(Emf.^2-k3^2)+Rs.^2.*Emf.^2))./(Emf.^2-k3^2));
f2=tan(thetai)- Xs/(R+Rs);
cendiff.m
function dfdx=cendiff(f,x,Na,Xd,Xq,Emf,thetai,Rarm,r,s,k3,h)
%cendiff.m
%approximates derivative by using central difference
if f==1
    if x==1
        fplus=getf1(Na,Xd,Xq,Emf+h,thetai,Rarm,r,s,k3);
        fminus=getf1(Na,Xd,Xq,Emf-h,thetai,Rarm,r,s,k3);
    else
        fplus=getf1(Na,Xd,Xq,Emf,thetai+h,Rarm,r,s,k3);
        fminus=getf1(Na,Xd,Xq,Emf,thetai-h,Rarm,r,s,k3);
    end
else
    if x==1
        fplus=getf2(Na,Xd,Xq,Emf+h,thetai,Rarm,r,s,k3);
        fminus=getf2(Na,Xd,Xq,Emf-h,thetai,Rarm,r,s,k3);
    else
        fplus=getf2(Na,Xd,Xq,Emf,thetai+h,Rarm,r,s,k3);
        fminus=getf2(Na,Xd,Xq,Emf,thetai-h,Rarm,r,s,k3);
    end
end
dfdx=(fplus-fminus)/(2*h);
poleface.m
%%poleface.m%%
%%calculates pole face losses%%

%average rotor radius
averotrad=(rotoprad+stattoprad)/2;

%index for harmonic

```



```

m=1;

%wavenumber
km=m*statsp*(2*pp)/averotrad;

%mechanical frequency
omegam=m*(statsp*2*pp)/pp*omegaelec;

%fundamental flux density at tip of stator tooth
%need new expression for higher harmonics
Bm=(4/pi*armwindingfac*Fs*(lambda0+lambda2/2)+Fr*lambda1)*statstang/stattoothang;

S=musteel*steelconductivity*omegam/(km^2);

alpha=km*sqrt(1+j*S);

kmoveralpha=km./alpha;

kmg=km*airgapwid1;

C=(kmoveralpha.*Bm)./( (kmoveralpha+1./tanh(kmg))*cosh(kmg) - 1./sinh(kmg));

%pole face losses
rotironloss=steelconductivity.*omegam./km.*(C.*conj(C))/2*1./(2*real(alpha))*averotrad.*omegaelec/pp*2*pi*averotrad*2*stacklen*rottoothfrac;
cost.m
%%cost.m%%
%%Evaluates the *materials cost* of acceptable machines; without overhead
if validmachine

%rotor centerpiece volume
rotcenterpiecevol=pi*(rotslotbotrad^2-innerrad^2)*totlen;

%rotor teeth volume
rotteethvol=(0.5*(rottoprad^2-rotslotbotrad^2)*rottoothang)*stacklen*(2*pp);

%stator back-iron volume
statbackironvol=pi*(outerrad^2-statbotrad^2)*totlen+2*pi*(statbotrad^2-statslotbotrad^2)*stacklen;

%volume of stator teeth
statteethvol=2*stattoothwid*(statslotbotrad-stattoprad)*stacklen*statteeth;

%mass of stator teeth
statteethmass=statteethvol*steeldensity;

```

```

%total steel cost
steelcost=(rotcenterpiecevol+rotteethvol+statbackironvol+statteethvol)*dollarspervolsteel;

%armature winding copper volume
armcoppervol=armmeanpathlen*usedslotarea*(0.5*statslots);

%field winding copper volume
fieldcoppervol=pi*(statbotrad^2-statslotbotrad^2)*interstacklen*packingfactor;

%total cost off copper
coppercost=(armcoppervol+fieldcoppervol)*dollarspervolcopper;

%total materials cost
totcost=steelcost+coppercost;
end

```

### **savecheap.m**

```

%%%savecheap.m%%%
%%% Saves a set number of cheapest machines %%%
if validmachine
    counter=counter+1;
[maxcost,maxcostloc]=max(dimensions(:,13));
if (totcost < maxcost)
    dimensions(maxcostloc,1)=outerrad;
    dimensions(maxcostloc,2)=statbotrad;
    dimensions(maxcostloc,3)=statslotbotrad;
    dimensions(maxcostloc,4)=airgapwid1;
    dimensions(maxcostloc,5)=airgapwid2;
    dimensions(maxcostloc,6)=rotslotbotrad;
    dimensions(maxcostloc,7)=innerrad;
    dimensions(maxcostloc,8)=stattoothang;
    dimensions(maxcostloc,9)=rottoothang;
    dimensions(maxcostloc,10)=stacklen;
    dimensions(maxcostloc,11)=interstacklen;
    dimensions(maxcostloc,12)=Ns;
    dimensions(maxcostloc,13)=totcost;

    save(eval('filename'), 'dimensions', 'desno', 'counter', 'pp', 'garratio','origfield','back-
emfaccuracy');

end
end

```

### **saveall.m**

```

%%%saveall.m%%%

```

```

%%Saves all acceptable machines (note file space occupied)
if validmachine
    counter=counter+1;
    dimensions(counter,1)=outerrad;
    dimensions(counter,2)=statbotrad;
    dimensions(counter,3)=statslotbotrad;
    dimensions(counter,4)=airgapwid1;
    dimensions(counter,5)=airgapwid2;
    dimensions(counter,6)=rotslotbotrad;
    dimensions(counter,7)=innerrad;
    dimensions(counter,8)=stattoothang;
    dimensions(counter,9)=rottoothang;
    dimensions(counter,10)=stacklen;
    dimensions(counter,11)=interstacklen;
    dimensions(counter,12)=Ns;
    dimensions(counter,13)=totcost;
    save(eval('filename'), 'dimensions', 'desno', 'counter', 'pp', 'gearratio','origfield','back-
emfaccuracy');
end
onerun.m
%%onerun.m
%%single iteration on a design given its dimensions and turns
filename='reforigp18com.mat';
loadfile=0; %load file above
draw=1; %1 draws machine
samescale=1; %1 draws all machines using the same image size
imagesize=250; %if samescale is 1, need image size in millimeters
newfigure=0; %0 draws in same figure
showproperties=1; %1 shows machine properties
showdimensions=0; %1 shows dimensions
origfield=1; %0 for modified structure (field adjacent to rotor);
backemfaccuracy=1; % 1 to be exact (refined search)
    % 2 to ignore resistance (broad search)
    % 3 to ignore resistance and saliency
    % 4 to use exact but calculate all three options
indexoption=1; %1 to handpick
    %2 to select in sequence with increasing index
    %3 to select minimum cost
    %4 to select at random
machinenumber=8; %if indexoption is 1, need machinenumber
%%
if loadfile
    load(eval('filename'))
end
if indexoption==1
index=machinenumber; %machine is hand picked

```

```

elseif indexoption==2
index=index+1; %select machines in sequence
elseif indexoption==3
[minval,minindex]=min(dimensions(:,13)); %select minimum cost machine
index=minindex;
elseif index==4
index=floor(rand*min(counter,size(dimensions,1))) +1; %select a machine at random
end
end
init;
outerrad = dimensions(index,1);
statbotrad = dimensions(index,2);
statslotbotrad = dimensions(index,3);
airgapwid1 = dimensions(index,4);
airgapwid2 = dimensions(index,5);
rotslotbotrad = dimensions(index,6);
innerrad = dimensions(index,7);
stattoothang = dimensions(index,8);
rottoothang = dimensions(index,9);
stacklen = dimensions(index,10);
interstacklen = dimensions(index,11);
Ns = dimensions(index,12);
totcost = dimensions(index,13);
%stattoothang=statstang/2;
%rottoothang=rotstang;
stattoprad = rotslotbotrad + airgapwid2;
rottoprad = rotslotbotrad + airgapwid2 - airgapwid1;
if showdimensions
outerrad
statbotrad
statslotbotrad
airgapwid1
airgapwid2
rotslotbotrad
innerrad
stattoothang
rottoothang
stacklen
interstacklen
Ns
totcost
stattoprad
rottoprad
end

cdim;
lumpparam;

```

```

perf;
cost;
%poleface %calculate pole face losses

if draw
    if newfigure
        figure
    else
        figure(10)
        clf
    end
subplot(121)
cross_section
title(totcost*2)
subplot(122)
if origfield
sideview
else
sideviewmod
end
title(totcost*2)
legend
end

%save for purposes of plotting vs. pole count
if validmachine
total_cost(pp)=2*totcost; %factor of two for overhead
dia(pp)=outerrad*2;
stack_len(pp)=stacklen;
inter_stack_length(pp)=interstacklen;
arm_turns_per_coil(pp)=Ns;
mass(pp)=(rotcenterpiecevol+rotteethvol+statbackironvol+statteethvol)*steeldensity+(armcopp-
ervol+fieldcoppervol)*copperdensity;
eff(pp)=efficiency2;
flux_den(pp)=max(Bstattooth);
field_cur_dens(pp)=max(Jfield);
stator_cur_dens(pp)=max(Jarm);
tip_speed(pp)=max(tipspeed);
shear_stress(pp)=max(shearstress);
rotor_inertia(pp)=inertia;

back_iron_thickness_a(pp)=backironthickness;
end_turn_width_a(pp)=endturnwid;
statbotrad_a(pp)=statbotrad;
statslotbotrad_a(pp)=statslotbotrad;
airgapwid1_a(pp)=airgapwid1;

```

```

airgapwid2_a(pp)=airgapwid2;
rotslotbotrad_a(pp)=rotslotbotrad;
stattoothang_a(pp)=stattoothang;
rottoothang_a(pp)=rottoothang;
image_dim(pp)=max(outerrad,(2*stacklen+interstacklen+2*endturnwid)/2)*1e3;
rottoothfrac_a(pp)=rottoothfrac;
end

%shows properties of machine
if showproperties
Total_cost=2*totcost
Diameter=outerrad*2
Stack_length=stacklen
Inter_stack_length=interstacklen
Armature_turns_per_coil=Ns
Mass=(rotcenterpiecevol+rotteethvol+statbackironvol+statteethvol)*steeldensity+(armcopper-
vol+fieldcoppervol)*copperdensity
Efficiency=efficiency2
Steel_flux_density=max(Bstattooth)
Field_current_density=max(Jfield)
Stator_current_density=max(Jarm)
Tip_speed=max(tipspeed)
Shear_stress=max(shearstress)
Rotor_inertia=inertia
end

```

### **cross\_section.m**

```

%% %% cross_section.m %% %%
%draws a cross-section of the machine
%clf reset;
%axis([-1 1 -1 1]*outerrad*1e3);
axis square
axis off
if samescale
axis([-1 1 -1 1]*ceil(imagesize/2));
else
axis([-1 1 -1 1]*ceil(max(outerrad,(2*stacklen+interstacklen+2*endturnwid)/2)*1e3));
end
%axis([-1 1 -1 1]*0.15*1e3);
hold on

fill(outerrad*1e3*cos(linspace(0,2*pi)),outerrad*1e3*sin(linspace(0,2*pi)), 'w');
if origfield
fill(statbotrad*1e3*cos(linspace(0,2*pi)),statbotrad*1e3*sin(linspace(0,2*pi)), 'w');

```

```

else
fill(statslotbotrad*1e3*cos(linspace(0,2*pi)),statslotbotrad*1e3*sin(linspace(0,2*pi)), 'w');
end

stattopradpluscloserlen=stattoprad*(1+0.75*halfstatslottopang);
statslotbotarcang=linspace(halfstatslotbotang,-halfstatslotbotang);
arcangno=length(statslotbotarcang);
rad=[stattopradpluscloserlen,stattoprad,stattoprad,stattopradpluscloserlen,statslot-
botrad*ones(1,arcangno)]*1e3;
slotcloserangle=(statstang-stattoprad*stattoothtopang/stattopradpluscloserlen)/2;
locang=[-slotcloserangle -halfstatslottopang/4 halfstatslottopang/4 slotcloserangle statslot-
botarcang];

for c=1:statslots,
    globang = [locang+(c-0.5)*statstang];
    fill(rad.*cos(globang),rad.*sin(globang),'r');
end

fill(stattoprad*1e3*cos(linspace(0,2*pi)),stattoprad*1e3*sin(linspace(0,2*pi)), 'k');
fill(rottograd*1e3*cos(linspace(0,2*pi)),rottograd*1e3*sin(linspace(0,2*pi)), 'w');

rottogradarcang=linspace(rotslotang/2, -rotslotang/2);
toparcangno=length(rottogradarcang);

rotslotbotarcang=linspace(-rotslotang/2, rotslotang/2);
slotbotarcangno=length(rotslotbotarcang);
%%% if rottoothfrac<0.5 just do as before, rottoothfrac>0.5, halve the number...of slots... do as
before but paint both white!!!
rad=[rotslotbotrad rottograd rottograd*ones(1,toparcangno) rottograd rotslotbotrad rotslot-
botrad*ones(1,slotbotarcangno)]*1e3;
locang=[rotslotang/2 rotslotang/2 rottogradarcang -rotslotang/2 -rotslotang/2 rotslotbotarcang];
if rottoothfrac<0.5
for c=1:rotslots,
    globang=[pi/2+locang+(c-0.5)*rotstang];
    fill(rad.*cos(globang),rad.*sin(globang),'k');
end
for c=1:rotslots
line(rotslotbotrad*1e3*cos(linspace(pi/2-rottoothang/2,pi/2+rottoothang/2 )+rotstang+2*c*rot-
stang),rotslotbotrad*1e3*sin(linspace(pi/2-rottoothang/2,pi/2+rottoothang/2)+rotstang+2*c*rot-
stang));
end
else
for c=1:rotslots/2,
    globang=[pi/2+locang+(c-0.5)*(2*rotstang)];
    fill(rad.*cos(globang),rad.*sin(globang),'w');

```

```

end
end

fill(innerrad*1e3*cos(linspace(0,2*pi)),innerrad*1e3*sin(linspace(0,2*pi)),'b');
sideview.m
%sideview.m
%sectional view of machine
%clf reset;
axis square
axis off
if samescale
    axis([-1 1 -1 1]*ceil(imagesize/2));
else
    axis([-1 1 -1 1]*ceil(max(outerrad,(2*stacklen+interstacklen+2*endturnwid)/2)*1e3));
end
%axis('square','off');
hold on;
halfshaftlen=(interstacklen+2*stacklen)/2;
halfinterstacklen=interstacklen/2;
fill([-halfshaftlen halfshaftlen halfshaftlen -halfshaftlen]*1e3,[-outerrad -outerrad outerrad outerrad]*1e3,'k')
fill([-halfshaftlen halfshaftlen halfshaftlen -halfshaftlen]*1e3,[-innerrad -innerrad innerrad innerrad]*1e3,'b')
fill([-halfshaftlen halfshaftlen halfshaftlen -halfinterstacklen -halfinterstacklen -halfshaftlen]*1e3,[innerrad innerrad rotslotbotrad rotslotbotrad rottoprad rottoprad]*1e3,'w')

line(-ones(1,100)*halfshaftlen*1e3,linspace(rottoprad,stattoprad)*1e3)

line(ones(1,100)*halfshaftlen*1e3,linspace(rotslotbotrad,stattoprad)*1e3)

if (mod(pp,2)==0)
    fill([-halfshaftlen halfshaftlen halfshaftlen -halfinterstacklen -halfinterstacklen -halfshaftlen]*1e3,[-innerrad -innerrad -rotslotbotrad -rotslotbotrad -rotoprad -rotoprad]*1e3,'w')
    line(ones(1,100)*halfshaftlen*1e3,linspace(-rotslotbotrad,-stattoprad)*1e3);
    line(-ones(1,100)*halfshaftlen*1e3,linspace(-rotoprad,-stattoprad)*1e3);
else
    fill([-halfshaftlen halfinterstacklen halfinterstacklen halfshaftlen halfshaftlen -halfshaftlen]*1e3,[-rotslotbotrad -rotslotbotrad -rotoprad -rotoprad -innerrad -innerrad]*1e3,'w')
    line(-ones(1,100)*halfshaftlen*1e3,linspace(-rotslotbotrad,-stattoprad)*1e3);
    line(ones(1,100)*halfshaftlen*1e3,linspace(-rotoprad,-stattoprad)*1e3);
end
fill([halfinterstacklen halfshaftlen halfshaftlen halfinterstacklen]*1e3,[stattoprad stattoprad statbotrad statbotrad]*1e3,'w')
fill([halfinterstacklen halfshaftlen halfshaftlen halfinterstacklen]*1e3,[-stattoprad -stattoprad -statbotrad -statbotrad]*1e3,'w')

```



```

fill([-halfinterstacklen -halfshaftlen -halfshaftlen -halfinterstacklen]*1e3,[stattoprad stattoprad
statbotrad statbotrad]*1e3,'w')
fill([-halfinterstacklen -halfshaftlen -halfshaftlen -halfinterstacklen]*1e3,[-stattoprad -stattoprad -
statbotrad -statbotrad]*1e3,'w')
fill([-halfshaftlen halfshaftlen halfshaftlen -halfshaftlen]*1e3,[statbotrad statbotrad outerrad out-
errad]*1e3,'w')
fill([-halfshaftlen halfshaftlen halfshaftlen -halfshaftlen]*1e3,[-statbotrad -statbotrad -outerrad -
outerrad]*1e3,'w')
fill([-halfinterstacklen halfinterstacklen halfinterstacklen -halfinterstacklen]*1e3,[statslotbotrad
statslotbotrad statbotrad statbotrad]*1e3,'y')
fill([-halfinterstacklen halfinterstacklen halfinterstacklen -halfinterstacklen]*1e3,[-statslotbotrad -
statslotbotrad -statbotrad -statbotrad]*1e3,'y')
fill([-halfinterstacklen halfinterstacklen halfinterstacklen -halfinterstacklen]*1e3,[stattoprad stat-
toprad statslotbotrad statslotbotrad]*1e3,'r')
fill([-halfinterstacklen halfinterstacklen halfinterstacklen -halfinterstacklen]*1e3,[-stattoprad -stat-
toprad -statslotbotrad -statslotbotrad]*1e3,'r')
fill([halfshaftlen halfshaftlen+endturnwid halfshaftlen+endturnwid halfshaftlen]*1e3,[stattoprad
stattoprad statslotbotrad statslotbotrad]*1e3,'r')
fill([-halfshaftlen -(halfshaftlen+endturnwid) -(halfshaftlen+endturnwid) -halfshaftlen]*1e3,[stat-
toprad stattoprad statslotbotrad statslotbotrad]*1e3,'r')
fill([halfshaftlen halfshaftlen+endturnwid halfshaftlen+endturnwid halfshaftlen]*1e3,[-stattoprad
-stattoprad -statslotbotrad -statslotbotrad]*1e3,'r')
fill([-halfshaftlen -(halfshaftlen+endturnwid) -(halfshaftlen+endturnwid) -halfshaftlen]*1e3,[-
stattoprad -stattoprad -statslotbotrad -statslotbotrad]*1e3,'r')

```

### sideviewmod.m

```

%figure
%clf reset;
axis square
axis off
if samescale
    axis([-1 1 -1 1]*ceil(imagesize/2));
else
    axis([-1 1 -1 1]*ceil(max(outerrad,(2*stacklen+interstacklen+2*endturnwid)/2)*1e3));
end
%axis('square','off');
hold on;
halfshaftlen=(interstacklen+2*stacklen)/2;
halfinterstacklen=interstacklen/2;
fill([-halfshaftlen halfshaftlen halfshaftlen -halfshaftlen]*1e3,[-outerrad -outerrad outerrad outer-
rad]*1e3,'k')
fill([-halfshaftlen halfshaftlen halfshaftlen -halfshaftlen]*1e3,[-innerrad -innerrad innerrad inner-
rad]*1e3,'b')
fill([-halfshaftlen halfshaftlen halfshaftlen -halfinterstacklen -halfinterstacklen -half-
shaftlen]*1e3,[innerrad innerrad rotslotbotrad rotslotbotrad rottoprad rottoprad]*1e3,'w')

```

```
line(-ones(1,100)*halfshaftlen*1e3, linspace(rotoprad,stattoprad)*1e3)
line(ones(1,100)*halfshaftlen*1e3, linspace(rotslotbotrad,stattoprad)*1e3)
```

```
if (mod(pp,2)==0)
```

```
fill([-halfshaftlen halfshaftlen halfshaftlen -halfinterstacklen -halfinterstacklen -half-
shaftlen]*1e3,[-innerrad -innerrad -rotslotbotrad -rotslotbotrad -rotoprad -rotoprad]*1e3,'w')
line(ones(1,100)*halfshaftlen*1e3, linspace(-rotslotbotrad,-stattoprad)*1e3);
line(-ones(1,100)*halfshaftlen*1e3, linspace(-rotoprad,-stattoprad)*1e3);
```

```
else
```

```
fill([-halfshaftlen halfinterstacklen halfinterstacklen halfshaftlen halfshaftlen -half-
shaftlen]*1e3,[-rotslotbotrad -rotslotbotrad -rotoprad -rotoprad -innerrad -innerrad]*1e3,'w')

line(-ones(1,100)*halfshaftlen*1e3, linspace(-rotslotbotrad,-stattoprad)*1e3);
line(ones(1,100)*halfshaftlen*1e3, linspace(-rotoprad,-stattoprad)*1e3);
```

```
end
```

```
fill([-halfshaftlen -halfinterstacklen -halfinterstacklen halfinterstacklen halfinterstacklen half-
shaftlen halfshaftlen -halfshaftlen]*1e3,[stattoprad stattoprad statslotbotrad statslotbotrad stat-
toprad stattoprad outerrad outerrad]*1e3,'w')
```

```
fill([-halfshaftlen -halfinterstacklen -halfinterstacklen halfinterstacklen halfinterstacklen half-
shaftlen halfshaftlen -halfshaftlen]*1e3,[-stattoprad -stattoprad -statslotbotrad -statslotbotrad -
stattoprad -stattoprad -outerrad -outerrad]*1e3,'w')
```

```
line(linspace(-halfshaftlen, halfshaftlen)*1e3, ones(1,100)*statslotbotrad*1e3);
line(linspace(-halfshaftlen, halfshaftlen)*1e3, ones(1,100)*(-statslotbotrad)*1e3);
```

```
fill([-halfinterstacklen halfinterstacklen halfinterstacklen -halfinterstacklen]*1e3,[rotslotbotrad
rotslotbotrad stattoprad stattoprad]*1e3,'y')
```

```
fill([-halfinterstacklen halfinterstacklen halfinterstacklen -halfinterstacklen]*1e3,[-rotslotbotrad -
rotslotbotrad -stattoprad -stattoprad]*1e3,'y')
```

```
fill([-halfinterstacklen halfinterstacklen halfinterstacklen -halfinterstacklen]*1e3,[stattoprad stat-
toprad statslotbotrad statslotbotrad]*1e3,'r')
```

```
fill([-halfinterstacklen halfinterstacklen halfinterstacklen -halfinterstacklen]*1e3,[-stattoprad -stat-
toprad -statslotbotrad -statslotbotrad]*1e3,'r')
```

```
fill([halfshaftlen halfshaftlen+endturnwid halfshaftlen+endturnwid halfshaftlen]*1e3,[stattoprad
stattoprad statslotbotrad statslotbotrad]*1e3,'r')
```

```
fill([-halfshaftlen -(halfshaftlen+endturnwid) -(halfshaftlen+endturnwid) -halfshaftlen]*1e3,[stat-
toprad stattoprad statslotbotrad statslotbotrad]*1e3,'r')
```

```
fill([halfshaftlen halfshaftlen+endturnwid halfshaftlen+endturnwid halfshaftlen]*1e3,[-stattoprad
-stattoprad -statslotbotrad -statslotbotrad]*1e3,'r')
```

```
fill([-halfshaftlen -(halfshaftlen+endturnwid) -(halfshaftlen+endturnwid) -halfshaftlen]*1e3,[-
stattoprad -stattoprad -statslotbotrad -statslotbotrad]*1e3,'r')
```

**distance.m**

```

%legend.m%
%shows scale corresponding to 50 mm
subplot(121)
zoom;
%clf reset;
clear theta rho;
clear thetac rhoc;
clear point1 point2;
grid off;
if samescale
    imdim=ceil(imageSize/2);
else
    imdim=ceil(max(outerrad,(2*stacklen+interstacklen+2*endturnwid)/2)*1e3);
end
axis([-1 1 -1 1]*imdim);
axis('square','off');
hold on;
xa=-(imdim-25)+linspace(-25,25);
ya=(imdim-10)+zeros(1,length(xa));
line(xa,ya)
for xin=1:6
    y=(imdim-10)+linspace(-5,5); %2
    x=-(imdim-25)+ones(1,length(y))*(xin-3.5)*10;
    line(x,y)
end

```

## References

- [1] J. G. Kassakian, H. C. Wolf, J. M. Miller and C. J. Hurton, "Automotive Electrical Systems circa 2005," *IEEE Spectrum*, pp 22.-27, August 1996.
- [2] K. G. Burger, H. P. Groter, H. J. Lutz, F. Meyer, W. Schleuter, "Alternators in Automotive Applications - State of the Art and Development Trends," symposium "*Nebenaggregate im Fahrzeug*," Haus der Technik Essen, Oct. 5 and 6, 1994.
- [3] A. Brown, "*The Analysis and Design of a High-Power, High-Efficiency Generator*," M.Eng. Thesis, Massachusetts Institute of Technology, Department of Electrical Engineering and Computer Science, May, 1999.
- [4] E. Richter, "New Developments in Very High Speed Electrical Alternators," *Intersociety Energy Conversion Engineering Conference*, 1971.
- [5] J. A. N. Msekela, P. N. Materu, A. H. Nzali, "Development of a Homopolar Electrical Machine for High Power Density High Speed Applications", *African Electrical Technology Conference*, 1996.
- [6] M. Siegl, V. Kotrba, "Losses and Cooling of a High-Speed and High-Output Power Homopolar Inductor Alternator," *Fifth International Conference on Electrical Machines and Drives*, 1991.
- [7] M. Hippner, R.G. Harley, "*High Speed Synchronous Homopolar and Permanent Magnet Machines Comparative Study*," article from Department of Electrical Engineering, University of Natal, South Africa.
- [8] A.E. Fitzgerald, C. Kingsley, Jr., S. D. Umans, *Electric Machinery*, McGraw-Hill, 1990.
- [9] V. Caliskan, D. J. Perreault, T.M. Jahns, J. G. Kassakian, "Analysis of Three-Phase Rectifiers with Constant-Voltage Loads", *IEEE Power Electronics Specialists Conference '99*, in press, Hune-July 1999, Charleston, SC.
- [10] P.K. Dash, A.K. Das Gupta, "Design Aspects of Three-Phase Inductor Alternators", *IEEE Transactions on Power Apparatus & Systems*, vol. PAS-88, no. 11, Nov. 1969, pp.1718-24, USA.
- [11] P.K. Dash, A.K. Das Gupta, "A Basic Analysis of Three-Phase Inductor Alternator", *Journal of the Institution of Engineers*, vol.50 , June 1970.
- [12] D.C. Jain, "*Design Aspects of a Homopolar Inductor-Alternator*", October, 1964.
- [13] P.C. Krause, K. Carlsen, "*Analysis of a Homopolar Inductor Alternator*", Department of Electrical Engineering, University of Wisconsin, Madison, Wisconsin.

[14] M. Siegl, “*Transient and Subtransient Behavior of Homopolar Inductor Alternators*”, University of Colorado, Ph.D. dissertation, 1972.

[15] H. Woodson, J. Melcher, *Electromechanical Dynamics*, John Wiley & Sons, Inc., 1968.